

Fabrication, Validation, and Performance Evaluation of a New Sampling System for the *In-Situ*
Chemical Speciation of Chromium Ions in Groundwater Using Supported Liquid Membranes
(SLMs)

Lesley S. Owens

Dissertation submitted to the faculty of the Virginia Polytechnic Institute and State University in
partial fulfillment of the requirements for the degree of

Doctor of Philosophy
In
Chemistry

Gary L. Long
James M. Tanko
Karen J. Brewer
John R. Morris
Matthew J. Eick

December 19, 2012
Blacksburg, VA

Keywords: Chromium (III), Chromium (VI), speciation, Supported Liquid Membranes (SLMs),
sampler, kinetics, environment

Copyright 2012

Fabrication, Validation, and Performance Evaluation of a New Sampling System for the *In-Situ* Chemical Speciation of Chromium Ions in Groundwater Using Supported Liquid Membranes (SLMs)

Lesley S. Owens

ABSTRACT

A sampler has been fabricated to facilitate the *in-situ* speciation of Cr. Teflon[®] was selected as the material for the samplers because of its inert chemical nature. The design of the sampler is based on the Supported Liquid Membrane (SLM) extraction technique, which utilizes charged organic carrier molecules loaded onto a polymeric (Teflon[®]) support membrane and the principles of electrostatics to selectively transport Cr ions through an ion-pairing mechanism. Cr ions in the feed solution that have an opposite charge from the carrier molecule form an ion-pair with the carrier and are transported through the membrane and deposited into a second aqueous phase referred to as the acceptor phase. A counter-ion from the acceptor phase is exchanged for the Cr ion to complete the extraction process. Since the acceptor phase is contained in a Teflon[®] bottle, the SLM sampler is capable of speciation and storage of Cr ions, which is a major advantage over current speciation techniques.

A food coloring test was used to check the samplers for leaks. A plastic barrier was used in place of the polymeric membrane and the acceptor phase bottle was filled with DI water. The sampler was submerged in a beaker containing food coloring and DI water. The bottle contents were checked for the presence of food coloring using UV-vis

spectroscopy. The sampler was determined to be leak-free if the bottle did not contain food coloring. All systems prepared were validated upon the initial test and required no further manipulation to ensure structural soundness.

The SLM extraction technique involves two liquid-liquid extractions (LLEs). Before the samplers could be evaluated for their performance and stability in Cr speciation applications, liquid-liquid extraction studies were conducted on both systems (Cr (III) and Cr (VI)) to determine the optimal operating parameters (carrier concentration, decanol concentration, and acceptor phase concentration) of the SLM system. The selectivity of each system was also evaluated to validate proper SLM function.

The performance of the samplers was evaluated in a series of tank studies that focused on the uptake of Cr into the acceptor phase as well as the depletion of Cr ion from this phase. The goal of the performance studies was to determine the mechanical and chemical stability of the SLM samplers. As part of the validation process, selectivity studies and studies without the carrier molecule were conducted to ensure that the systems were functioning according to SLM theory. Tank studies that simulated natural sampling condition were also conducted.

The results of the tests conducted in the laboratory indicate that the SLM samplers are a stable, reliable, and viable method for Cr speciation. Future directions of this project will include the incorporation of the SLM sampler into the existing Multi-layer Sampler (MLS) technology as well as the analysis of the stability and performance of the incorporated systems in the *in-situ* speciation application.

Table of Contents

Chapter 1: Literature Review	1
1.1 Introduction	1
1.2 Environmental Problem	2
1.3 Chromium Chemistry	4
1.4 Chemical Speciation	10
1.5 Supported Liquid Membrane (SLM) Theory	12
1.6 Supported Liquid Membrane (SLM) Problems	19
1.7 Kinetics of Liquid-Liquid Extraction	24
1.8 Project Goals	26
1.9 References	26
Chapter 2: Design and Fabrication of a Sampling System Capable of Chemical Speciation of Chromium Ions in Groundwater	32
2.1 Introduction	32
2.2 Experimental	33
2.2.1 <i>Materials and Reagents</i>	33
2.2.2 <i>Sampler Design and Fabrication</i>	36
2.2.3 <i>Membrane Preparation</i>	37
2.2.4 <i>Sampler Preparation</i>	37
2.2.5 <i>Equipment</i>	38
2.2.6 <i>Sampler Validation</i>	38
2.2.7 <i>Sampler Performance Evaluation</i>	39
2.3 Results and Discussion	41
2.3.1 <i>Sampler Integrity</i>	41
2.3.2 <i>Uptake Studies of Individual Ions</i>	41
2.3.3 <i>Sampler Lifetime</i>	46
2.4 Summary	48
2.5 References	49
Chapter 3: Liquid-Liquid Extraction Studies for Determining Optimal Supported Liquid Membrane (SLM) Operating Parameters and Determining Cr Extraction Kinetics	50
3.1 Introduction	50
3.2 Parameter Optimization	53
3.2.1 <i>Experimental</i>	53
3.2.2 <i>Results and Discussion</i>	58
3.2.2.1 <i>Carrier Concentration Studies</i>	60
3.2.2.2 <i>Decanol Concentration Studies</i>	63
3.2.2.3 <i>Acceptor Phase Concentration Studies</i>	65

3.2.2.4 Selectivity Studies.....	68
3.3 Extraction Kinetics.....	69
3.3.1 <i>Experimental</i>	70
3.3.2 <i>Results and Discussion</i>	72
3.3.3 <i>Occam's Razor</i>	90
3.4 Summary.....	94
3.5 References.....	95

Chapter 4: Validation of the Supported Liquid Membrane (SLM) Based Samplers in Laboratory- Controlled and Simulated Natural Groundwater Conditions.....	98
4.1 Introduction.....	98
4.2 Experimental.....	98
4.2.1 <i>Cr (III) Uptake</i>	100
4.2.2 <i>Cr (VI) Uptake</i>	101
4.2.3 <i>Cr (III) Depletion</i>	101
4.2.4 <i>Cr (III) Depletion with EDTA</i>	102
4.2.5 <i>Cr (VI) Depletion</i>	102
4.2.6 <i>Cr (III) Uptake with no carrier</i>	102
4.2.7 <i>Cr (VI) Uptake with no carrier</i>	102
4.2.8 <i>Cr (III) Depletion with no carrier</i>	103
4.2.9 <i>Cr (III) Uptake – Selectivity</i>	103
4.2.10 <i>Cr (VI) Uptake – Selectivity</i>	103
4.2.11 <i>Cr (III) Depletion – Selectivity</i>	103
4.2.12 <i>Simulated Natural Sampling</i>	104
4.3 Results and Discussion.....	110
4.3.1 <i>Uptake</i>	111
4.3.1.1 <i>Cr (III)</i>	112
4.3.1.2 <i>Cr (VI)</i>	113
4.3.1.3 <i>Uptake Summary</i>	114
4.3.2 <i>Depletion</i>	115
4.3.2.1 <i>Cr (III) Depletion</i>	116
4.3.2.2 <i>Cr (VI) Depletion</i>	118
4.3.2.3 <i>Cr (III) Depletion with EDTA</i>	120
4.3.2.4 <i>Depletion Summary</i>	121
4.3.3 <i>No Carrier</i>	122
4.3.3.1 <i>Cr (III) Uptake</i>	124
4.3.3.2 <i>Cr (VI) Uptake</i>	125
4.3.3.3 <i>Cr (III) Depletion</i>	127
4.3.3.4 <i>No Carrier Summary</i>	129
4.3.4 <i>Selectivity</i>	129
4.3.4.1 <i>Cr (III) Uptake</i>	130
4.3.4.2 <i>Cr (VI) Uptake</i>	131
4.3.4.3 <i>Cr (III) Depletion</i>	133
4.3.4.4 <i>Selectivity Summary</i>	134
4.3.5 <i>Double Membrane</i>	135

4.3.5.3 Cr (III) Depletion	137
4.3.5.4 Double Membrane Summary	137
4.3.6 <i>Mixed Systems</i>	138
4.3.6.1 Mixed Systems Summary	139
4.3.7 <i>Simulated Natural Sampling</i>	139
4.3.7.1 Simulated Natural Cr Uptake	140
4.3.7.2 Elizabeth City Simulated Natural Sampling	140
4.3.7.3 Simulated Natural Systems Summary	142
4.4 Summary	142
4.4 References	143
Chapter 5: Summary and Potential Applications	144
5.1 Summary	144
5.2 Potential Applications	148

List of Figures

Figure 1.1. Dose-response curve for essential trace elements, including Cr.	6
Figure 1.2. A Pourbaix diagram of Cr species.	8
Figure 1.3. Illustration of the major redox pathways present in soil systems.	11
Figure 1.4. A diagram of the general transport mechanism for the extraction of Cr ions in a carrier-facilitated Supported Liquid Membrane (SLM) system.	14
Figure 1.5. (a) Structure of Aliquat-336 (tricaprylammonium chloride).	15
Figure 1.6. Diagram of the flux of Cr ions through the organic phase of a Supported Liquid Membrane (SLM) system.	17
Figure 2.1. (a) Structure of Aliquat-336 (tricaprylmethylammonium chloride). (b) Structure of D2EHPA (di-(2-ethylhexyl)phosphoric acid).	32
Figure 2.2. Drawing of an assembled Selective Ion Trap (SIT) sampler.	34
Figure 2.3. Photograph of the components (base plate and collection bottle) and dimensions of the Selective Ion Trap (SIT) sampler.	34
Figure 2.4. Photograph of Supported Liquid Membrane (SLM) samplers positioned in HDPE tank.	39
Figure 2.5. Uptake of Cr (III) and Cr (VI).	42
Figure 3.1. Equilibrium Cr (III) distribution as a function of D2EHPA (carrier) concentration.	62
Figure 3.2. Equilibrium Cr (VI) distribution as a function of Aliquat-336 (carrier) concentration.	63
Figure 3.3. Equilibrium Cr distribution as a function of decanol concentration.	65
Figure 3.4. Equilibrium Cr (III) distribution as a function of acceptor phase composition.	67
Figure 3.5. Equilibrium Cr (VI) distribution as a function of acceptor phase composition.	68
Figure 3.6. Equilibrium distribution of Cr in the organic carrier selectivity studies.	69
Figure 3.7. Photograph of the modified Lewis cell used in the Cr extraction kinetics studies.	71
Figure 3.8. Long-term (>1 day) Cr (III) and Cr (VI) liquid-liquid extraction (LLE). The dashed lines represent the half-life (τ) values for each extraction system.	72

Figure 3.9. Determination of reaction order with respect to initial Cr (III) concentration. Reaction Conditions: D2EHPA: 0.329 M, Decanol: 0.7865 M, pH = 5.25, $\Delta t = 4$ min.....	75
Figure 3.10. Determination of reaction order with respect to initial D2EHPA concentration. Reaction conditions: Cr (III): 0.0009616 M, Decanol: 0.7865 M, pH = 3.89, $\Delta t = 4$ min.	76
Figure 3.11. Determination of reaction order with respect to initial decanol concentration. Reaction conditions: Cr (III): 0.0009616 M, D2EHPA: 0.329 M, pH = 3.89, $\Delta t = 4$ min.	77
Figure 3.12. Determination of reaction order with respect to initial proton concentration. Reaction conditions: Cr (III): 0.0009616 M, D2EHPA: 0.329 M, Decanol: 0.7865 M, $\Delta t = 4$ min.	78
Figure 3.13. Determination of reaction order with respect to initial Cr (VI) concentration. Reaction conditions: Aliquat-336: 0.04392 M, Decanol: 1.0325 M, pH = 5.14, $\Delta t = 4$ min.	79
Figure 3.14. Determination of reaction order with respect to initial Aliquat-336 concentration. Reaction conditions: Cr (VI): 0.0009616 M, Decanol: 1.0325 M, pH = 5.14, $\Delta t = 4$ min.	80
Figure 3.15. Determination of reaction order with respect to initial decanol concentration. Reaction conditions: Cr (VI): 0.0009616 M, Aliquat-336: 0.04392 M, pH = 5.14, $\Delta t = 4$ min...	81
Figure 3.16. Determination of reaction order with respect to initial proton concentration. Reaction conditions: Cr (VI): 0.0009616 M, Aliquat-336: 0.04392 M, Decanol: 1.0325 M, $\Delta t = 4$ min.	82
Figure 3.17. Species distribution of Cr (III). The red vertical lines denote the pH range studied in the liquid-liquid extraction kinetics experiments.....	84
Figure 3.18. Species distribution of Cr (VI). The red vertical lines denote the pH range studied in the liquid-liquid extraction kinetics experiments.....	84
Figure 3.19. Overlay of extraction rate laws (equations 3.9 and 3.10) on experimental Cr liquid-liquid extraction.	86
Figure 3.20. Overlay of extraction rate laws (equations 3.9 and 3.10) on experimental sampler extraction data.....	87
Figure 3.21. Overlay of overall extraction rate laws with adjusted rate constants (equations 3.11 and 3.12) on experimental sampler extraction data.	89
Figure 3.22. Overlay of Occam's Razor extraction rate laws (equations 3.13 and 3.14) on experimental Cr liquid-liquid extraction kinetics data.....	91
Figure 3.23. Overlay of Occam's Razor extraction rate laws (equations 3.13 and 3.14) on experimental sampler extraction data.	92

Figure 3.24. Overlay of Occam’s Razor extraction rate laws (equations 3.15 and 3.16) on experimental sampler extraction data.	93
Figure 4.1. Photograph of SLM samplers positioned in HDPE tank.....	99
Figure 4.2. Graph of Cr uptake using the SLM-based sampling systems.....	112
Figure 4.3. Graph of Cr depletion using the SLM-based sampling systems.	116
Figure 4.4. Cr uptake with no carrier present in the organic phase.	123
Figure 4.5. Cr depletion with no carrier present in the organic phase.	124
Figure 4.6. Selectivity of organic carrier molecule as a function of Cr uptake.	130
Figure 4.7. Selectivity of Cr depletion.....	133
Figure 4.8. Comparison of double and single membrane depletion for Cr (III).....	136
Figure 4.9. Comparison of mixed and normal uptake for Cr (III) and Cr (VI).	138
Figure 4.10. Uptake of Cr (III) and Cr (VI) in Elizabeth City simulated groundwater sampling conditions.....	141

List of Tables

Table 2.1. Experimental conditions for Supported Liquid Membrane (SLM) tank studies.	40
Table 2.2. Cr (III) uptake data (units of ppm) with 95% confidence error.	43
Table 2.3. Cr (VI) uptake data (units of ppm) with 95% confidence error.	44
Table 2.4. Enrichment factors for Cr uptake.	45
Table 3.1. Experimental conditions for equilibrium carrier concentration studies.	54
Table 3.2. ICP-OES operating parameters for aqueous and organic samples.	55
Table 3.3. Experimental conditions for equilibrium decanol concentration studies.	56
Table 3.4. Experimental conditions for equilibrium selectivity studies.	57
Table 3.5. Experimental conditions for equilibrium acceptor phase studies.	58
Table 3.6. Legend information for liquid-liquid extraction (LLE) graphs.	59
Table 3.7. ICP-OES data for the equilibrium carrier concentration studies in units of micrograms (μg) and partition coefficient.	61
Table 3.8. ICP-OES data for the equilibrium decanol concentration studies in units of micrograms (μg) and partition coefficient.	64
Table 3.9. ICP-OES data for the equilibrium acceptor phase studies in units of (μg) and partition coefficient.	66
Table 3.10. ICP-OES data for the equilibrium carrier selectivity studies in units of micrograms (μg) and partition coefficient.	69
Table 3.11. Apparent reaction orders of Cr ^{+x} , carrier, decanol, and proton for Cr (III) and Cr (VI) as well as apparent rate constants determined by liquid-liquid extraction kinetics.	83
Table 4.1. Experimental conditions for SLM tank studies.	100
Table 4.2. Components and ppm concentrations of 30 groundwater sources found in the Appalachian Plateau region of West Virginia.	104
Table 4.3. Components of Appalachian Plateau simulated natural groundwater.	106

Table 4.4. Ionic composition and concentration of the simulated natural groundwater prepared for the simulated natural uptake studies. †The concentration of each component was compared to the data in Table 4.4. ‡The carbonate concentration was assumed to be approximately equal to the bicarbonate concentration presented in Table 4.4.....	107
Table 4.5. Components of Elizabeth City, NC simulated natural groundwater.	108
Table 4.6. Composition of modified Elizabeth City simulated natural groundwater.	109
Table 4.7. Data markers used in Chapter 4 graphs.	111
Table 4.8. Cr (III) uptake data (in units of ppm) with 95% confidence error (n = 5).....	113
Table 4.9. Cr (VI) uptake data (in units of ppm) with 95% confidence error (n = 5).....	114
Table 4.10. Normalized (against initial Cr (III) concentration) Cr (III) depletion data with 95% confidence error (n = 5).	117
Table 4.11. Normalized (against initial Cr (VI) concentration) Cr (VI) depletion data with 95% confidence error (n = 5).	119
Table 4.12. Normalized (against initial Cr (III) concentration) Cr (III)-EDTA depletion data with 95% confidence error (n = 5).	121
Table 4.13. Cr (III)-no carrier uptake data with 95% confidence error (n = 5).....	125
Table 4.14. Cr (VI)-no carrier uptake data with 95% confidence error (n = 5).....	126
Table 4.15. Cr (III)-no carrier depletion data with 95% confidence error (n = 5).....	128
Table 4.16. Cr (III)-selectivity uptake data with 95% confidence error (n = 5).....	131
Table 4.17. Cr (VI)-selectivity uptake data with 95% confidence error (n = 5).....	132
Table 4.18. Cr (III)-selectivity depletion data with 95% confidence error (n = 5).....	134
Table 4.19. Cr (III) double membrane depletion data with 95% confidence error (n = 5).....	137
Table 4.20. Mixed system uptake data with 95% confidence error (n = 5).....	139

Chapter 1

Literature Review

1.1 Introduction

Chromium contamination results from improper disposal of Cr-containing industrial waste and is one of the biggest environmental problems we face today. Although the disposal is regulated, various pathways exist for the transport of Cr into groundwater systems. Current methods used to assess Cr contamination in groundwater require the removal of a sample from the source and the subsequent analysis takes place away from the source. Furthermore, the analysis generally only takes into account the total Cr content of the sample. This approach is problematic due to the fact that Cr is among a variety of elements whose oxidation states display varying degrees of toxicity and mobility in natural systems (soil and water); Cr (VI) is toxic and relatively mobile, whereas Cr (III) is a non-toxic micronutrient and relatively non-mobile. Since toxicity, solubility, and mobility of Cr depend on the oxidation state, it is important for agencies overseeing human health to be able to differentiate between the states. This differentiation is achieved through the process of chemical speciation. However, when sampling from natural systems, chemical speciation is often difficult due to interconversion of the species during the time between collection and analysis. Therefore, there is a need for a sampling technique that is capable of collection, speciation, and storage. Thus, a new sampling system based on the SLM speciation technique has been designed to be used *in-situ* for the speciation of Cr ions in groundwater systems. The goal of this dissertation is to illustrate the fabrication, validation, and performance evaluation of the newly designed sampling system.

The SLM speciation technique has been shown in the literature to be an adequate method of differentiating Cr ions based on charge. However, these experiments are conducted as part of a clean-up procedure in the industrial process stream. The overall goal of the designed SLM

sampler is for the sampler to be incorporated into a multilayer sampler and be used for the *in-situ* speciation of Cr in groundwater systems.

The use of Supported Liquid Membranes (SLMs) in the chemical speciation of Cr ions presents a movement in the direction of improved collection and handling of environmental samples. The technique employs carriers that selectively extract either Cr (VI) or Cr (III) ions. Since the separated species are stored in different vessels, interconversion is not detrimental to the analysis. The total Cr content of each vessel can be analyzed to determine the distribution of Cr (VI) and Cr (III), and hence the risk to human health.

To date, the majority of work in SLM-based extraction focuses on adjusting experimental parameters to obtain more efficient extraction, rather than understanding the chemistry involved in the system and in turn developing new methods to enhance stability. Therefore, a kinetic approach was employed to gain a better understanding of the extraction processes that occur during SLM-based chemical speciation.

1.2 Environmental Problem

Over the past decade, the determination of Cr (III) and Cr (VI) in groundwater has become an increasingly important problem for environmental scientists.¹⁻⁵ The emergence of chromium in natural systems has been linked to improper disposal of industrial waste containing chromium.⁶ Cr is the second most abundant inorganic contaminant in the groundwater present beneath hazardous waste sites.⁷ The most common Cr compounds are chromate (CrO_4^{-2}), dichromate ($\text{Cr}_2\text{O}_7^{-2}$), chromium hydroxide ($\text{Cr}(\text{OH})_3$), and chromium dioxide (CrO_2).⁸

Environmental scientists have been struggling to adapt existing methods, as well as to create new techniques, that would permit the collection of the specific Cr ion of interest and also

permit the subsequent detection of this ion at trace to ultra-trace levels. The various forms of chromium display varying degrees of toxicity and mobility in natural systems. Generally, Cr (III) is essential⁹ and immobile in soil systems^{8,10} while Cr (VI) is toxic¹¹ and can be transported from soil systems to groundwater.¹⁰ Therefore, it is necessary to be able to distinguish between the various Cr species in order to know the extent of Cr contamination.

Some methods for assessing Cr contamination in groundwater sources are only designed to determine total Cr content. As mentioned above, the toxicity, solubility, and mobility depend on the oxidation state. While it is important to know total Cr content, techniques capable of determining the species distribution of Cr (III) and Cr (VI) provide a better assessment of the extent of Cr contamination. Current methods of Cr speciation in groundwater sources include capturing and removing a sample from its natural environment prior to speciation analysis. Since redox pathways exist that can facilitate the conversion of one species to another, the Cr species distribution can shift upon removal from the groundwater environment. Hence, an ideal sampling system for Cr contamination would be capable of *in-situ* speciation, as well as collection and storage of the speciated Cr ions. One technique that is capable of *in-situ* speciation is the Supported Liquid Membrane (SLM) extraction technique. The basics of the SLM technique and its role in sampler design which will be discussed briefly below and in more detail in Section 1.5.

The use of Supported Liquid Membranes (SLMs) has proven to be an adequate technique for the speciation of Cr. The theory of extraction in an SLM system is rooted in biochemistry, specifically in the area of cellular uptake/transport via biological membranes. Cells have specific transport mechanisms for various biologically relevant compounds. Facilitated pathways exist which use phosphate/sulfate carrier to selectively transport ions into and out of the cell. In these systems, the transport mechanism is preferential to certain molecules and discriminates all other

molecules. Accordingly, these transport systems move the target molecule into the cell and leave the non-specific molecules outside the cell. It is this specificity and selectivity that is desired for SLM extraction. Therefore, the SLM extraction of Cr ions is based on the anion exchange (phosphate/sulfate carrier) mechanism of biological membranes.¹²

1.3 Chromium Chemistry

Chromium (Cr) is a first row transition metal with the electron configuration $1s^2 2s^2 2p^6 3s^2 3p^6 4s^1 3d^5$. Due to the presence of the outer shell *s* and *d* electrons, the element has the ability to exist in a variety of oxidation states. The two thermodynamically favored oxidation states are +3 (trivalent) and +6 (hexavalent).¹³ The two states vary not only in their charge, but also in their reactivity and physiochemical properties.¹⁴ The most common hexavalent Cr compounds are the oxyanions chromate (CrO_4^{-2}) and dichromate ($\text{Cr}_2\text{O}_7^{-2}$), and the most common trivalent Cr compounds are chromium hydroxide ($\text{Cr}(\text{OH})_3$) and chromium dioxide (CrO_2).⁸ Of the two relevant oxidation states, Cr (III) is the most stable, due to the large amount of energy required for its oxidation.^{14,15} However, in natural systems, the oxidation of Cr (III) to Cr (VI) is possible via manganese (Mn) oxides.¹⁶⁻²⁰

Cr, in its various oxidation states, is found in the earth's crust as the sixth most abundant element and as the fifteenth most abundant element in sea water;⁹ there is no naturally occurring metallic chromium.⁶ The average concentration of Cr in the earth's crust is 200 ppm and the Cr concentration ranges from 1 to 2.5 ppb in sea water.²¹ The majority of Cr found in the environment is the result of anthropogenic activities,⁶ such as metallurgy,^{14,22} refractory,^{14,22} chemical manufacturing,^{10,14} mining,²³ smelting,²³ leather tanning,^{10,22} and electroplating.^{10,22,24} Accordingly, Cr is the second most abundant inorganic contaminant in the groundwater present beneath hazardous waste sites.⁷

Cr is an essential trace element necessary in sustaining human life.⁹ Cr is involved with two important metabolic pathways in the body: glucose and lipids.^{25,26} The specific role of Cr in the mechanisms of glucose and lipid metabolism has not been stated in the literature. However, the existence of the glucose tolerance factor has revealed that Cr (III) is involved with the metabolism of glucose. The glucose tolerance factor is a Cr (III) complex, which contains nicotinic and glutamic acids, glycine, and cysteine,²⁷ and is associated with insulin in the proper regulation of blood glucose levels.

Cr enters human cells via facilitated transporters. Wiegand studied the cellular transport of Cr.²⁸ The transport of hexavalent Cr into cells is facilitated by anion exchange carriers, such as phosphate or sulfate. Contrastingly, the entry of trivalent Cr into cells is via passive diffusion and phagocytosis, where the cell membrane deforms to encapsulate the molecule of interest. Additionally, the cellular uptake of Cr (III) is low.⁶ For orally ingested Cr (VI), the acidic nature of the stomach has the ability to reduce Cr (VI) to the less toxic and essential Cr (III).^{29,30} The *in vivo* reduction of hexavalent Cr to trivalent Cr has also been reported by De Flora^{30,31} and a step-wise mechanism for the reduction has been presented by Kasprzak.³² Furthermore, the reduction can be facilitated by glutathione in a non-enzymatic process,³³ or glutathione reductase in an enzymatic process.³⁴

In 1980, the United States National Academy of Sciences established a daily intake value of 50–200 μg ;²⁵ however, suggested intake values do not account for the specific form of Cr.⁶ The most important way for humans to obtain Cr is through the diet. Cr is found in foods, such as brown sugar, animal fats, and butter.³⁵ Water plays a slight, but important role in supplying Cr to the body. It has been estimated that one-sixth of the daily intake of Cr is from water.³⁶

However, the significance of water as a source of Cr has been disputed.⁹ The dose-response curve for Cr and other essential trace metals is U-shaped and is shown in Figure 1.1.

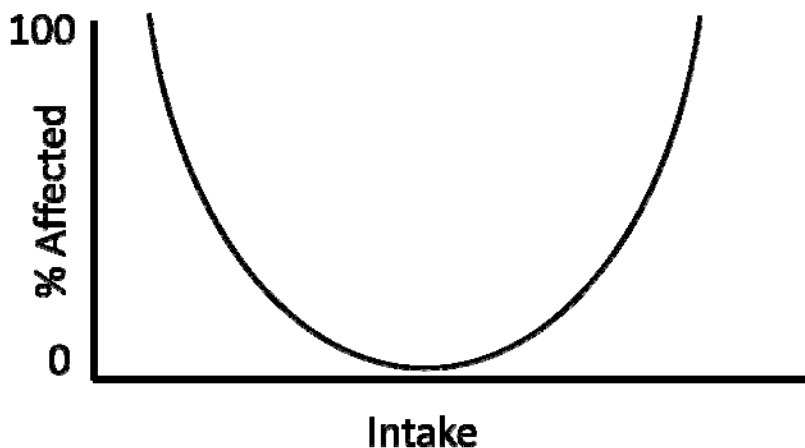


Figure 1.1. Dose-response curve for essential trace elements, including Cr.

Health problems arise if the amount of Cr in the body is outside the optimal range, which is represented as the portion of the curve located near the baseline in Figure 1.1. Below this range, signs of deficiency, which include impaired growth,^{9,15} pseudo diabetes,^{9,15} impaired fertility,¹⁵ protein-calorie malnutrition,¹⁵ and lifespan reduction in laboratory animals³⁸ are seen. Above the daily intake range, problems also occur. Too much Cr in the diet is associated with death.

Despite the necessity of Cr for biochemical processes, Cr is toxic. This is an irony that is common for essential trace elements. The toxic effects of Cr (VI) result from either inhalation or skin exposure.^{11,26} The symptoms of hexavalent Cr inhalation include nasal septum perforation,^{14,39,40} asthma,^{14,39} bronchitis,¹⁴ pneumonitis,¹⁴ liver and larynx inflammation,¹⁴ lung cancer,^{6,41,42} nasal cancer,⁶ rhinitis,⁴³ and a greater risk of bronchogenic carcinoma.¹⁴ Contact of Cr (VI) compounds with the skin produces skin allergies and dermatitis,^{44,45} as well as necrosis

and/or corrosion of the skin.²⁶ The danger of hexavalent Cr compounds lies in their strong oxidative potential.^{6,14,15} Despite lower toxicity of trivalent Cr compounds, there is still danger to the body when the Cr (III) concentration is too high. It has been observed that Cr (III) can coordinate organics which can inhibit the function of metallo-enzymes.¹⁴ It has been found that the oral toxicity of Cr (III) is low.⁶

Carcinogenicity is the ability of a substance to cause cancer. As with toxicity, Cr (VI) and Cr (III) display various levels of carcinogenicity. It has been shown that there is little or no evidence of trivalent Cr carcinogenicity.¹⁵ Of the hexavalent Cr compounds, the less soluble forms are the most carcinogenic, whereas there is less of a threat of cancer formation with the more soluble forms.¹⁵

Genotoxicity refers to the ability of a substance to cause damage to the DNA. Due to the fact that it takes a long time to accumulate enough DNA damage to form a tumor, a genotoxic substance may not be carcinogenic. Accordingly, a carcinogenic compound may not exhibit genotoxicity. The damage can result from either direct DNA interactions, such as the formation of covalent bonds, or interaction with processes that regulate DNA replication mechanisms, such as the inhibition of enzyme systems. The genotoxicity of Cr is connected to the solubility of the species. If the compound is not soluble, the bioavailability is reduced, which decreases the probability of the compound entering the body/cell and inducing DNA damage. The threat of genotoxicity of Cr-containing compounds, especially the hexavalent compounds, resides in the high oxidative potential. It has been reported that the genotoxic effects of Cr result after the reduction of Cr (VI) to Cr (III) inside the cell.¹⁵

Bioavailability refers to the potential of a compound to become part of biological pathways. The bioavailability of Cr is a function of the species distribution (Cr (III), Cr (VI)). Species distribution refers to how the various oxidation states are partitioned between the compounds associated with each oxidation state. The species distribution of Cr is shown in Figure 1.2. Typically for redox active elements, the species distribution is a function of the redox potential (E) and pH. The plot shown in Figure 1.2 is a Pourbaix diagram, which illustrates the speciation of Cr as a function of E and pH. The species that fall within the dashed lines in Figure 1.2, which indicates the environmentally-relevant pH range, are the Cr species that occur in natural systems.

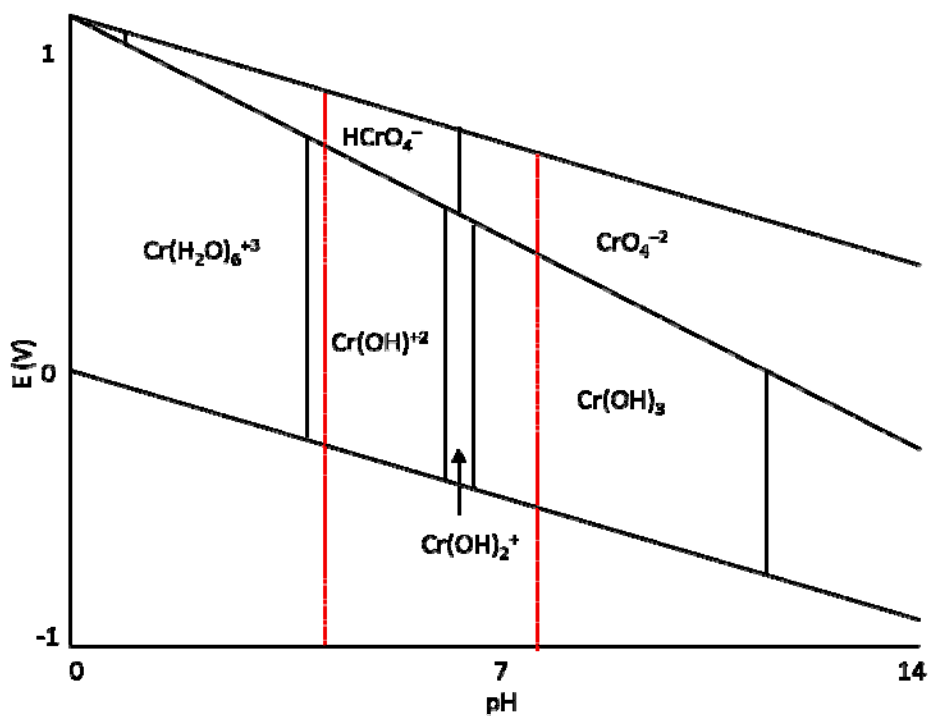


Figure 1.2. A Pourbaix diagram of Cr species.

As shown in Figure 1.2, the thermodynamically most stable forms of Cr in the environmentally-relevant pH range (4-9), which is given by the dashed vertical lines, include HCrO_4^- and CrO_4^{2-} for hexavalent Cr, and CrOH^{+2} , Cr(OH)_2^+ , and aqueous Cr(OH)_3 for trivalent

Cr. The empirical parameters used in the construction of the Pourbaix diagram include formation constants, acid/base equilibria, and redox equilibria. It should be noted that the Pourbaix diagrams are constructed using experimental results that are obtained in homogenous systems; the effects of naturally occurring ligands are not included in the diagrams. Therefore, the Pourbaix diagram is a useful tool in approximating the form of Cr in the environment, but it is not a complete picture of the speciation of Cr in natural systems.

Cr (III) has a large hydrolysis constant, K_{hyd} ($\text{p}K_{\text{hyd}} = 4.0$), which means that Cr (III) will hydrolyze as pH increases. When the pH exceeds 4.0, the Cr (III) will precipitate as $\text{Cr}(\text{OH})_3$.⁴⁶ In the presence of ferric iron (Fe (III)), hydrolysis is still observed and the result is the co-precipitation of Cr (III) with Fe (III) as $(\text{Cr}_x\text{Fe}_{1-x})(\text{OH})_3$.^{46,47} Cr (III) has low solubility in soil due to its precipitation⁴⁶ as $\text{Cr}(\text{OH})_3$ or co-precipitation with iron as $(\text{Cr}_x\text{Fe}_{1-x})(\text{OH})_3$.^{46,47} Complexation of Cr (III) with ligands present in the soil environment, such as humic acid, also renders Cr (III) insoluble.¹⁴ The ability of Cr (III) to complex with soil ligands in octahedral coordination is because Cr (III) functions as a hard Lewis acid.^{18,19} On the other hand, Cr (VI) is highly soluble in soil and natural waters.^{6,10} However, the Cr (VI) oxyanions can adsorb to the positively-charged surfaces of iron oxides in soil.

The transport of Cr in soils and natural waters also varies according to the solubility of the Cr ions. Since Cr (III) is insoluble in soil and natural waters due to its precipitation at environmentally-relevant pHs, trivalent Cr is immobilized as $\text{Cr}(\text{OH})_3$, $(\text{Cr}_x\text{Fe}_{1-x})(\text{OH})_3$ (in Fe (III)-containing environments),^{46,47} or as a complex with organic ligands.^{48,49} On the other hand, the oxyanions of Cr (VI) are soluble in soil and natural water systems and can be transported from the soil to water systems, as well as through water systems.

1.4 Chemical Speciation

Chemical speciation is the separation of various elements based on different physical properties, including oxidation state. As previously mentioned, it is imperative from an environmental or toxicological standpoint to be able to distinguish between various chemical forms. The scientific community is having difficulty assigning a thorough definition for chemical speciation that is acceptable to community.⁶ According to the First, Second, and Third Symposia on Speciation of Elements in Toxicology and Environmental and Biological Sciences, chemical speciation is the existence of distinguishable forms based on the state of the element (chemical, physical, or morphological).⁵⁰ The International Union of Pure and Applied Chemistry (IUPAC) defines chemical speciation as the distribution of the distinguishable elemental forms.⁵¹ While these definitions are a good start at providing a more unified understanding about chemical speciation, these definitions need further clarifications in order to accurately describe the specifics of chemical speciation.

Chemical speciation of Cr is necessary due to the existence of interconversion between the +3 and +6 states. The interconversion is possible because of redox pathways.^{22,52} Figure 1.3 shows the major redox pathways that exist in natural systems.

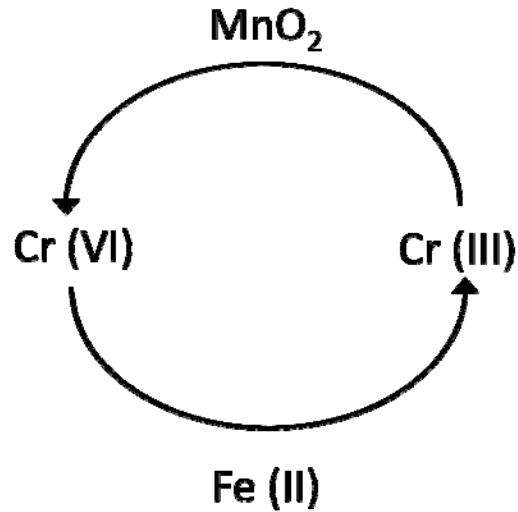


Figure 1.3. Illustration of the major redox pathways present in soil systems.

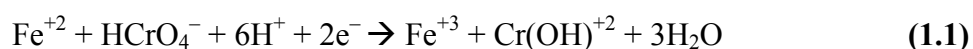
From an analytical viewpoint, the possibility of redox interconversion between Cr species makes representative sampling problematic. It is difficult to ascertain whether or not the collected sample accurately represents the species distribution at the time of collection. Examples of possible cause of interconversion of samples include chemical reactions, such as redox reactions or reactions between the container and analyte, temperature, pH, the presence of light.⁵³

Mn oxides play an important role in the redox chemistry of natural systems.¹⁶⁻²⁰ These oxides are ubiquitous in natural systems and reside on iron oxide surfaces and clay mineral surfaces.¹⁷ Due to their redox activity, Mn oxides contribute to the remobilization of Cr in natural systems.¹⁶ Remobilization occurs because the Mn oxides serve as oxidizing agents for the conversion of immobile Cr (III) to mobile Cr (VI) (oxidation).

Conversely, the organic matter found in natural systems is capable of reducing Cr (VI) to Cr (III). Like Mn oxides, organic matter is ubiquitous in natural systems. Organic matter

functions as a reducing agent by donating the electrons necessary for the reduction of the Cr (VI) species.⁵⁴ Some examples of the organic matter found in natural systems include humic substances, such as humic acids, fulvic acids, and humin, as well as non-humic substances, such as lipids, amino acids, carbohydrates, and other biochemical material.

Another source of redox activity in natural systems is ferrous iron (Fe (II)).⁵⁵ Compared to the Mn oxides, Fe (II) oxides are more abundant. Ferrous iron acts as a reducing agent and promotes the reduction of Cr (VI) to Cr (III) (see Equation 1.1).⁵⁶



Chemical speciation of Cr is important to the field of toxicology due to the various toxicological activities of Cr (III) and Cr (VI). Despite the observation that the toxicity of Cr varies with oxidation state, many regulations concerning human and environmental health deal only with total metal concentration.⁵⁷

1.5 Supported Liquid Membrane (SLM) Theory

The basis of SLM theory is rooted in biochemistry, specifically in the area of cellular uptake/transport via biological membranes. Cells have specific transport mechanisms for various biologically relevant compounds. Facilitated pathways exist that use phosphate/sulfate carriers to selectively transport ions into and out of the cell. In these systems, the transport mechanism is preferential to certain molecules and discriminates all other molecules. Accordingly, these transport systems move the target molecule into the cell and leave the non-specific molecules outside the cell. It is this specificity and selectivity that is desired for SLM extraction. Therefore, the SLM extraction of Cr ions is based on the anion exchange (phosphate/sulfate carrier) mechanism of biological membranes.¹²

SLMs have been studied since the late 1980s.⁵⁸ The first reported use of SLMs was in 1986 by Audunsson.⁵⁹ Since this time, interest in the study of SLMs has increased. The general theory of SLM extraction has been discussed in the literature by Jonsson⁶⁰ and will be presented below.

The basic components of a SLM system include a feed phase, an organic phase, and an acceptor phase. The system is fashioned like a sandwich. The feed phase (top layer) is aqueous and contains the analyte of interest. The organic phase (middle layer) includes a carrier dissolved in an organic solvent, which is impregnated on a membrane.⁶¹ The acceptor phase (bottom layer) is also aqueous and contains the strip solution, which promotes the transport of the analyte into the acceptor phase.

The membranes used in SLM extraction are porous and hydrophobic.^{58,62} The hydrophobic nature of the membranes maximizes the phase separation of the three liquid components. The types of membranes used are cellulose (acetate or nitrate), and Teflon[®] (PTFE; plain or polypropylene-backed). One disadvantage of the cellulose membranes is that these membranes are very fragile. It has been stated that PTFE membranes are slightly better than polypropylene⁶³ due to longer lifetimes.²⁴ However, the polypropylene backing tends to peel off of the Teflon[®] membranes. For this reason, the plain PTFE membranes are more robust.

The specific composition of the three phase system of SLMs varies based on the type of analyte to be extracted. The most common system is an aqueous/organic/aqueous system. The feed solution is aqueous and contains the analyte of interest, usually in a complex matrix. The membrane phase consists of the hydrophobic membrane, which functions as a support to hold the carrier/organic solution. The importance of the organic solvent has been stated in the literature.⁶⁴

However, there is no clear method described for choosing a solvent. It is not agreed upon in the literature whether one should choose a solvent based on polarity or on the idea of stability of the system vs. rapid transport of the analyte through the organic phase. The carrier provides selectivity to the SLM extraction. The carrier functions as the ion transporter which moves the specific form of Cr from the feed solution to the strip solution. Then, the strip solution meets the Cr ion at the membrane-strip interface and transports the Cr ion into the acceptor phase where it remains.

The mechanism of SLM extraction can be visualized as a revolving door process with the Cr ion being transported from the feed phase through the organic phase and a strip phase ion being counter-transported through the organic phase to the feed phase. The counter-transport mechanism is the driving force of the SLM process.⁵⁶ The general transport mechanism for Cr ions is shown in Figure 1.4.

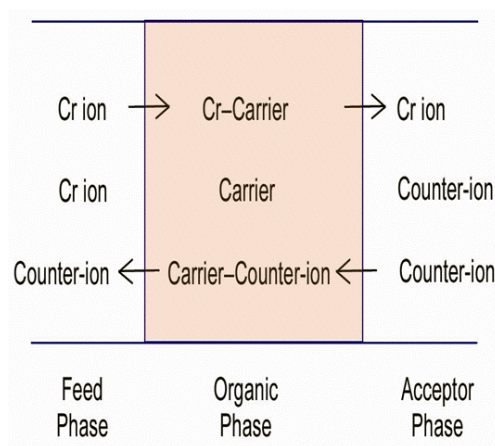
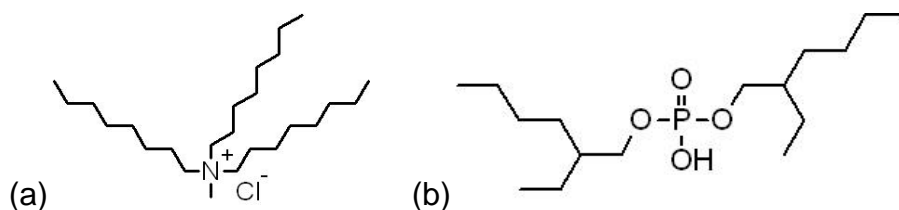


Figure 1.4. A diagram of the general transport mechanism for the extraction of Cr ions in a carrier-facilitated Supported Liquid Membrane (SLM) system.

The Cr ion starts on one side of the membrane, passes through the membrane, and remains on the other side. The specific Cr ion forms an ion-pair with the carrier at the feed-

organic interface, which is shown on the left side of Figure 1.4. The ion-pair moves through the organic phase to the organic-acceptor interface. Here, the carrier ion in the analyte-carrier pair is replaced with an ion from the strip solution. The new ion-pair moves into the acceptor phase, which is shown on the right side of Figure 1.4. The transported Cr ion will remain in the acceptor phase.

The chemistry of the Cr ion of interest influences the choice of carrier. The two common carriers for Cr are Aliquat-336 (tricaprylammonium chloride),^{23,56,65-68} which is selective of Cr (VI) over Cr (III), and D2EHPA (di-(2-ethylhexyl)phosphoric acid),^{23,69} which is selective of Cr (III) over Cr (VI). The structures of Aliquat-336 and D2EHPA are shown in Figure 1.5 (a) and Figure 1.5 (b), respectively.



**Figure 1.5. (a) Structure of Aliquat-336 (tricaprylammonium chloride).
(b) Structure of D2EHPA (di-(2-ethylhexyl)phosphoric acid).**

As shown in Figure 1.5(a), Aliquat-336 is a quaternary ammonium compound with low water solubility.⁵⁶ The positively charged carrier and the negatively charged Cr (VI) compounds (oxyanions) form an electrostatic ion-pair. This specific quaternary ammonium compound is selected for SLM extraction of Cr (VI) ions due to its excellent ion-pair forming stability.⁵⁶ On the other hand, D2EHPA (Figure 1.5(b)) is a neutral phosphoric acid compound which is deprotonated in the organic phase of the SLM system. Since the acid is deprotonated, the carrier has a negative charge which electrostatically attracts the positively charged trivalent Cr. The strip

solution used for Aliquat-336 extraction is NaCl, which exchanges Cl^- for the Cr oxyanion,⁵⁶ whereas the strip solution used for D2EHPA extraction is acidic, which provides H^+ for the exchange of the Cr (III) ion.

The driving force of the SLM process is the counter-transport of an acceptor phase ion. The counter-transport mechanism is based on molecular diffusion and the existence of a concentration gradient between the two aqueous phases. The counter-transport mechanism for Cr (VI) is based on the Cl^- concentration gradient between the feed and acceptor phases. The counter-transport for Cr (III) is based on the pH (or H^+ concentration) gradient between the feed and acceptor phases.

There are two transport steps involved in the SLM process: transport of the Cr ion from the feed phase to the acceptor phase and the counter-transport of an ion from the acceptor phase to the feed phase. The transport of Cr through SLMs is based on ion-pair formation between the analyte and the carrier, as well as counter-transport of an ion from the strip solution. The most common way of determining the analyte transport through the system is by using mass transfer.

Mass transfer is the transportation of an analyte along a concentration gradient. In the absence of flow, the mass transfer will be molecular in nature as opposed to convective, which is the type of mass transfer seen in flowing systems. Since the mass transfer is molecular in nature, the terms mass transfer and molecular diffusion are used interchangeably in non-flowing systems. Mass transfer in SLMs occurs in two distinct processes: one for the Cr ion and the second for the counter ion transport. The steps for Cr ion mass transfer are as follows: diffusion of the Cr ion through the feed solution and across the feed-organic interface, transport of the ion-pair through the organic phase and across the organic-acceptor interface, and diffusion of the Cr

ion through the acceptor solution. The mass transfer process for the counter-transport is similar. The steps are as follows: diffusion of the counter-transport ion through the acceptor phase and across the acceptor-organic interface, transport of the ion-pair (original carrier) through the organic phase and across the organic-feed interface, and diffusion of the counter-transport ion through the feed phase. The transport steps are described by the two-resistance theory, which was originally developed by Whitman in the 1920s.⁷⁰ Whitman's theory states that the transfer rate between the two adjacent phases (feed-organic and organic-acceptor) is governed by the diffusion rate and that there is no resistance to mass transfer from the interface of the two phases.⁷⁰ In SLM, there are two interfaces: the feed-organic interface and the organic-acceptor interface. Also, the membrane plays a role in the properties of the interface. The membranes must not provide resistance to mass transfer.

The classic definition of flux is a vector quantity that refers to the amount per unit time that passes through a given area. This area is defined to be normal to the flux vector. In the SLM process, flux is defined as the amount of Cr ion which passes through the organic phase per unit time and is depicted in Figure 1.6.

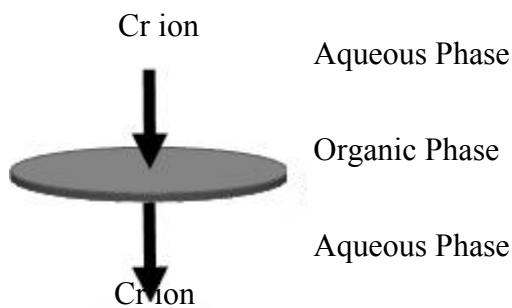


Figure 1.6. Diagram of the flux of Cr ions through the organic phase of a Supported Liquid Membrane (SLM) system.

Flux is dependent on the concentration gradient. The simplest mathematical representation of flux in a stagnant chemical system is described by de Groot⁷¹ (see Equation 1.2).

$$Flux = - \left(\begin{matrix} overall \\ density \end{matrix} \right) \left(\begin{matrix} diffusion \\ coefficient \end{matrix} \right) \left(\begin{matrix} concentration \\ gradient \end{matrix} \right) \quad (1.2)$$

or

$$J_{A,z} = -cD_{AB} \frac{dy_A}{dz} \quad (1.3)$$

Equation 1.3 describes the flux of analyte A in the z-direction, where c is the concentration, D_{AB} is the diffusion coefficient for analyte A through B, and $\frac{dy_A}{dz}$ is the concentration gradient of A in the z-direction. In the SLM system, the z-direction is taken to be through the organic phase. For the SLM process, the flux depends on the concentration of Cr ions in the feed solution, the pH of the feed solution, as well as the concentration of the carrier in the organic phase.⁷²

There are a variety of applications of SLM extraction of Cr ions presented in the literature. These applications include the determination of Cr in urine,²³ as well as effluent treatment,⁷³ trace metal enrichment,^{74,75} and ion-selective electrodes.⁷⁶

The use of SLMs for the extraction of Cr ions has several advantages. The selectivity of this technique is one of the greatest advantages.^{12,61} The choice of carrier influences the type of analyte that will be extracted. Therefore, the carrier is responsible for the selectivity in an SLM system. Sample enrichment is important due to the fact that Cr may exist in trace amount in environmental samples.⁶¹ The process of enrichment occurs if the acceptor phase is stagnant or non-flowing.⁶⁰ Since the total volume of the acceptor phase is constant and the amount of Cr ion

in the phase increases, the concentration of Cr ion in the acceptor phase can surpass the amount in the original feed solution. This process is known as enrichment. Enrichment allows for the progression from trace amounts of Cr to detectable amounts. Enrichment factors are easily calculated and the relationship between initial concentration and enrichment is straightforward.⁷⁷ Equation 1.4 shows the dependence of the enrichment factor (E_e) on the concentrations of the feed (c_F) and acceptor (c_A) phases.

$$E_e = \frac{c_A}{c_F} \quad (1.4)$$

Under non-flowing conditions and non-replenishment of the feed phase, the concentration of Cr in the feed phase decreases with time, while the concentration of Cr in the acceptor phase increase with time. Thus, the enrichment increases. Another advantage of the SLM technique is the reduction in solvent use. Compared to conventional solvent extraction, the volume of solvent used is minimal.^{61,78}

1.6 Supported Liquid Membrane (SLM) Problems

Despite the advantages presented above, the SLM extraction technique is plagued by its disadvantages. The most notable disadvantage is instability. There have been a variety of mechanisms proposed in the literature to attempt to explain the cause of membrane instability.^{12,58,64} The possible causes of instability are the existence of a pressure difference across the membrane, the solubility of the organic phase in the aqueous phase (feed and/or acceptor), pore wetting, pore blocking, the existence of an osmotic pressure difference across the membrane, and emulsion formation.

Danesi⁷⁹ and Takeuchi⁸⁰ have independently investigated the effects of a pressure gradient on membrane stability in flowing systems. However, Neplenbroek found that membrane

instability still occurs in the absence of a pressure gradient.⁸¹ Working independently, Lamb⁸² and Deblay⁸³ found that there is an inversely proportional relationship between solubility and membrane stability. Along the same lines, Dozol reported the relationship between aqueous solubility of the solvent and membrane lifetime.⁸⁴

First proposed by Danesi,⁷⁹ then clarified by Takeuchi,^{85,86} pore wetting refers to the replacement of the organic phase in the membrane by the aqueous phase (feed and/or acceptor). The interfacial tension of an aqueous droplet on the membrane surface is key to the understanding of the pore wetting mechanism. Once the interfacial tension falls below a critical value, the droplet will displace the organic phase present in the membrane pore. Hence the term pore wetting. An indicator of pore wetting is that the organic phase lost should have the same composition as the remaining organic phase. Again, Neplenbroek disputes the validity of the pore wetting mechanism as the main contributor to membrane stability in that the composition of the lost and remaining phases is different.⁸¹ Pore blocking refers to carrier precipitation or the presence of water in the membrane pores.⁶⁴ The effects of water present in the membrane are similar to those in the pore wetting mechanism.

In the area of carrier precipitation in the membrane pores, Belfer⁸⁷ and Chiarizia^{88,89} have studied this mechanism for SLM instability. The precipitation of the carrier in the pores decreases the rate of permeability through the membrane, which decreases the flux of the system. Research in the area of osmotic pressure has been conducted by Fabiani⁹⁰ and Danesi.⁹¹ Fabiani found that water transport through the membrane increased as the osmotic pressure across the membrane increases, and concluded that the organic phase is lost from the membrane because the water is dragging the organic phase out of the pores.⁹⁰ Danesi

investigated salt permeability in addition to water transport and concurs that the organic phase is removed by the transported water.⁹¹

Finally, the emulsion formation mechanism for membrane instability was investigated initially by Neplenbroek^{92,93} and Zha⁹⁴⁻⁹⁶ provided an extension of Neplenbroek's work through a series of papers. Both authors have determined that there is a relationship between SLM instability and emulsion formation stability. As more stable emulsions are formed, the instability of the SLM system increases. Thermodynamics indicates that emulsions are unstable,⁶⁴ which means that an energy source must be present in order to produce more stable emulsions. A higher flow rate provides enough energy to the system to stabilize emulsion formation in that the probability of forming emulsions increases with increasing flow rate.⁶⁴

All of the proposed mechanisms for SLM instability deal with the loss of the organic phase from the system. Therefore, the main contributor to the instability of SLMs is the loss of organic phase.^{58,64} In this mechanism, the volume of the organic phase is decreased either due to the solubility of the organic phase in either aqueous phase or the emulsification of the organic phase as a result of shear forces.^{58,64,92} Recently, one group has ruled out organic phase solubility as a loss mechanism.⁹² This was achieved by observing a similar level of instability from two organic systems with varying degrees of solubility in the aqueous phases.

A second disadvantage of the SLM technique is membrane lifetime, which is a direct consequence of membrane instability. The lifetimes tend to be short and limited, as well as inconsistent.^{12,58} Membrane lifetime and instability are related inversely: as instability increases, the lifetime decreases. When the lifetime of the membrane is reached, the system breaks down. One major sign of system breakdown is the loss of selectivity, which is observed as the

establishment of direct channels through the organic phase which allows for the transport of all of the components in the feed solution. The loss of organic phase results in the ability to establish direct channels through the organic phase. As the organic phase is removed from the system, there is less volume available to cover the porous membrane. Therefore, there is a greater probability of the aqueous phases contacting the membrane and the contents of the aqueous phase to pass through the membrane pores. It has been suggested that several parameters can be modified to increase membrane lifetime: pore size, hydrophobicity, solubility, and shear forces.^{58,64} It is recommended to use highly hydrophobic membranes that have smaller pore sizes. The more hydrophobic the membrane, the less likely channeling will occur. Smaller pore sizes are recommended due to the inverse relationship between stability and the size of the membrane pore. Also, the organic solvent should have low solubility in water and vice-versa.⁶⁴ The concept of low solubility helps to reduce loss of organic phase. Finally, shear forces should be minimized, which is accomplished by decreasing flow rates in flowing systems or eliminating the flowing component (stagnant phases).⁹² The reduction of shear forces also reduces the loss of organic phase.

The number of parameters and the need to optimize each parameter adds to the list of SLM disadvantages. The parameter optimization process is time-consuming and each set of parameters is unique for each SLM system.¹² Both the pH and ionic strength must be optimized for both the feed and acceptor phases.⁷⁷ It has been discovered that the use of high ionic strengths suppresses emulsion formation, which increases membrane stability.⁹² The pH of the system is important from the aspect of analyte precipitation (Cr (III)) in the feed phase and the establishment of an H^+ concentration gradient across the organic phase when acidic carriers, such

as D2EHPA, are used. The concentration of the acceptor phase must be optimized so that leaching of the carrier from the organic phase is not induced.⁵⁶

The carrier concentration affects the efficiency of the process. According to Choi and Moon, higher concentrations of Aliquat-336 produce stronger bonding in the carrier-Cr (VI) ion pair.⁵⁶ When this occurs, the extraction time increases as a result of slower stripping rates. The carrier itself must be specific to the desired form of Cr. The solvent must be non-viscous and have low water solubility. The solvent also influences the transfer rate and thus the efficiency with respect to time. Also, the type of membrane used influences the transfer rate and the efficiency of the system.^{20,77} Furthermore, membrane preparation is a parameter that affects SLM instability and lifetime. Membrane preparation deals with how the membrane is treated following removal from the carrier/organic solution. In the wet preparation method, the excess liquid is removed from the membrane surface by gently blotting both sides with a laboratory tissue. This is the most common method found in the literature. However, not all preparation methods are explicit in the literature. On the other hand, the dry preparation method is the same as the wet method except the wet membrane is allowed to air dry for 30 minutes.⁹⁷ It was concluded that the dry membrane preparation method produces more stable membranes due to the observation that the loss of organic phase is less for the dry membranes.⁹⁷

The affect of interfering ions must be determined. In a recent study of Cr (VI) SLM extraction, Choi and Moon examine cations and anions that could interfere with the process.⁵⁶ The cations investigated were Cr (III), Fe (II & III), Al (III), Mg (II), Ni (II), Cu (II), and Pb (II) in the form of chloride salts, and the anions investigated were SO_4^{-2} , NO_3^- , NO_2^- , and Cl^- in the form of potassium salts. The presence of interfering ions decreases the efficiency of the SLM process. The flux and recovery of Cr (VI) decreases when Pb (II) is present due to the formation

of the PbCrO_4 species.⁵⁶ Recovery decreases when all anions studied are present at 100 times the concentration of Cr (VI), with the exception of NO_2^- and NO_3^- , which affects the recovery when present at 10 times the concentration of Cr (VI).⁵⁶

1.7 Kinetics of Liquid-Liquid Extraction

An understanding of solvent extraction processes using liquid ion exchangers is useful when thinking about the LLE processes involved in the SLM system. The carrier molecule functions as a liquid ion exchanger. Specifically, the liquid ion exchanger can be a cation or anion exchanger depending on which Cr species is studied. Historically, liquid ion exchangers have been used in a variety of applications, such as industrial waste treatment tasks which focus on reagent recycling.^{98,99,98} LLE with liquid ion exchangers have proved to be a useful technique for a number of reasons. This technique is capable of reaching equilibria in a matter of seconds as well as separating very small amounts (μg) of reagent. However, the key benefit that makes the SLM process attractive for the speciation of Cr ions is the fact that LLE with liquid ion exchangers is capable of separating elements in different oxidation states (SES with LIEs).

The driving force of the LLE with liquid ion exchangers technique is the formation of an ion-pair or uncharged complex that is extractable into the organic phase.¹⁰⁰ The ion-pair formation is thought to occur in the interfacial region between the aqueous and organic phases.¹⁰⁰ The interfacial chemistry has been studied in these systems has been studied by Watarai et al.¹⁰¹ This group has used fluorescence and Raman techniques to study the interfacial species. The results of these experiments have determined that molecular recognition of the ion of interest is achieved through carrier aggregation and that the ion-pairing reaction rate at the interface is rapid.

Lewis cell experiments have been conducted in the literature on a variety of LLE systems to determine the reaction order of various LLE components. However, these works focus on the

extraction of metal ions from various media, such as those found in industrial wastewater treatment. It has been shown that the reaction orders, rate constants, and overall rate laws differ based on the extraction conditions. Although these studies differ on some results, the majority agree on reaction order with respect to carrier concentration. The LLE parameters that were investigated in the literature include pH, carrier concentration, and Cr concentration. Given the fact that decanol is necessary for the prevention of third phase formation, it was proposed in this work that the decanol concentration plays a role in the rate of reaction. Therefore, the Lewis cell studies conducted in this work are similar to those conducted in the literature with the addition of a decanol study.

The method of initial rates was employed in the treatment of the Lewis cell data. In this method, the extraction rate can be expressed as

$$rate = -\left(\frac{d[Cr]}{dt}\right)_o = k_f [Cr]^a [H^+]^b [Carrier]^c [Decanol]^d \quad (1.5)$$

By taking the log of both sides, we have

$$\log rate = \log k_f + a \log [Cr] + b \log [H^+] + c \log [Carrier] + d \log [Decanol] \quad (1.6)$$

When 3 of the 4 components on the right hand side of equation 1.6 are held constant, the log vs. log plot should produce a line with slope equal to the reaction order and y-intercept equal to the sum of log k_f and the constant log values of the other parameters. Once all reaction orders have been determined, the value of k_f can be found.

A model can be developed using the rate laws obtained from the method of initial rates analysis. This model can be used to predict the extraction of Cr from the SLM-based sampler.

1.8 Project Goals

The goals of this project are as follows:

1. Design and fabricate a sampler based on the SLM extraction technique that is capable of the *in-situ* speciation of Cr ions.
2. Validate the structural integrity of the sampling systems to ensure that the assembled samplers are free of leaks that would be detrimental to their use.
3. Determine the optimized operating parameters of the SLM systems using classic liquid-liquid extraction (LLE) studies.
4. Evaluate the LLE kinetics and develop a kinetic model to predict sampler-based extraction.
5. Evaluate the performance of the samplers in tank studies that aid in the validation of proper SLM function.

1.9 References

- (1) Kozuh, N.; Stupar, J.; Gorenc, B. *Environ. Sci. Technol.* **1999**, *34*, 112.
- (2) Wittbrodt, P. R.; Palmer, C. D. *Environ. Sci. Technol.* **1996**, *30*, 2470.
- (3) Abu-Saba, K. E.; Flegal, A. R. *Environ. Sci. Technol.* **1997**, *31*, 3455.
- (4) Buerge, I. J.; Hug, S. J. *Environ. Sci. Technol.* **1997**, *31*, 1426.
- (5) Jardine, P. M.; Fendorf, S. E.; Mayes, M. A.; Larsen, I. L.; Brooks, S. C.; Bailey, W. B. *Environ. Sci. Technol.* **1999**, *33*, 2939.
- (6) Yokel, R. J. *Toxicol. Environ. Health, Part B* **2006**, *9*, 63.
- (7) Baird, C.; Cann, M. *Environmental Chemistry*; 3rd ed.; W. H. Freeman and Company: New York, 2005.
- (8) Bartlett, R. J.; Kimble, J. M. *J. Environ. Qual.* **1976**, *5*, 379.

- (9) Mertz, W. *Phys. Rev.* **1969**, *49*, 163.
- (10) Richard, F. C.; Bourg, A. C. M. *Water Res.* **1991**, *25*, 807.
- (11) *Biological and environmental aspects of chromium*; Langård, S., Ed.; Elsevier Biomedical Press: Amsterdam, 1982; Vol. 5.
- (12) Franken, T. *Membr. Technol.* **1997**, *1997*, 6.
- (13) Elderfield, H. *Earth Planet. Sci. Lett.* **1970**, *9*, 10.
- (14) Kotas, J.; Stasicka, Z. *Environ. Pollut.* **2000**, *107*, 263.
- (15) Katz, S. A.; Salem, H. *J. Appl. Toxicol.* **1993**, *13*, 217.
- (16) Schroeder, D. C.; Lee, G. F. *Water, Air, Soil Pollut.* **1975**, *4*, 355.
- (17) Bartlett, R.; James, B. *J. Environ. Qual.* **1979**, *8*, 31.
- (18) Nakayama, E.; Kuwamoto, T.; Tsurubo, S.; Fujinaga, T. *Anal. Chim. Acta* **1981**, *130*, 401.
- (19) Saleh, F. Y.; Parkerton, T. F.; Lewis, R. V.; Huang, J. H.; Dickson, K. L. *Sci. Total Environ.* **1989**, *86*, 25.
- (20) Johnson, C. A.; Xyla, A. G. *Geochim. Cosmochim. Acta* **1991**, *55*, 2861.
- (21) Love, A. G. H. In *Chromium: Metabolism and Toxicity*; Burrows, D., Ed.; CRC Press Inc. : Boca Raton, 1983, p 3.
- (22) Bartlett, R. J.; James, B. R. In *Chromium in the Natural and Human Environment*; Niragu, J., Nieboer, E., Eds.; John Wiley & Sons: New York, 1988, p 267.
- (23) Soko, L.; Cukrowska, E.; Chimuka, L. *Anal. Chim. Acta* **2002**, *474*, 59.
- (24) Yang, X. J.; Fane, A. G.; MacNaughton, S. *Water Sci. Technol.* **2001**, *43*, 341.
- (25) Anderson, R. A. *Sci. Total Environ.* **1989**, *86*, 75.
- (26) Gad, S. C. *Sci. Total Environ.* **1989**, *86*, 149.
- (27) Nieboer, E.; Jusys, A. A. E. In *Chromium in Natural and Human Environments*; Nriagu, J. O., Nieboer, E., Eds.; Wiley Interscience: New York, 1988, p 21.
- (28) Wiegand, H. J.; Ottenwalder, H.; Bolt, H. M. *Arch. Toxicol.* **1985**, *57*, 31.
- (29) Finley, B. L.; Kerger, B. D.; Katona, M. W.; Gargas, M. L.; Corbett, G. C.; Paustenbach, D. J. *Toxicol. Appl. Pharmacol.* **1997**, *142*, 151.

- (30) Deflora, S.; Badolati, G. S.; Serra, D.; Picciotto, A.; Magnolia, M. R.; Savarino, V. *Mutat. Res.* **1987**, *192*, 169.
- (31) Deflora, S.; Serra, D.; Camoirano, A.; Znacchi, P. *Biol. Trace Elem. Res.* **1989**, *21*, 179.
- (32) Kasprzak, K. S. *Chem. Res. Toxicol.* **1991**, *4*, 604.
- (33) Kortenkamp, A.; Ozolins, Z.; Beyersmann, D.; Obrien, P. *Mutat. Res.* **1989**, *216*, 19.
- (34) Gunaratnam, M.; Grant, M. H. *Chem.-Biol. Interact.* **2001**, *134*, 191.
- (35) *Chromium: Metabolism and Toxicity*; Burrows, D., Ed.; CRC Press, Inc.: Boca Raton, 1983.
- (36) Hammond, P. B.; Beliles, R. P. In *Toxicology: The Basic Science of Poisons*; 2nd ed.; Doull, J., Klaassen, C. D., Amdur, M. O., Eds.; Macmillan: New York, 1980, p 409.
- (37) Olin, S. S. *J. Nutr.* **1998**, *128*, 364S.
- (38) Schroeder, H. A.; Vinton, W. H.; Balassa, J. J. *J. Nutr.* **1963**, *80*, 39.
- (39) Feron, V. J.; Arts, J. H. E.; Kuper, C. F.; Slootweg, P. J.; Woutersen, R. A. *Crit. Rev. Toxicol.* **2001**, *31*, 313.
- (40) MacKenzie, J. N. *JAMA* **1884**, *3*, 601.
- (41) Baetjer, A. M. *Arch. Ind. Hyg. Occup. Med.* **1950**, *2*, 505.
- (42) Gross, E.; Kosch *Arch. Gewerbepathol. Gewerbehyg.* **1943**, *112*, 164.
- (43) Sunderman, F. W. *Ann. Clin. Lab. Sci.* **2001**, *31*, 3.
- (44) Cumin, W. *Edinburgh Med. Surg. J.* **1827**, *28*, 295.
- (45) Parkhurst, H. J. *Arch. Dermatol. Syphilol.* **1925**, *12*, 253.
- (46) Sass, B. M.; Rai, D. *Inorg. Chem.* **1987**, *26*, 2228.
- (47) Bartlett, R. J.; Kimble, J. M. *J. Environ. Qual.* **1976**, *5*, 383.
- (48) Stumm, W.; Morgan, J. J. *Aquatic Chemistry*; Wiley Interscience: New York, 1996.
- (49) Johnson, C. A.; Sigg, L.; Lindauer, U. *Limnol. Oceanogr.* **1992**, *37*, 315.
- (50) Nieboer, E.; Fletcher, G. G.; Thomassen, Y. J. *J. Environ. Monit.* **1999**, *1*, 1.
- (51) Templeton, D. M.; Ariese, F.; Cornelis, R.; Danielsson, L. G.; Muntau, H.; Van Leeuwen, H. P.; Lobinski, R. *Pure Appl. Chem.* **2000**, *72*, 1453.

- (52) Seigneur, C.; Constantinou, E. *Environ. Sci. Technol.* **1995**, *29*, 222.
- (53) Gomez Ariza, J. L.; Morales, E.; Sanchez-Rodas, D.; Giraldez, I. *Trends Anal. Chem.* **2000**, *19*, 200.
- (54) Stollenwerk, K. G.; Grove, D. B. *J. Environ. Qual.* **1985**, *14*, 396.
- (55) Lin, C. J. *Water, Air, Soil Pollut.* **2002**, *139*, 137.
- (56) Choi, Y.-W.; Moon, S.-H. *Sep. Sci. Technol.* **2004**, *39*, 1663.
- (57) Larsen, E. K.; Berg, T. In *Trace Element Speciation for Environment, Food and Health*; Ebdon, L., Pitts, L., Cornelis, R., Crews, H., Donard, O. F. X., Quevauviller, P., Eds.; Royal Society of Chemistry: Cambridge, 2001, p 251.
- (58) Yang, X. J.; Fane, A. G.; Soldenhoff, K. *Ind. Eng. Chem. Res.* **2003**, *42*, 392.
- (59) Audunsson, G. *Anal. Chem.* **1986**, *58*, 2714.
- (60) Jonsson, J. A.; Lovkvist, P.; Audunsson, G. *Anal. Chim. Acta* **1993**, *277*, 9.
- (61) Jonsson, J. A.; Mathiasson, L. *Trends Anal. Chem.* **1999**, *18*, 318.
- (62) Zha, F. F.; Fane, A. G.; Fell, C. J. D. *Ind. Eng. Chem. Res.* **1995**, *34*, 1799.
- (63) Jonsson, J. A.; Mathiasson, L. *Trends Anal. Chem.* **1999**, *18*, 325.
- (64) Kemperman, A. J. B.; Bargeman, D.; van den Boomgaard, T.; Strathmann, H. *Sep. Sci. Technol.* **1996**, *31*, 2733.
- (65) Alguacil, F. J.; Caravaca, C.; Martin, M. I. *J. Chem. Technol. Biotechnol.* **2003**, *78*, 1048.
- (66) Alonso, A. I.; Pantelides, C. C. *J. Membr. Sci.* **1996**, *110*, 151.
- (67) Alonso, A. I.; Urriaga, A. M.; Irabien, A.; Ortiz, M. I. *Chem. Eng. Sci.* **1994**, *49*, 901.
- (68) Castillo, E.; Granados, M.; Cortina, J. L. *Anal. Chim. Acta* **2002**, *464*, 197.
- (69) Buonomenna, M. G.; Oranges, T.; Molinari, R.; Drioli, E. *Water Environ. Res.* **2006**, *78*, 69.
- (70) Whitman, W. G. *Chem. Met. Eng.* **1923**, *29*, 146.
- (71) de Groot, S. R. *Thermodynamics of Irreversible Processes*; North-Holland: Amsterdam, 1951.
- (72) Huang, T. C.; Huang, C. C.; Chen, D. H. *Sep. Sci. Technol.* **1998**, *33*, 1919.

- (73) Chaudry, M. A.; Ahmad, S.; Malik, M. T. *Waste Manage.* **1998**, *17*, 211.
- (74) Papantoni, M.; Djane, N. K.; Ndungu, K.; Jonsson, J. A.; Mathiasson, L. *Analyst* **1995**, *120*, 1471.
- (75) Malcus, F.; Djane, N. K.; Mathiasson, L.; Johansson, G. *Anal. Chim. Acta* **1996**, *327*, 295.
- (76) Choi, Y. W.; Moon, S. H. *Environ. Monit. Assess.* **2001**, *70*, 167.
- (77) Chimuka, L.; Megersa, N.; Jonsson, J. A. *Anal. Chem.* **1998**, *70*, 3906.
- (78) Venkateswaran, P.; Palanivelu, K. *Hydrometallurgy* **2005**, *78*, 107.
- (79) Danesi, P. R. *Sep. Sci. Technol.* **1984**, *19*, 857.
- (80) Takeuchi, H.; Takahashi, K.; Goto, W. *J. Membr. Sci.* **1987**, *34*, 19.
- (81) Neplenbroek, A. M.; Bargeman, D.; Smolders, C. A. *J. Membr. Sci.* **1992**, *67*, 121.
- (82) Lamb, J. D.; Bruening, R. L.; Izatt, R. M.; Hirashima, Y.; Tse, P. K.; Christensen, J. J. *J. Membr. Sci.* **1988**, *37*, 13.
- (83) Deblay, P.; Delepine, S.; Minier, M.; Renon, H. *Sep. Sci. Technol.* **1991**, *26*, 97.
- (84) Dozol, J. F.; Casas, J.; Sastre, A. *J. Membr. Sci.* **1993**, *82*, 237.
- (85) Takahashi, K.; Takeuchi, H. *J. Chem. Eng. Jpn.* **1985**, *18*, 205.
- (86) Takeuchi, H.; Nakano, M. *J. Membr. Sci.* **1989**, *42*, 183.
- (87) Belfer, S.; Binman, S.; Lati, Y.; Zolotov, S. *J. Appl. Polym. Sci.* **1990**, *40*, 2073.
- (88) Chiarizia, R. *J. Membr. Sci.* **1991**, *55*, 65.
- (89) Chiarizia, R. *J. Membr. Sci.* **1991**, *55*, 39.
- (90) Fabiani, C.; Merigiola, M.; Scibona, G.; Castagnola, A. M. *J. Membr. Sci.* **1987**, *30*, 97.
- (91) Danesi, P. R.; Reichleyyinger, L.; Rickert, P. G. *J. Membr. Sci.* **1987**, *31*, 117.
- (92) Neplenbroek, A. M.; Bargeman, D.; Smoulders, C. A. *J. Membr. Sci.* **1992**, *67*, 133.
- (93) Neplenbroek, A. M.; Bargeman, D.; Smolders, C. A. *Desalination* **1990**, *79*, 303.
- (94) Zha, F. F.; Fane, A. G.; Fell, C. J. D. *J. Membr. Sci.* **1995**, *107*, 59.
- (95) Zha, F. F.; Coster, H. G. L.; Fane, A. G. *J. Membr. Sci.* **1994**, *93*, 255.

- (96) Zha, F. F.; Fane, A. G.; Fell, C. J. D. *J. Membr. Sci.* **1995**, *107*, 75.
- (97) Yang, X. J.; Fane, T. *J. Membr. Sci.* **1997**, *133*, 269.
- (98) De, A. K.; Khopkar, S. M.; Chalmers, R. A. *Solvent Extraction of Metals*; Van Nostrand Reinhold: London, 1970.
- (99) Marcus, Y.; Kertes, A. S. *Ion exchange and solvent extraction of metal complexes*; Wiley-Interscience, 1969.
- (100) Khopkar, S. M. *Solvent Extraction Separation of Elements with Liquid Ion Exchangers*; New Age Science Limited Tunbridge Wells, UK, 2009.
- (101) Watarai, H.; Tsukahara, S.; Nagatani, H.; Ohashi, A. *B. Chem. Soc. Jpn* **2003**, *76*, 1471.

Chapter 2

Design and Fabrication of a Sampling System Capable of Chemical Speciation of Chromium Ions in Groundwater

2.1 Introduction

The sampler designed in this work is termed a Selective Ion Trap (SIT). The SIT is capable of in-situ chemical speciation of Cr ions as well as preservation of the speciated ions. The SITs are fashioned to fit within existing dialysis-based samplers (Multi-Layer sampler, MLS).^{1,2} The sampling system is based on the supported liquid membrane (SLM) extraction technique. In the SLM technique, a carrier molecule (liquid ion exchanger) is used to selectively transport Cr ions across a membrane into a collection bottle. Tricaprylmethylammonium chloride (Aliquat-336) or di-(2-ethylhexyl) phosphoric acid (D2EHPA) is used for the selective extraction and enrichment of the anionic Cr (VI) and cationic Cr (III) species, respectively. The liquid ion exchangers used in this work are shown in Figure 2.1. Since the process is based on the ion-pairing of Cr ions with the carrier molecule, the system is selective of one Cr species over the other.

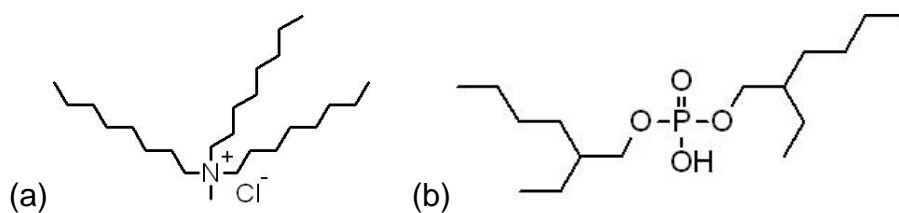


Figure 2.1. (a) Structure of Aliquat-336 (tricaprylmethylammonium chloride). (b) Structure of D2EHPA (di-(2-ethylhexyl)phosphoric acid).

This sampling system differs from existing samplers in that a polymeric support membrane is used as opposed to a dialysis-based membrane. The polymeric membrane functions as a barrier separating the aqueous phases (source and collection), as well as a support material for the liquid ion exchanger of the organic phase. Teflon[®] membranes were selected for this work because of their chemical inertness and acid resistance. Also, Teflon[®] membranes are more robust than cellulose-based membrane (acetate and nitrate) and are less susceptible to perforation.

Another difference in this system is the scale on which the sampler is used. The sampler, as designed to fit within the existing multilayer sampler (MLS) framework, has a membrane that is 25 mm in diameter and a collection bottle of 50 mL. Coupled with the MLS system, the sampler could afford in-situ chemical speciation, as well as depth profiling analysis of a contaminant plume. Such information would be invaluable to scientists and engineers tasked with the verification of remediation efforts.

2.2 Experimental

2.2.1 Materials and Reagents

The sampling system is constructed from commercially-available products. A schematic of the sampler is shown in Figure 2.2 and a photograph of the components of the sampler (base plate and collection bottle) is shown in Figure 2.3. To avoid contamination from metal pieces, the sampler was constructed from Teflon[®]; associated apparatuses were plastic as well. Teflon[®] sheets (12" x 12" x 3/8") and a Teflon[®] Bonding Kit were purchased from McMaster-Carr (Atlanta, GA). HPLC-grade acetone (Fisher Scientific) was used as the cleaning agent according to the instructions included in the Teflon[®] Bonding Kit. Nylon screws and nuts were also

purchased from McMaster-Carr for the assembly of the SLM samplers. The screws were 1¼” in length with an 8-32 thread and were a slotted drive style. The nuts were right-hand thread with a matching 8-32 thread. These screws and nuts were considered disposable as new ones were used each time a sampler was assembled. Teflon® bottles (50 mL) with caps were purchased from Fisher Scientific.

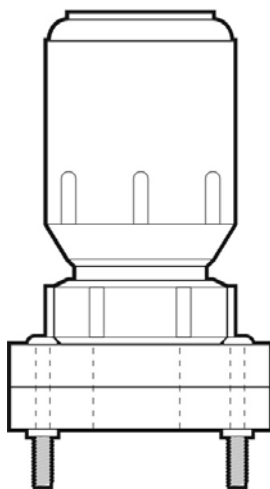


Figure 2.2. Drawing of an assembled Selective Ion Trap (SIT) sampler.

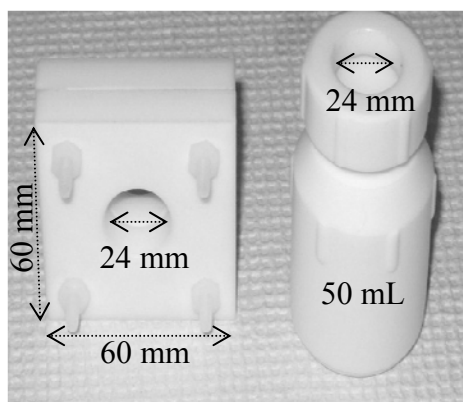


Figure 2.3. Photograph of the components (base plate and collection bottle) and dimensions of the Selective Ion Trap (SIT) sampler.

Three HDPE tanks (8"x 8"x 8") were purchased from Fisher Scientific and were used as the feed phase container in the sampler validation studies. Up to 4 samplers can be placed in a tank during the validation experiments. The Teflon[®] membranes used in the samplers were purchased from VWR on a "made to order" basis. The membranes have a diameter of 25 mm, a thickness of 220 μm, and a porosity of 0.45 μm.

Materials utilized for the testing of leaks in each cell are food coloring and PVC film. Several drops of yellow food coloring were added to a beaker of DI water to produce an intensely colored bulk solution. A 1:10 dilution of the bulk solution produced an absorbance of 0.55 AU at $\lambda_{\text{max}} = 425$ nm. For the uptake studies, Cr stock solutions were prepared using chromium (III) nitrate nonahydrate ($\text{Cr}(\text{NO}_3)_3 \cdot 9 \text{H}_2\text{O}$, 99% purity, Sigma-Aldrich, Allentown, PA) and potassium dichromate ($\text{K}_2\text{Cr}_2\text{O}_7$, $\geq 99.5\%$ purity, Fluka, Allentown, PA). The organic carrier molecules (Figure 2.2) used in this work were Aliquat-336 and bis-2-ethylhexyl phosphoric acid (D2EHPA). Aliquat-336 (97% purity) was obtained from Sigma-Aldrich. The D2EHPA (97% purity) compound was obtained from Aldrich (Allentown, PA). The carrier molecules were used as-is with no further purification. Other components of the organic phases of this work include decanol (99% purity, Sigma-Aldrich) as a phase modifier (co-surfactant) and kerosene (Fluka) as the solvent. Perylene ($>98\%$, Alfa Aesar, Ward Hill, MA) was used as an organic dye to test the stability of the organic phase in the membrane. Omni Trace hydrochloric acid (EMD; Gibbstown, NJ) was used to prepare the acceptor phases of this work. HCl is an appropriate acceptor phase for both Cr (III) and Cr (VI) SLM extraction since it provides the appropriate counter-ion for each mechanism; H^+ for Cr (III) extraction and Cl^- for Cr (VI) extraction.

All glassware (grade A) and Teflon[®] materials were washed after use with Citronox[®], which is manufactured by Alconox (NJ). This soap was purchased from Spectrum and is specifically designed for cleaning equipment associated with trace metal analysis.

2.2.2 Sampler Design and Fabrication

The dimensions of the sampling system have been selected with consideration of the existing MLS framework. The Teflon[®] sheet was cut into 60 mm x 60 mm plates. Four screw holes were drilled into the corner of each square (see Figures 2.2 and 2.3). A 24 mm hole was drilled through the center of each square. The center hole diameter is smaller than the membrane diameter (25 mm) to ensure that the plates sandwiched the membrane correctly. A matching 24 mm hole was drilled through the cap of the Teflon[®] bottle.

Once the Teflon[®] sheet was cut and the holes drilled, the bottle caps were bonded to one of the plates using the Teflon[®] Bonding Kit. The kit contains a treating agent (Na in a naphthalene matrix) and the epoxy materials (resin and curing agent). The treating and bonding procedures were followed according to the instructions contained in the kit. The Teflon[®] pieces were prepared for bonding by soaking in acetone for one hour. The pieces were then allowed to air dry for an hour. The treating agent was shaken thoroughly and a thin layer was dispensed on the surface using a disposable pipette. **CAUTION: The treating agent contains sodium metal. Take the following precautions: use vinyl gloves, work in a hood, and DO NOT use water.** The etched surface will turn black or dark brown after 15-60 seconds. After the etching process is complete, the pieces are soaked in fresh acetone to remove any residual treating agent. Then, the pieces are rinsed in soapy, hot water followed by fresh acetone again and allowed to air dry. The pieces were inspected to determine the quality of the etching procedure; any piece deemed

poorly-etched (non-uniform discoloration) was re-treated. The initial acetone soak and air dry steps were shortened to 15 minutes each for the re-treatment procedure.

The etched pieces were allowed to dry overnight before bonded to each other. The epoxy was prepared by mixing equal lengths of Chemgrip Cement A (red) and B (amber) on the provided mixing sheet to produce a uniform, dark pink paste. The cement was applied to both of the etched pieces (plate and bottle cap) and spread to a uniform thickness. Then the pieces were pressed together for a few seconds. The bonded pieces were placed plate-down on the bench top and a bar clamp (or brick in later fabrications) was set on top of the assembly to ensure intimate contact. The epoxy was allowed to cure for 4 days.

2.2.3 Membrane Preparation

The membrane was prepared according to the wet preparation procedure described by Yang and Fane.³ Accordingly, a Teflon[®] membrane was soaked for 10 minutes in a 10 mL organic phase solution corresponding to the Cr ion of interest: 10% D2EHPA and 15% decanol in kerosene for Cr (III) and 2% Aliquat-336 and 20% decanol in a kerosene matrix for Cr (VI). The organic phase solutions were prepared by weighing the appropriate mass of organic carrier and volumetrically delivering the appropriate volumes of decanol and kerosene. The membrane was removed from solution and placed between the sampler plates.

2.2.4 Sampler Preparation

The Teflon[®] membrane is placed with the polypropylene backing touching the Teflon[®] plate equipped with a bottle cap. Plastic screws are placed through the four corner holes of the

plain Teflon[®] plate (without a bottle cap). The plain plate is affixed to the bottle cap plate. Nuts with matching threads are placed on the screws and tightened such that the plates are sealed. Needle-nose pliers are used to hold the nut in place while the screws are tightened. Once the plates are sealed, the Teflon[®] bottle, filled with 50 mL of acceptor phase solution, is attached to the bottle cap portion of the Teflon[®] plate assembly.

2.2.5 Equipment

Equipment used in this work concerned measurement for sampler integrity and Cr uptake. Sampler integrity was confirmed by monitoring the lack of intrusion of a colored solution into the sampler bottle. Spectral measurements were obtained using an Ocean Optics UV-vis spectrometer.

Cr levels were determined using ICP-OES. The instrument used was a Perkin Elmer 4300DV. The instrument was equipped with a high solids nebulizer and an on-line internal standard (Yttrium) kit. Normal parameters were used for Cr analysis at 283.563 nm. Stock solutions of Cr (III) and Cr (VI) were prepared as described in the Materials and Reagents section. All solutions were prepared in Class A glassware. A set of calibration standards were prepared using serial dilution. Data were generated from 5 replicate measurements. The % RSD of spectrometric data is less than 1%.

2.2.6 Sampler Validation

A four day curing process was required to ensure the bonding of the Teflon[®] cap and plate. The bonded pieces were checked manually for weakness; the bottle cap and plate were twisted in opposite directions to see if the epoxy had cured properly. No system failed during the

manual checks. The integrity of the sampling system from leakage was accomplished using a simple food coloring test. The samplers were equipped with a thin sheet of PVC film over the holes of the bonded plate and a second (unbonded) plate. The Teflon[®] bottle was filled with DI water and attached to the bottle cap. The assembled systems were placed in a beaker filled with the food coloring solution and allowed to sit for 4 days. The liquid in the sampler bottle was checked for evidence of leakage (orange color). An Ocean Optics UV-Vis spectrometer was used to determine the absorbance of sampler bottle contents at 425 nm ($\lambda_{\text{max, food coloring}}$).

2.2.7 Sampler Performance Evaluation

The testing phase of the SLM samplers involves tank studies. The arrangement of the samplers is shown in Figure 2.4. The studies initially focused on the uptake of Cr (III) and Cr (VI) separately; later studies were conducted under mixed conditions where Cr (III) and Cr (VI) are present together. The experimental conditions of each tank study are given in Table 2.1.



Figure 2.4. Photograph of Supported Liquid Membrane (SLM) samplers positioned in HDPE tank.

Table 2.1. Experimental conditions for Supported Liquid Membrane (SLM) tank studies.

Ion	Feed Phase	Organic Phase	Acceptor Phase
Cr (III)	10 ppm Cr (III)	10% D2EHPA; 15% Decanol	0.1 M HCl
Cr (VI)	10 ppm Cr (VI)	2% Aliquat-336; 20% Decanol	5 M HCl
Cr (III) & Cr (VI)	10 ppm Cr (III)	10% D2EHPA; 15% Decanol	0.1 M HCl
	10 ppm Cr (VI)	2% Aliquat-336; 20% Decanol	5 M HCl

In the individual Cr ion studies, the HDPE tank was filled with ~2.5 L of the appropriate 10 ppm Cr solution. The samplers were placed in the tank on their sides. A Teflon[®] plate was placed under the bottle of the sampler to ensure that the entire membrane was covered by the acceptor phase solution. The tank was covered with its lid and the samplers were allowed to sit in the tank undisturbed for a fixed time. The removal dates were based on residence time in the tank and were selected to be 1, 2, 4, 5, 6, 7, 8, 10, 12, 14, and 21 days. The Cr concentration in each sampler bottle was quantified using ICP-OES.

For the mixed sampling conditions, the tank was filled with ~2.5 L of a solution containing 10 ppm Cr (VI) and 10 ppm Cr (III). Two Cr (VI) and two Cr (III) samplers were

prepared and assembled according to the procedure described in the previous sections. The completed samplers were placed in the tank and removed after 4 and 8 days. ICP-OES was used to quantify the amount of Cr present in each sampler bottle.

2.3 Results and Discussion

2.3.1 Sampler Integrity

Upon removal from the food coloring solution, the sampler integrity was validated if no food coloring could be measured in the Teflon[®] bottle. Six sampling systems were prepared and validated according to the procedures detailed in this work. All samplers were determined to be leak-free.

2.3.2 Uptake Studies of Individual Ions

Uptake studies for both Cr (III) and Cr (VI), separately, were conducted as part of the SLM sampler evaluation. The results of the uptake experiments are presented in Figure 2.5 and Tables 2.2 and 2.3. The x-axis for all graphs will represent the sampler's residence time (days) in the tank and the y-axis is the concentration of Cr in the acceptor phase (ppm). The data is corrected for the Cr concentration in the corresponding blank samples; the uptake data is corrected by subtracting the Cr concentration in the HCl stock solution from the sample concentration. Error bars for the Cr concentration are present. However, since the error associated with the measurement is less than 1% RSD, most error bars cannot be seen because the data marker covers them.

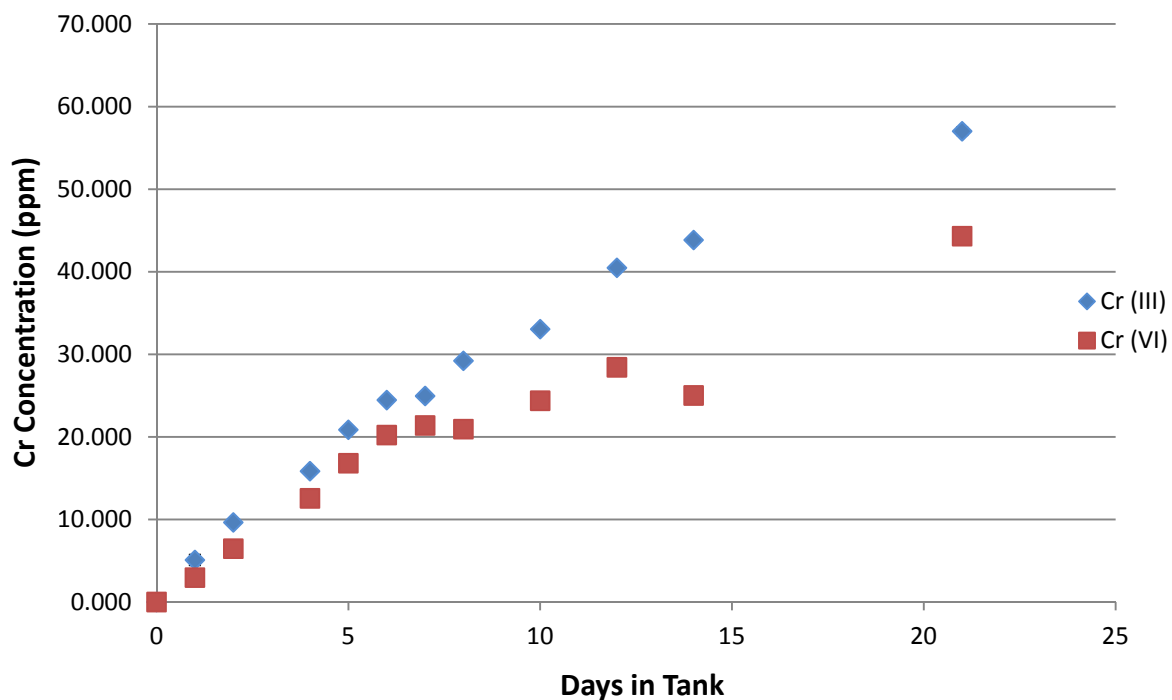


Figure 2.5. Uptake of Cr (III) and Cr (VI).

The Cr (III) uptake profile is linear in shape (see Table 2.2 for numeric values). The system displays enrichment after 2 days or residence in the tank. The concentration doubles again (from 10 ppm to 20 ppm) at 5 days of residence. After 8 days in the tank, the system reaches approximately 30 ppm. The 40 ppm mark is achieved at 12 days residence. The sampler surpasses 50 ppm at day 21.

Table 2.2. Cr (III) uptake data (units of ppm) with 95% confidence error.

Days	[Cr] (ppm)	95% confidence (n=5)
0	0.000	
1	5.094	0.639
2	9.645	0.083
4	15.85	0.13
5	20.86	0.17
6	24.46	0.32
7	24.96	0.19
8	29.22	0.27
10	33.05	0.33
12	40.48	0.30
14	43.85	0.18
21	57.02	0.46

The Cr (VI) uptake profile is similar to that of Cr (III); the concentration increases linearly throughout the experiment. The numeric data is given in Table 2.3. However, the rate of increase is much slower than that of Cr (III). The concentration of Cr (VI) in the sampler surpasses the initial concentration of the feed phase (10 ppm) after 4 days in the tank. The Cr (VI) concentration exceeds 20 ppm at day 6. The 30 ppm mark is approached on days 12, but is not surpassed until day 21. At this point, the concentration of Cr (VI) exceeds 40 ppm.

Table 2.3. Cr (VI) uptake data (units of ppm) with 95% confidence error.

Days	[Cr] (ppm)	95% Confidence (n=5)
0	0.000	
1	2.956	0.083
2	6.457	0.065
4	12.56	0.11
5	16.81	0.09
6	20.22	0.20
7	21.39	0.12
8	20.94	0.61
10	24.38	0.17
12	28.43	0.37
14	25.02	0.09
21	44.31	0.16

The process of enrichment occurs if the acceptor phase is stagnant or non-flowing.⁴ Since the total volume of the acceptor phase is constant and the amount of Cr ion in the acceptor phase increases, the concentration of Cr ion in the acceptor phase can surpass the amount in the original feed solution. This process is known as enrichment. Enrichment factors are easily calculated and the relationship between initial concentration and enrichment is straightforward.⁵ Equation 2.1 shows the dependence of the enrichment factor (E_e) on the concentrations of the feed (c_F) and acceptor (c_A) phases. If the sampling environment is non-flowing and the feed

phase is not replenished, the concentration of Cr in the feed phase is approximately constant throughout the experiment, while the concentration of Cr in the acceptor phase increase with time. Thus, the enrichment increases with increased sampling time. The enrichment factors for Cr uptake are shown in Table 2.4.

$$E_e = \frac{c_A}{c_F} \quad (2.1)$$

Table 2.4. Enrichment factors for Cr uptake.

Days	E_e (Cr (III))	E_e (Cr (VI))
0	0.000	0.000
1	0.5094	0.2956
2	0.9645	0.6457
4	1.585	1.256
5	2.086	1.681
6	2.446	2.022
7	2.496	2.139
8	2.922	2.094
10	3.305	2.438
12	4.048	2.843
14	4.385	2.502
21	5.702	4.431

From the data presented in Figure 2.5, it can be determined that both systems (Cr (III) and Cr (VI)) have similarly-shaped uptake curves, which suggests that both systems function in a similar fashion. However, the data indicate that Cr (III) uptake is faster than Cr (VI). Also, it should be noted that Cr (III) uptake is more complete at the end of the sampling period (21 days). Despite the differences in rate, both systems display enrichment. Since the acceptor phase has a smaller volume than the feed phase (50 mL vs. 2500 mL), the transport of Cr into the acceptor phase concentrates or enriches the concentration of Cr compared to that of the original solution (feed phase). This is especially important when one considers the fact that Cr in natural systems can occur in trace amounts; enrichment allows for the progression from trace amounts of Cr to detectable amounts.

2.3.3 Sampler Lifetime

The results of the uptake studies indicate that the samplers are stable in ambient laboratory-controlled conditions for 3 weeks. There was no membrane failure or sampler degradation during the duration of the uptake experiments. Since environmental sampling occurs over an extended period (weeks to months) to ensure representative sampling, the stability of the sampling system is imperative for the environmental viability of the sampler.

It has been noted in the literature that loss of organic phase from SLM-based sampling systems can occur and is detrimental to sampler performance and lifetime.^{6,7} The stability of the organic phase in the membrane was verified using an organic dye (perylene). Perylene fluoresces in the presence of UV light, while there is no background fluorescence from the membrane or kerosene. If the organic phase is removed from the membrane, the fluorescence will decrease as

a result of perylene loss. Therefore, the stability of the organic phase was verified if membrane fluorescence did not decrease over a period of one month.

A solution was prepared which consisted of 0.0061g perylene in 10 mL kerosene. The membrane was prepared according to the standard procedure and placed in the sampling system. A hand-held UV light source was used to induce perylene fluorescence. The sampler was placed on its side in a 1 L beaker filled with water. The sampler was checked several times over a period of one month. A qualitative inspection of perylene fluorescence indicates that the dye did not leach out of the kerosene/membrane matrix. Hence, the organic phase of the sampling system was determined to be stable for at least one month. This result supports the observed sampler lifetime from the laboratory-controlled uptake experiments.

It has been discovered that exposure to high acidity (5 M HCl) will cause degradation of the sampler. The samplers were submerged in 5 M HCl, which is far more acidic than any potential groundwater sampling environment. The plastic screws and nuts used to hold the sampler plates together are not designed nor expected to withstand extremely acidic solution for extended periods of time (i.e. several days). It was noted that after 5 days residence in 5 M HCl the nylon screws begin to degrade. After 6 days in 5 M HCl, the nylon screw degradation results in separation of the sampler plates. Thus, the plates that sandwich the membrane separate. This plate separation compromises the integrity of the sampling system. The membrane can potentially slip out of place, which would uncover the hole. In this situation, a direct channel would be established for the unassisted flow of Cr to and from the acceptor bottle.

Furthermore, the epoxy used to bond the bottle cap to the plate does not withstand the harsh sampling conditions. The plate/cap assembly remained intact in the 5 M HCl solution.

However, it was discovered that the epoxy of some of the samplers had weakened. This resulted in the bottle cap separating from the plate and twisting off during subsequent sampler assembly.

The damaged systems were repaired (re-bonded) using the procedure outline above. Re-bonding does not appear to have a negative impact on the lifetime of the sampler system; the re-bonded samplers do not come apart faster than the original samplers. However, these results show that the samplers are not infinitely stable under extreme conditions.

2.4 Summary

A sampling system has been designed and fabricated for the chemical speciation of chromium ions, Cr (III) or Cr (VI), in groundwater systems. The sampler is fabricated from Teflon[®] and is based on the SLM speciation mechanism. The motivation for the design and development of this sampler is based on the needs of environmental scientists and engineers to be able to differentiate between Cr oxidation states (speciation), given the varying degrees of toxicity and mobility of Cr ions in the environment. This sampling system, termed the Selective Ion Trap (SIT), utilizes a charged organic carrier that is contained within a supported liquid membrane (SLM) for the selective extraction of the hexavalent form (which exists as HCrO_4^-) or the trivalent form (which exists as $\text{Cr}(\text{OH})^{+2}$) from natural waters and soils. The selectivity of the sampler for one form of Cr over the other is controlled via the charged organic carrier, which is referred to as a liquid ion exchanger. The positively charged carrier Aliquat-336 is used for Cr (VI), while the negatively charged carrier D2EHPA is used for Cr (III). In addition to the trap ensuring the specificity of the sample, it also provides stabilization for subsequent sample analysis. Accordingly, an important advantage to this design is that it allows for both the in-situ separation and storage of the Cr species. Hence, this system avoids problems associated with the

stabilization and the preservation of the individual fractions of the chemical species in environmental solutions that occurs using normal sampling methods.

2.5 References

- (1) Ronen, D.; Magaritz, M.; Weber, U.; Amiel, A. J.; Klein, E. *Water Resour. Res.* **1992**, *28*, 1279.
- (2) Long, G. L.; Amiel, A. J.; Magaritz, M.; Ronen, D.; Brenner, I. B. In *The Eighteenth Annual Meeting of the Federation of Analytical Chemistry and Spectroscopic Societies* 1991.
- (3) Yang, X. J.; Fane, T. J. *J. Membr. Sci.* **1997**, *133*, 269.
- (4) Jonsson, J. A.; Lovkvist, P.; Audunsson, G. *Anal. Chim. Acta* **1993**, *277*, 9.
- (5) Chimuka, L.; Megersa, N.; Jonsson, J. A. *Anal. Chem.* **1998**, *70*, 3906.
- (6) Kemperman, A. J. B.; Bargeman, D.; van den Boomgaard, T.; Strathmann, H. *Sep. Sci. Technol.* **1996**, *31*, 2733.
- (7) Yang, X. J.; Fane, A. G.; Soldenhoff, K. *Ind. Eng. Chem. Res.* **2003**, *42*, 392.

Chapter 3

Liquid-Liquid Extraction Studies for Determining Optimal Supported Liquid Membrane (SLM) Operating Parameters and Determining Cr Extraction Kinetics

3.1 Introduction

Despite the numerous occurrences of Supported Liquid Membrane (SLM) extraction applications for Cr in the literature,¹⁻¹² reports that describe the rationale for selecting certain operating parameters (carrier concentration, acceptor phase composition and concentration, etc.) are missing from the literature. The purpose of the work conducted in the liquid-liquid extraction phase studies is to provide insight into what parameters influence the SLM extraction of Cr, and how optimal experimental conditions are determined. The studies conducted here examine the effect of carrier concentration, co-surfactant (modifier) concentration, as well as acceptor phase concentration on the efficiency of the SLM extraction technique for Cr speciation. The selectivity of the carrier molecule is also determined using the optimized organic phase conditions (carrier concentration and decanol concentration).

The use of SLMs has proven to be an adequate technique for the speciation of Cr in the literature^{4-7,9,12} as well as in this work. The SLM extraction process, which is illustrated in Figure 1.4, can be thought of as two concerted liquid-liquid extractions (LLEs). The first occurs when a Cr ion is transported from the feed phase into the organic phase. Then, the second LLE occurs when the Cr ion is transported from the organic phase into the acceptor phase. Since the two steps form a consecutive mechanism, the SLM displays greater efficiency than that achieved from the two processes separately.¹⁰

The use of the SLM technique is abundant in the literature.¹⁻¹² While these works indicate that the SLM extraction technique is invaluable in the speciation of Cr, a discussion of how to determine and select optimal operating parameters is absent. It is the purpose of this work to explore the effect of SLM operating parameters (carrier concentration, modifier concentration, and counter-ion concentration) in order to develop a better understanding of the SLM extraction mechanism and optimize the efficiency of the SLM-based sampling system.

The SLM process functions using basic LLE. Here, the analyte is partitioned between an aqueous and an organic phase. The extent of partitioning is governed by the solubility of the analyte in each phase, as well as the affinity of the analyte for each phase. The degree of partitioning is expressed using the partition coefficient, K .

$$K = \frac{[analyte]_{organic}}{[analyte]_{aqueous}} \quad (3.1)$$

For the experiments conducted in this work, the volume of the aqueous and organic phases are equal, which means that

$$K = \frac{mass_{organic}}{mass_{aqueous}} \quad (3.2)$$

An understanding of solvent extraction processes using liquid ion exchangers is useful when considering the LLE processes involved in the SLM system. The carrier molecule functions as a liquid ion exchanger. Specifically, the liquid ion exchanger can be a cation or anion depending on which Cr species is studied. Historically, liquid ion exchangers have been used in a variety of applications, such as industrial waste treatment tasks, which focus on reagent recycling.¹³⁻¹⁶

LLE with liquid ion exchangers have proved to be a useful technique for a number of reasons. This technique is capable of reaching equilibria in a matter of seconds as well as separating very small amounts (μg) of reagent. However, the key benefit that makes the SLM process attractive for the speciation of Cr ions is the fact that LLE with liquid ion exchangers is capable of separating elements in different oxidation states.¹⁷

The driving force of the LLE with liquid ion exchangers technique is the formation of an organic soluble ion-pair or uncharged complex that is extractable into the organic phase.¹⁷ The ion-pair formation is thought to occur in the interfacial region between the aqueous and organic phases.¹⁷ The interfacial chemistry has been studied in these systems by Watarai et al.¹⁸ This group has used fluorescence and Raman techniques to study the nature and structure of the interfacial species. The results of these experiments have determined that molecular recognition of the ion of interest is achieved through carrier aggregation and that the ion-pairing reaction rate at the interface is rapid.

Lewis cell experiments have been conducted in the literature on a variety of LLE systems to determine the reaction order of various LLE components.¹⁹ Although these studies differ on some aspects of the results, the majority agree on reaction order with respect to carrier concentration. The LLE parameters that were investigated in the literature include pH, carrier concentration, and Cr concentration. Given the fact that decanol is necessary to prevent the formation of a third phase, it is proposed in this dissertation that the decanol concentration plays a role in the rate of reaction. Therefore, the Lewis cell studies conducted in this work are similar to those conducted in the literature²⁰⁻³² with the addition of a decanol concentration study.

The method of initial rates was employed in the treatment of the Lewis cell data. In this method, the extraction rate can be expressed as

$$J = k_f [Cr]^a [H^+]^b [Carrier]^c [Decanol]^d \quad (3.3)$$

where J is the flux of Cr from one phase to the other, k_f is the rate constant, and a , b , c , and d are the reaction orders of chromium ion, proton, carrier molecule, and decanol, respectively (equation 3.3). By taking the log of both sides of equation 3.3, we have

$$\log J = \log k_f + a \log [Cr] + b \log [H^+] + c \log [Carrier] + d \log [Decanol] \quad (3.4)$$

When three of the four concentrations on the right hand side of equation 3.4 are held constant, the $\log J$ vs. \log concentration plot should produce a line with slope equal to the reaction order of the species whose concentration is varied, and y-intercept equal to the sum of $\log k_f$ and the sum of the remaining \log concentration terms. Once all reaction orders have been determined, the value of k_f can be found.

3.2 Parameter Optimization

3.2.1 Experimental

A stock solution of 1000 ppm Cr (VI) was made volumetrically by dissolving 1.4145 g potassium dichromate (Fluka) in 500.00 mL Milli-Q H₂O. A stock solution of 1000 ppm Cr (III) was made by dissolving 1.9239 g chromium (III) nitrate nonahydrate (Sigma) in 250.00 mL Milli-Q H₂O. Stock solutions of varying concentrations of hydrochloric acid were made by diluting OmniTrace[®] hydrochloric acid (EMD) with Milli-Q H₂O. Kerosene (Acros), decanol (Aldrich), Aliquat-336 (Aldrich), and D2EHPA (Aldrich) were used as received.

Qorpak[®] vials (60 mL) were used in the LLE parameter optimization studies. Exactly 10.0 mL of the appropriate 10 ppm Cr solution for a total of 100 µg Cr was added to the vials: Cr (III) for the D2EHPA systems and Cr (VI) for the Aliquat-336 systems. A series of varying carrier concentrations were prepared. For Cr (III), the concentrations of D2EHPA were 0%, 2.5%, 5%, 10%, and 20%. For Cr (VI), the concentrations of Aliquat-336 were 0%, 0.5%, 1%, 1.5%, 2%, and 2.5%. The dependence of the modifier was also investigated. The carrier concentration studies were performed in duplicate for Cr (III) and Cr (VI), with the presence or absence of 10% decanol in the organic phase. Kerosene was used as the solvent in the organic phase for all experiments. The total volume of the organic phase was 10 mL. Table 3.1 illustrates the experimental conditions for the carrier concentration studies. It should be noted that data will not be presented for the Cr (VI) studies without decanol due to the existence of a two layer organic phase in these systems. The observation of a biphasic organic phase in the absence of a co-surfactant is supported by the literature.³³

Table 3.1. Experimental conditions for equilibrium carrier concentration studies.

Phase	<i>Cr (III)</i>	<i>Cr (III)</i> <i>With Decanol</i>	<i>Cr (VI)</i>	<i>Cr (VI)</i> <i>With Decanol</i>
Feed (10 mL)	10 ppm Cr (III)	10 ppm Cr (III)	10 ppm Cr (VI)	10 ppm Cr (VI)
Organic (10 mL)	X% D2EHPA	X% D2EHPA; 10% Decanol	X% Aliquat-336	X% Aliquat-336; 10% Decanol

The organic components were mixed in vials and allowed to dissolve/incorporate completely before the feed phase was pipetted into the vials. Next, the vials were placed on an orbit-shaker table, shaken at 125 rpm for 2 hours (in order to reach equilibrium), and allowed to settle. The contents of the vials were placed in a separatory funnel and allowed to settle. The aqueous phase was drained into a clean vial and the organic phase was drained into the original vial. Each phase was analyzed using a Perkin-Elmer 4300 DV ICP-OES, according to Table 3.2. All ICP-OES data is reported at the 283.563 nm Cr wavelength, except for the acceptor phase Cr (VI) study, which is reported at the 357.869 nm Cr wavelength in order to avoid spectral interferences.

Table 3.2. ICP-OES operating parameters for aqueous and organic samples.

<i>ICP-OES PARAMETER</i>	<i>AQUEOUS</i>	<i>ORGANIC</i>
RF Power	1300W	1300W
Nebulizer Flow	0.8 L/min	0.5 L/min
Plasma Flow	15 L/min	15 L/min
Aux Flow	0.2 L/min	0.1 L/min
Sample Flow	1.5 mL/min	0.8 mL/min
Cr wavelengths	283.563 nm	283.563 nm
	357.869 nm	357.869 nm

A series of varying decanol concentrations (v/v%) was prepared for both Cr (III) and Cr (VI). The optimal D2EHPA and Aliquat-336 concentrations were chosen according to the results of the carrier concentration studies. The decanol concentrations were 0%, 5%, 10%, 15%,

and 20%. Kerosene was used as the solvent. The feed phase (10 mL) was 10 ppm Cr (III) for the D2EHPA systems and 10.0 mL of 10 ppm Cr (VI) for the Aliquat-336 systems. The experimental conditions for the decanol studies are shown in Table 3.3. The shaking and separation procedures from the previous studies were followed. ICP-OES was used to analyze the Cr concentration in the aqueous and organic phases.

Table 3.3. Experimental conditions for equilibrium decanol concentration studies.

Phase	<i>Cr (III)</i>	<i>Cr (VI)</i>
Feed (10 mL)	10 ppm Cr (III)	10 ppm Cr (VI)
Organic (10 mL)	10% D2EHPA X% Decanol	2% Aliquat-336 X% Decanol

The purpose of the selectivity study was to determine how effective the carrier is at discriminating against the Cr ion of the same charge. Based on the SLM theory and the principles of electrostatics, the charged carrier should ion-pair only with the Cr ion of the opposite charge. Thus, the carrier charge dictates which Cr ion will be transported into the acceptor phase.

In these studies, the carrier ion and Cr ion possess the same charge, which means that the carrier demonstrates selectivity if no Cr is transported into the organic phase. The experimental conditions are shown in Table 3.4. For Cr (III), the optimum conditions for the Cr (VI) organic phase were used: 2% Aliquat-336 and 20% decanol in kerosene (10 mL). The aqueous phase was 10 mL 10 ppm Cr (III). For Cr (VI), the optimum conditions for the Cr (III) organic phase were

used: 10% D2EHPA and 15% decanol in kerosene (10 mL). The aqueous phase was 10 mL of 10.0 ppm Cr (VI). ICP-OES was used to analyze the aqueous and organic phases.

Table 3.4. Experimental conditions for equilibrium selectivity studies.

Phase	<i>Cr (III)</i>	<i>Cr (VI)</i>
Aqueous (10 mL)	10 ppm Cr (III)	10 ppm Cr (VI)
Organic (10 mL)	2% Aliquat-336, 20% Decanol	10% D2EHPA, 15% Decanol

Four vials were prepared using identical feed and organic phases for both Cr (III) and Cr (VI) (Table 3.5). The shaking and separating procedures were followed as previously described. In each original vial, 10 mL of the acceptor phase was added to the organic phase. A series of HCl concentrations (0.1, 0.5, 1M HCl – Cr (III); 1, 2, 5M HCl – Cr (VI)) as well as a blank (DI water) were used to determine the optimum acceptor phase concentration. The shaking and separating procedures were followed again. ICP-OES was used to analyze the aqueous, organic, and acceptor phases.

Table 3.5. Experimental conditions for equilibrium acceptor phase studies.

Phase	<i>Cr (III)</i>	<i>Cr (VI)</i>
Aqueous (10 mL)	10 ppm Cr (III)	10 ppm Cr (VI)
Organic (10 mL)	10% D2EHPA, 15% Decanol	2% Aliquat-336, 20% Decanol
Acceptor (10 mL)	DI Water or XM HCl	DI Water or XM HCl

3.2.2 Results and Discussion

The data from the LLE studies are presented in tabular and graphical forms. The tables give the [Cr] determined from the ICP experiments in units of micrograms (μg). The graphs display the distribution of Cr in the aqueous (feed and/or acceptor) phases. Since the LLE studies were conducted in closed systems, the partitioning, which is defined as the organic phase concentration divided by the aqueous phase concentration, takes place between the aqueous and organic phases. The y-axis is the mass of Cr (μg) and the x-axis represents the parameter being investigated (i.e. carrier concentration, decanol concentration, acceptor phase concentration, or carrier selectivity). Errors bars are included, which represent the 95% confidence interval for each data point. The legend information for the parameter optimization and carrier selectivity studies, which is summarized below, is found in each graph as well as in Table 3.6.

Table 3.6. Legend information for liquid-liquid extraction (LLE) graphs.

Experiment	Data Series	Bar Style
D2EHPA concentration	Cr (III) feed	White with dots (▣)
	Cr (III) feed w/decanol	White (□)
Aliquat-336 concentration	Cr (VI) feed w/decanol	White (□)
Decanol concentration	Cr (III) feed	White with dots (▣)
	Cr (VI) feed	White (□)
Acceptor Phase concentration	Acceptor	White (□)
Selectivity	Feed	White with dots (▣)
	Organic	Gray (■)

In the carrier concentration studies, the feed phase Cr (III) data is represented as white bars with black dots while the feed phase Cr (III) with decanol data is represented as white bars, and the feed phase Cr (VI) with decanol data is represented as white bars. The bars corresponding to the systems that contained decanol are dotted. The feed phase Cr (III) data for decanol concentration studies are represented as white bars with black dots and the feed phase Cr (VI) organic phase data are represented with white bars. For the acceptor phase studies, the acceptor phase is white for both data sets (Cr (III) and Cr (VI)). Finally, the feed phase for the selectivity studies is white with black dots and the organic phase is gray.

3.2.2.1 Carrier Concentration Studies

Table 3.7 summarizes the data obtained from the carrier concentration studies. Figure 3.1 illustrates the distribution of Cr in the aqueous phase for the Cr (III)/D2EHPA systems. For both experiments (\pm 10% Decanol), the data displays a similar trend. As the carrier concentration increases, the distribution of Cr (III) favors the organic phase. The trend peaks at 10%, then decreases for the 20% D2EHPA system. These results indicate that the LLE is most complete for the 10% D2EHPA systems studied. However, the extraction is more complete for the 10% decanol systems than for the 0% decanol systems.

Table 3.7. ICP-OES data for the equilibrium carrier concentration studies in units of micrograms (μg) and partition coefficient.

	<i>Sample</i>	<i>Feed</i>	<i>Partitioning</i>
Cr (III)	0% D2EHPA	92.75	0.00
	2.5% D2EHPA	29.36	2.14
	5% D2EHPA	16.90	4.27
	10% D2EHPA	12.10	6.36
	20% D2EHPA	3.270	22.08
Cr (III) With Decanol	0% D2EHPA	91.40	0
	2.5% D2EHPA	29.83	2.33
	5% D2EHPA	14.38	5.77
	10% D2EHPA	5.110	17.44
	20% D2EHPA	1.650	46.91
Cr (VI) With Decanol	0% Aliquat-336	109.5	0
	0.5% Aliquat-336	10.39	7.13
	1% Aliquat-336	0.000	∞
	1.5% Aliquat-336	0.2200	315.0
	2% Aliquat-336	0.000	∞
	2.5% Aliquat-336	1.800	41.55

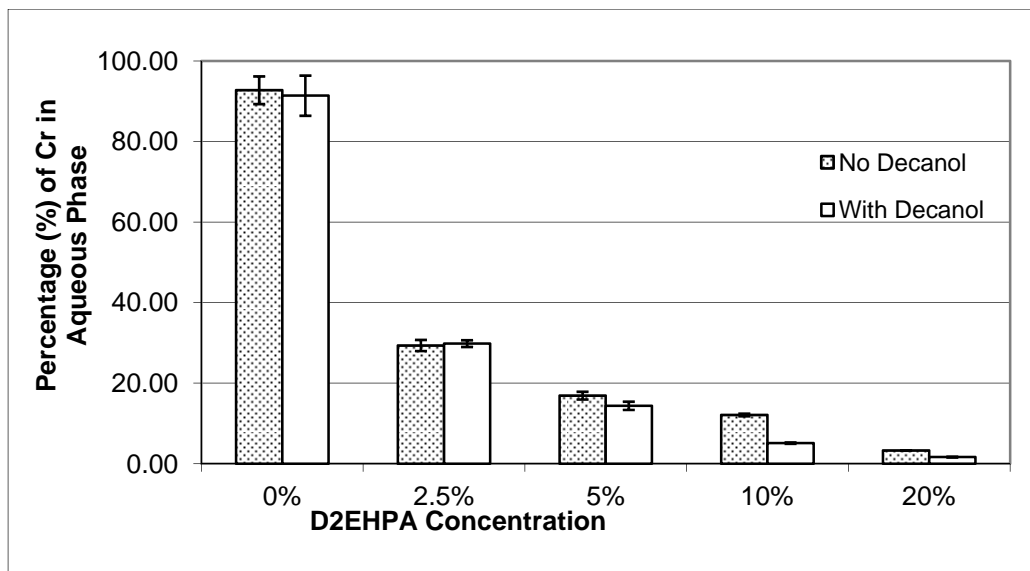


Figure 3.1. Equilibrium Cr (III) distribution as a function of D2EHPA (carrier) concentration.

Figure 3.2 presents the distribution of Cr (VI) as a function of Aliquat-336 concentration. As mentioned previously, the decanol is required in the Aliquat-336 systems in order to prevent the formation of a second organic phase. Accordingly, no useful data was obtained from the systems without decanol. The graph shows that the aqueous phase Cr concentration fluctuates as the carrier concentration increases. The optimal carrier concentration is such that the organic phase Cr is maximized and the aqueous phase Cr is minimized. According to the data presented in Figure 2, the optimal Aliquat-336 concentration is 2%.

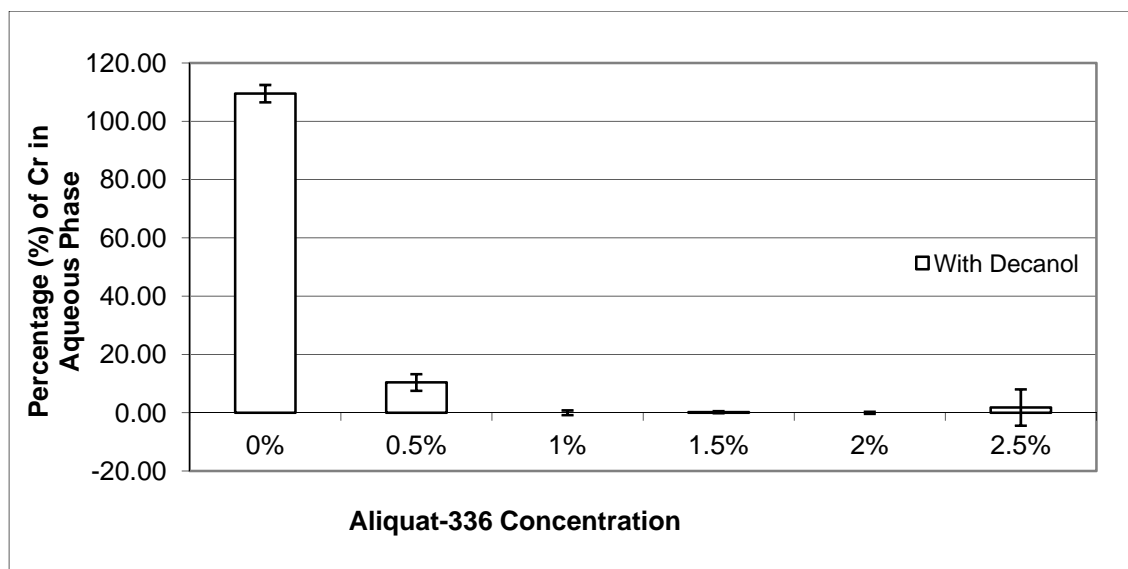


Figure 3.2. Equilibrium Cr (VI) distribution as a function of Aliquat-336 (carrier) concentration.

3.2.2.2 Decanol Concentration Studies

There are reports in the literature that state the importance of a co-surfactant. These co-surfactants are also referred to as phase modifiers. They are commonly alcohols and play a vital role in the formation of inverse/reverse micelles. The dependence of Cr in the aqueous phase on decanol concentration is presented in Figure 3.3 for both Cr systems. Both sets of data suggest that the presence of decanol enhances the extraction process and that increasing decanol concentration increases the completeness of the extraction process. The optimal decanol concentration is 15% for Cr (III) and 20% for Cr (VI). As seen in the previous section, the decanol must be present for the existence of a homogeneous organic phase with the use of a cationic carrier molecule. On the other hand, the decanol does not have an effect on the homogeneity of the D2EHPA-containing organic phase (anionic carrier). These results are consistent with the observation of co-surfactants for ionic carriers; anionic carriers/surfactants

(i.e. D2EHPA) do not need a co-surfactant to form inverse/reverse micelles where as cationic carriers/surfactants (i.e. Aliquat-336) require a co-solvent.³³

Table 3.8. ICP-OES data for the equilibrium decanol concentration studies in units of micrograms (μg) and partition coefficient.

	<i>Sample</i>	<i>Feed</i>	<i>Partitioning</i>
Cr (III)	0% Decanol	14.7	5.57
	5% Decanol	10.7	8.35
	10% Decanol	3.67	27.2
	15% Decanol	5.39	18.7
	20% Decanol	5.74	17.3
Cr (VI)	0% Decanol	N/A	N/A
	5% Decanol	0.24	374
	10% Decanol	0.00	∞
	15% Decanol	0.00	∞
	20% Decanol	0.00	∞

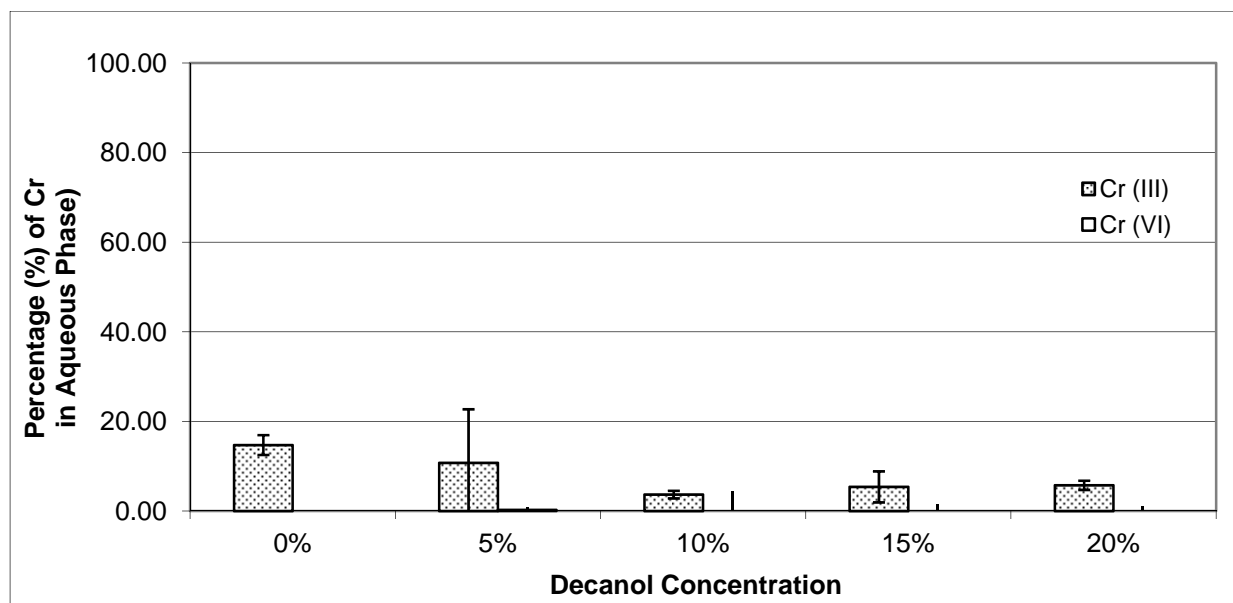


Figure 3.3. Equilibrium Cr distribution as a function of decanol concentration.

3.2.2.3 Acceptor Phase Concentration Studies

In the SLM mechanism, the counter-ion from the acceptor phase provides the driving force for the extraction mechanism. The presence of a concentration gradient between the feed and acceptor phase drives the extraction of the Cr ion from the feed phase into the acceptor phase. The counter-ion of the acceptor phase is exchanged for the Cr ion of the ion pair in the organic phase. For both systems, the acceptor phase is HCl. The counter-ion for Cr (III) extraction is H^+ , whereas the counter-ion for Cr (VI) extraction is Cl^- .

The data for the acceptor phase studies is presented in Table 9. For Cr (III), the Cr content in the feed phase is relatively constant for all systems studied. The acceptor phase Cr is very small for the control system (0M HCl – DI Water acceptor phase). The Cr content increases dramatically for the 0.1M system. Then, there is a slight decrease for the 0.5M system and a similar value for the 1M HCl system. The Cr (VI) acceptor phase data shows that the amount of Cr increases as the HCl concentration increases.

Table 3.9. ICP-OES data for the equilibrium acceptor phase studies in units of (μg) and partition coefficient.

<i>Sample</i>		<i>Acceptor</i>	<i>Partitioning (acceptor)</i>
Cr (III)	0M HCl	2.900	0.039
	0.1M HCl	78.62	3.99
	0.5M HCl	74.43	5.39
	1M HCl	57.3	3.43
Cr (VI)	0M HCl	0	0.000
	1M HCl	4.790	0.130
	2M HCl	11.49	0.385
	5M HCl	43.67	2.97

Figure 3.4 illustrates the dependence Cr (III) concentration in the acceptor phase on the acidity of the acceptor phase. As noted previously, the 0.1M HCl vial produces the greatest transport of Cr into the acceptor phase.

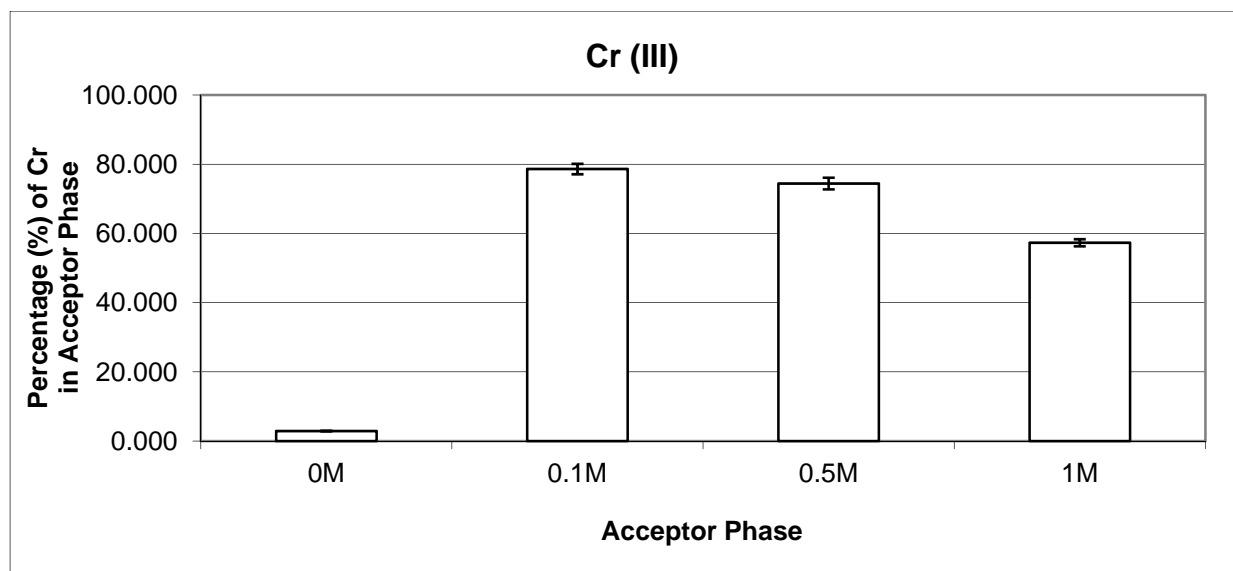


Figure 3.4. Equilibrium Cr (III) distribution as a function of acceptor phase composition.

The relationship between acceptor phase Cr (VI) concentration and the H^+ concentration in the acceptor phase is presented in Figure 3.5. As discussed previously, the Cr concentration increases in the acceptor phase as the H^+ concentration increases. Since there is no peak in the data, one might suggest continuing to increase the HCl concentration to determine the optimal operating condition. However, since the acceptor phase solution is in contact with the polymeric membrane in the SLM setup, the acceptor phase solution cannot be infinitely concentrated. Highly acidic solutions can cause damage to the membrane (holes) and extraction instability can result. Therefore, 5 M HCl is the most concentrated acceptor phase solution that will be used.

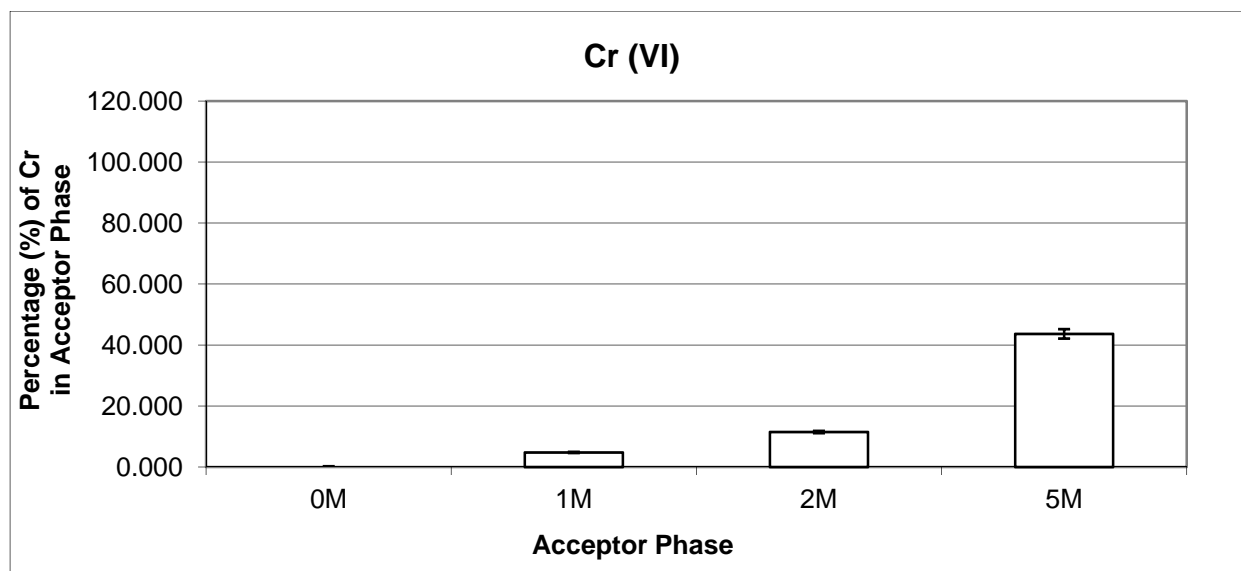


Figure 3.5. Equilibrium Cr (VI) distribution as a function of acceptor phase composition.

3.2.2.4 Selectivity Studies

Selectivity refers to the SLM system's ability to discriminate between the positively-charged and negatively-charged Cr ions and transport the appropriately-charged ion into the acceptor phase. In these studies, the SLM system has been modified such that the carrier molecule has the same charge as the Cr ion. Under these LLE conditions, the carrier cannot ion-pair with the Cr ion and transport of the Cr ion from the aqueous phase into the organic phase will not be facilitated.

The ICP-OES data is presented in Table 3.10. The ICP data suggests that (within experimental error) nearly all of the 100 μg Cr sample remained in the feed phase. It should be noted that the partition coefficients (K) are the same (0.08) for both systems.

Table 3.10. ICP-OES data for the equilibrium carrier selectivity studies in units of micrograms (μg) and partition coefficient.

<i>Sample</i>	<i>Feed</i>	<i>Organic</i>	<i>Partitioning</i>
Cr (III) with Aliquat-336	99.43	8.18	0.08
Cr (VI) with D2EHPA	104.90	8.79	0.08

The distribution of Cr between the feed and organic phases of the selectivity studies for D2EHPA and Aliquat-336 is shown in Figure 3.6. As noted from inspection of the ICP data, the majority of the Cr remains in the aqueous phase. Since there was very little Cr transported from the feed phase into the organic phase, these results prove the selectivity that the SLM theory indicates.

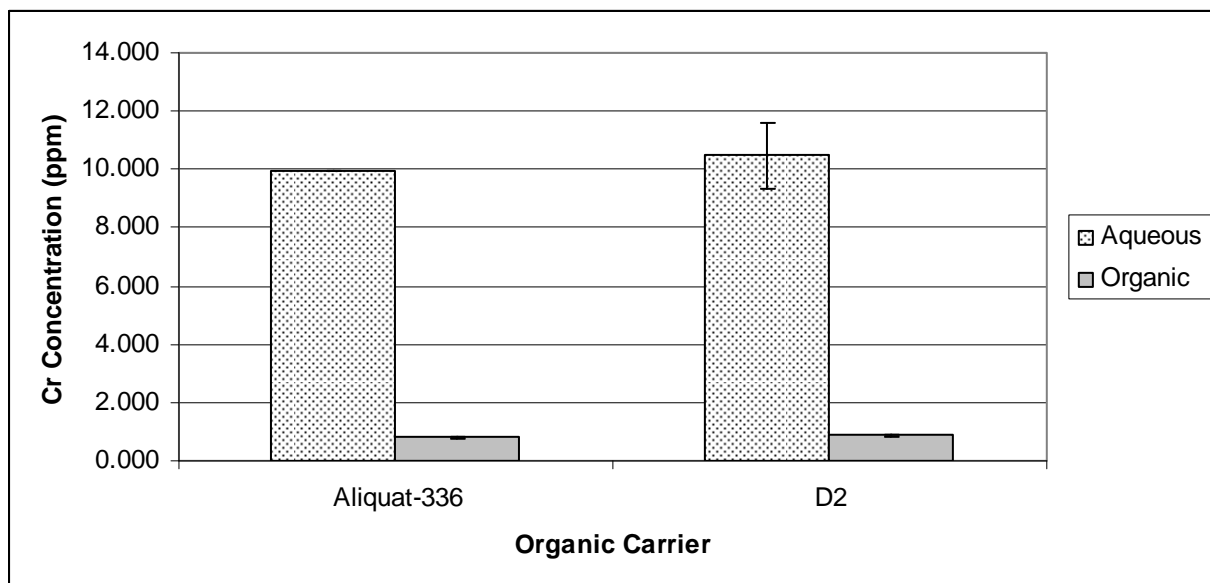


Figure 3.6. Equilibrium distribution of Cr in the organic carrier selectivity studies.

3.3 Extraction Kinetics

Kinetic investigations were conducted in order to gain a better understanding of the chemistry involved in the liquid-liquid extraction of Cr. Since the SLM-based sampling system is

comprised of two liquid-liquid extractions, a fundamental understanding of the kinetics of Cr extraction affords a more complete assessment of sampler function. Kinetics provides a tool for predicting SLM-based sampler behavior. The ability to predict Cr extraction from natural systems is powerful considering the sampling system does not have an infinite lifetime. However, if a kinetic model can predict adequate Cr extraction within the known sampler lifetime (at least 3 weeks), the integrity and viability of the sampling system is confirmed.

The method of initial rates was employed to determine rate laws and rate constants for each Cr LLE. From these rate laws, a kinetic model for Cr extraction in the SLM-based sampler will be developed. The model was tested against experimental SLM-based sampling data.

3.3.1 Experimental

A modified Lewis cell¹⁹ (Figure 3.7) was used in the LLE kinetics studies. A 400 mL beaker was used as the Lewis cell. Equal volumes (100 mL) of aqueous and organic phases were added to the beaker. The aqueous phase contained the Cr ion of interest and was pipetted into the cell first. A stir bar and a length of capillary tubing were placed into the aqueous phase. The tubing provides a method of *in-situ* aqueous phase sampling without disturbing the interface between the aqueous and organic phases. The organic phase, which contained the appropriate carrier molecule and decanol (phase modifier) in a kerosene matrix, was prepared volumetrically and pipetted slowly into the beaker so as not to disturb the interface. Both stirring mechanisms (overhead stirrer and stir bar) were adjusted so that the interface was not disturbed during the experiment.

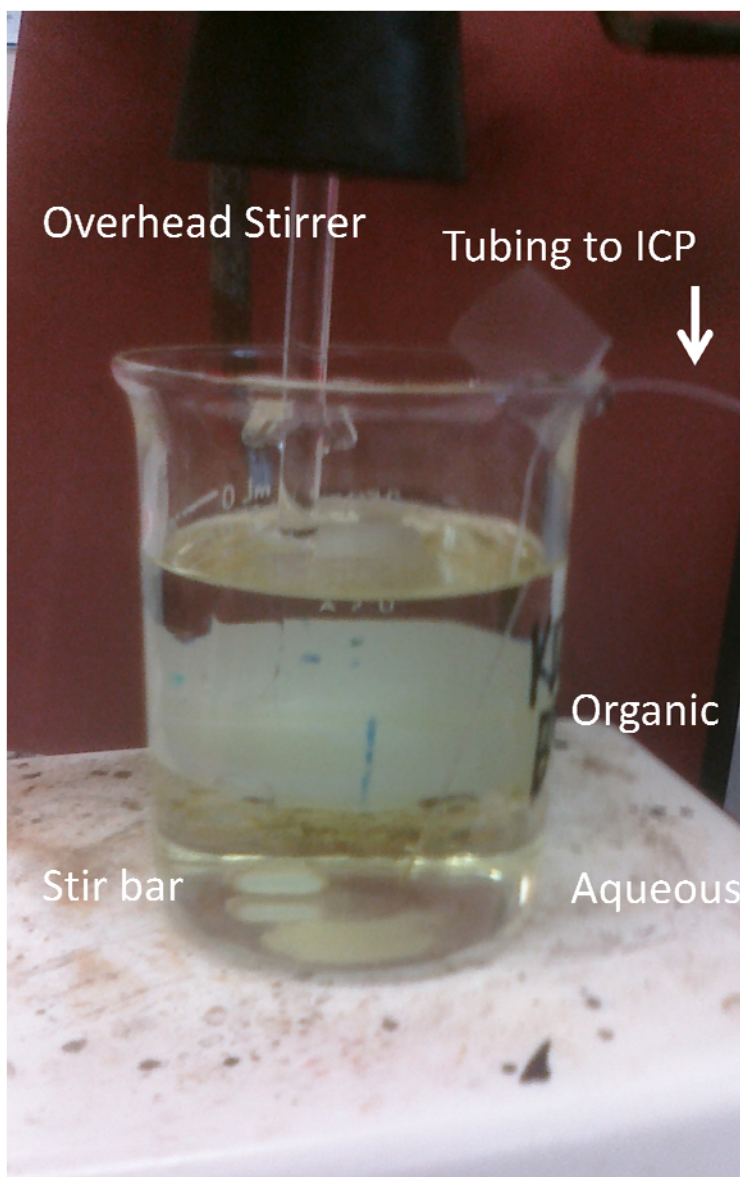


Figure 3.7. Photograph of the modified Lewis cell used in the Cr extraction kinetics studies.

A long-term extraction study was performed for each optimized LLE system. Samples were collected over a period of 24 hours from the aqueous phase via a length of capillary tubing in the aqueous phase and the peristaltic pump on the ICP-OES. Samples were pumped into a small test tube then capped and stored until analysis. For the method of initial rates analysis, samples were taken at 4 minutes from the onset of stirring. *In-situ* ICP-OES was used to analyze the aqueous phase Cr concentration during the method of initial rate analysis.

3.3.2 Results and Discussion

A long-term extraction was performed with both systems in order to determine the appropriate timeframe for kinetic analysis. The concentration-time profile is shown in Figure 3.8. The graph illustrates the normalized removal of Cr from each optimized extraction system. The error bars represent an estimated experimental error of 10%. Both systems appear to exhibit exponential decay. The half-life (τ) values for Cr (III) and Cr (VI) are illustrated by the dashed lines and are approximately 1 and 3 hours, respectively.

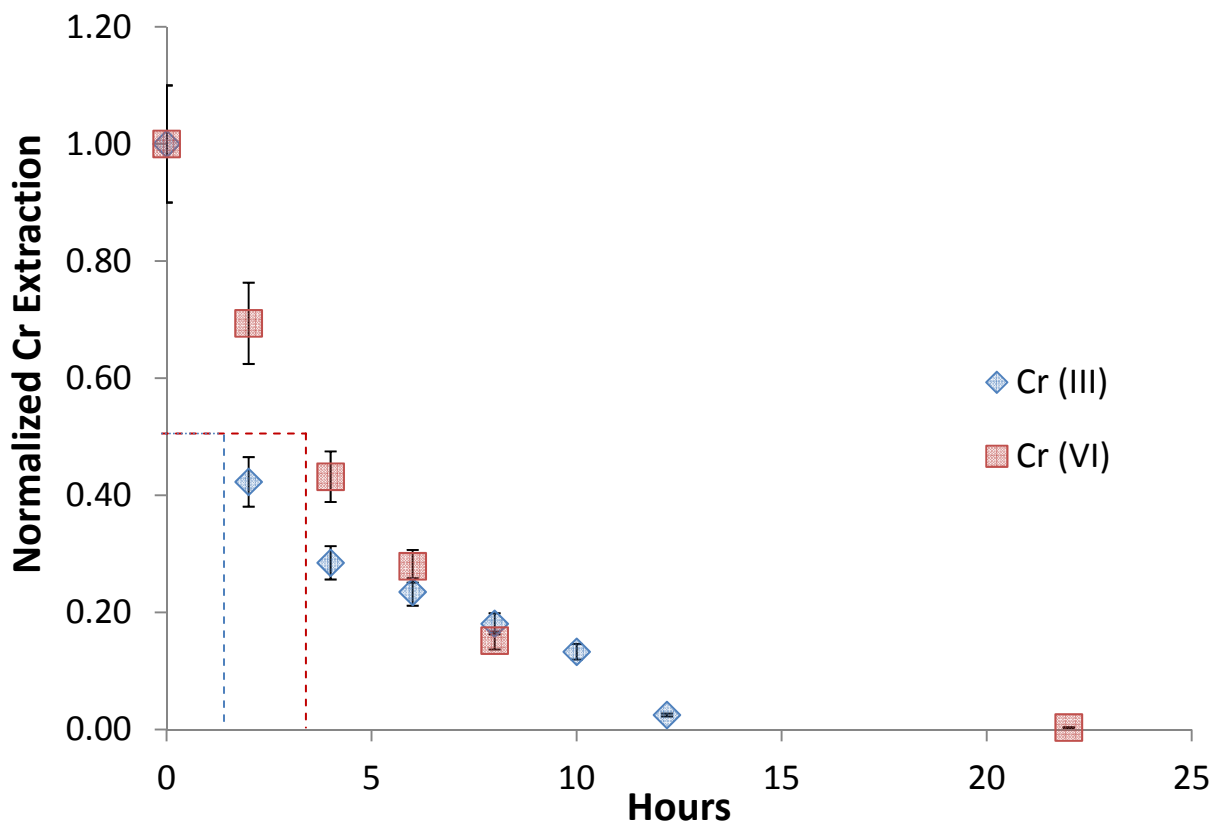


Figure 3.8. Long-term (>1 day) Cr (III) and Cr (VI) liquid-liquid extraction (LLE). The dashed lines represent the half-life (τ) values for each extraction system.

Since the concentration-time profile of each Cr species appears exponential with a well-defined linear region at sampling times less than 2 hours, the method of initial rates is a valid kinetic analysis for both Cr liquid-liquid extraction systems. According to the method of initial rates, the [Cr] is monitored in the linear portion of the curve. Less than 10% of the Cr present in the system has been removed (or converted) in the linear region. A convenience that accompanies the method of initial rates is that there is no assumption about the actual rate law.

In the method of initial rates, the initial rate, or the amount of Cr extracted at 4 minutes from the onset of stirring, is defined according to equation 3.5. Equation 3.6 is generated by taking the log of both sides of equation 3.5. When one parameter is varied and the other three parameters remain constant, equation 3.6 simplifies to equation 3.7, where C is defined in equation 3.8. A plot of the log of the initial rate versus the log of the initial Cr concentration generates a line with a slope equal to the reaction order with respect to the initial Cr concentration. The intercept of the line is equal to the constant C, which contains the observed rate constant (k_{obs}). To determine the remaining reaction orders, $\log k_{obs}$ versus varied parameter plots were generated and reaction order were the slope of the line.

$$Rate = \left(-\frac{d[Cr]}{dt} \right)_o \cong \left(-\frac{\Delta[Cr]}{\Delta t} \right)_o = k[Cr^{+x}]^a[H^+]^b[Carrier]^c[Decanol]^d \quad (3.5)$$

$$\log \left(-\frac{d[Cr]}{dt} \right)_o = \log k_{obs} + a \log[Cr^{+x}] + b \log[H^+] + c \log[Carrier] + d \log[Decanol] \quad (3.6)$$

$$\log \left(-\frac{d[Cr]}{dt} \right)_o = a \log[Cr^{+x}] + C \quad (3.7)$$

$$C = \log k_{obs} = \log k + b \log[H^+] + c \log[Carrier] + d \log[Decanol] \quad (3.8)$$

Assumptions were made during the method of initial rate analysis. The first assumption was that no back extraction (movement of a Cr ion from the organic phase into the aqueous phase) occurred. The second assumption was that the diffusion rates in the system remain constant (Cr through the aqueous phase and the carrier molecule through the organic phase). It should be noted that the transition state of the LLE process is not a discrete transition state as one would obtain in a chemical reaction; it is an ensemble of species likely involved in the extraction process.

The graphs used to determine reaction orders in the kinetics experiments are presented with the x-axis corresponding to the log of the parameter of interest (initial Cr concentration, initial carrier concentration, initial decanol concentration, or initial H^+ concentration) and the y-axis representing the log of Cr extracted (Figures 3.9 and 3.13) or the log of the apparent rate constant ($\log k_{obs}$) (Figures 3.10–3.16). The experimental conditions are listed in the graph captions. All axes are formatted to the same scale to allow for direct comparison. Experimental error was determined to be approximately 10% and is indicated by the error bars in each graph.

Figure 3.9 shows the determination of the reaction order with respect to initial Cr (III) concentration. The concentrations of D2EHPA (Cr (III) carrier molecule), decanol, and H^+ are held constant while the feed phase Cr (III) concentration is varied. The plot illustrates the amount of Cr extracted as a function of initial Cr (III) concentration. The slope of the regression equation ($m = 1.3$) is the reaction order with respect to the initial Cr (III) concentration.

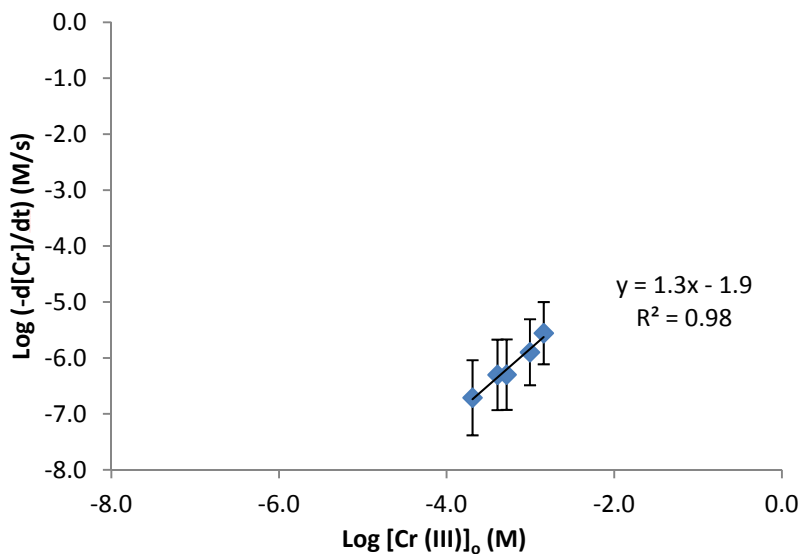


Figure 3.9. Determination of reaction order with respect to initial Cr (III) concentration. Reaction Conditions: D2EHPA: 0.329 M, Decanol: 0.7865 M, pH = 5.25, $\Delta t = 4$ min.

Figure 3.10 shows the determination of the reaction order with respect to initial D2EHPA concentration. The concentrations of Cr (III), decanol, and H^+ are held constant while the organic phase D2EHPA concentration is varied. The plot illustrates the log of the apparent rate constant ($\log k_{obs}$) as a function of initial D2EHPA concentration. The slope of the regression equation ($m = 1.3$) is the reaction order with respect to the initial D2EHPA concentration.

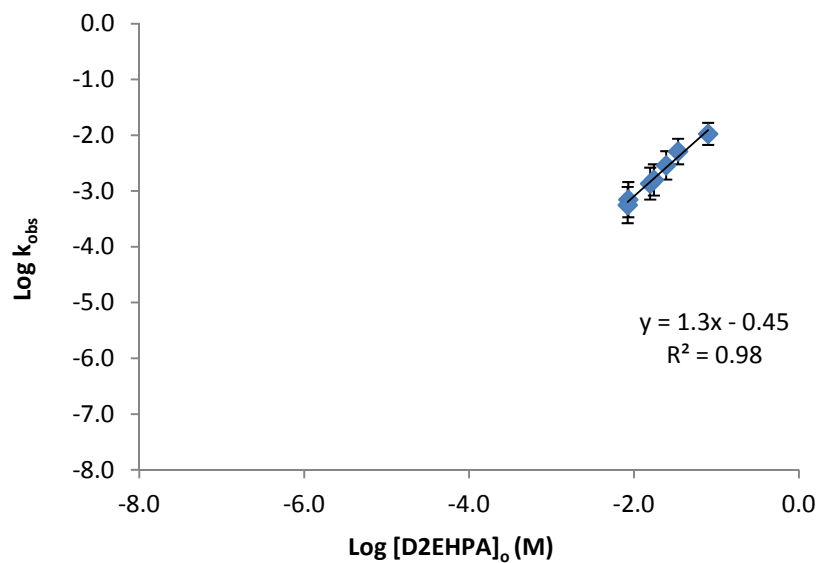


Figure 3.10. Determination of reaction order with respect to initial D2EHPA concentration.
Reaction conditions: Cr (III): 0.0009616 M, Decanol: 0.7865 M, pH = 3.89, $\Delta t = 4$ min.

Figure 3.11 shows the determination of the reaction order with respect to initial decanol concentration. The concentrations of Cr (III), D2EHPA, and H^+ are held constant while the organic phase decanol concentration is varied. The plot illustrates the log of the apparent rate constant ($\log k_{obs}$) as a function of initial decanol concentration. The slope of the regression equation ($m = 0.34$) is the reaction order with respect to the initial decanol concentration.

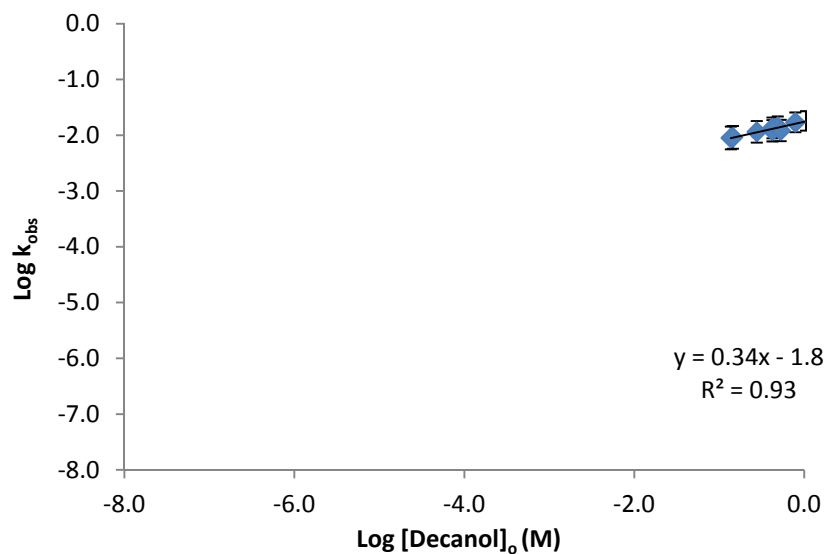


Figure 3.11. Determination of reaction order with respect to initial decanol concentration. Reaction conditions: Cr (III): 0.0009616 M, D2EHPA: 0.329 M, pH = 3.89, $\Delta t = 4$ min.

Figure 3.12 shows the determination of the reaction order with respect to initial H^+ concentration. The concentrations of Cr (III), D2EHPA, and decanol are held constant while the organic phase decanol concentration is varied. The plot illustrates the log of the apparent rate constant ($\log k_{obs}$) as a function of initial proton concentration. The slope of the regression equation ($m = 0.06$) is the reaction order with respect to the initial H^+ concentration.

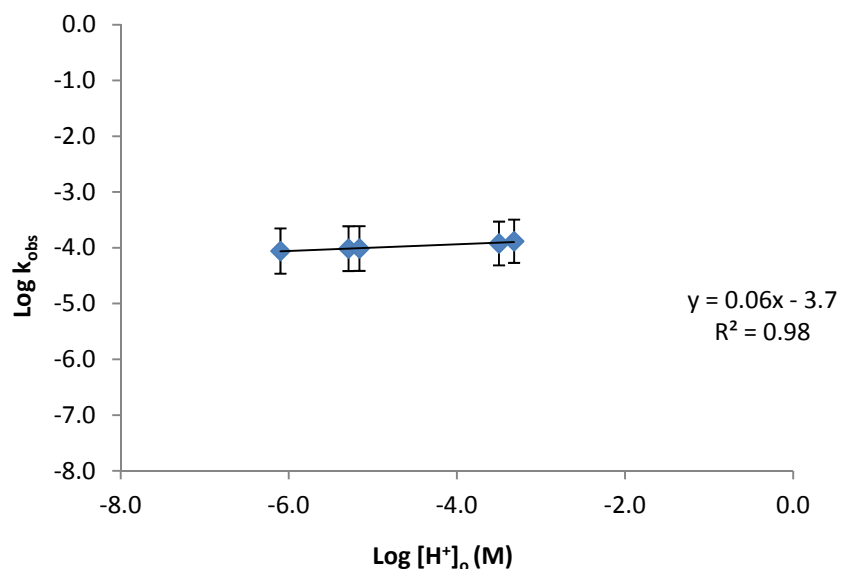


Figure 3.12. Determination of reaction order with respect to initial proton concentration.
Reaction conditions: Cr (III): 0.0009616 M, D2EHPA: 0.329 M, Decanol: 0.7865 M,
 $\Delta t=4$ min.

Figure 3.13 shows the determination of the reaction order with respect to initial Cr (VI) concentration. The concentrations of Aliquat-336 (Cr (VI) carrier molecule), decanol, and H^+ are held constant while the feed phase Cr (VI) concentration is varies. The plot illustrates the amount of Cr extracted as a function of initial Cr (VI) concentration. The slope of the regression equation ($m = 0.61$) is the reaction order with respect to the initial Cr (VI) concentration.

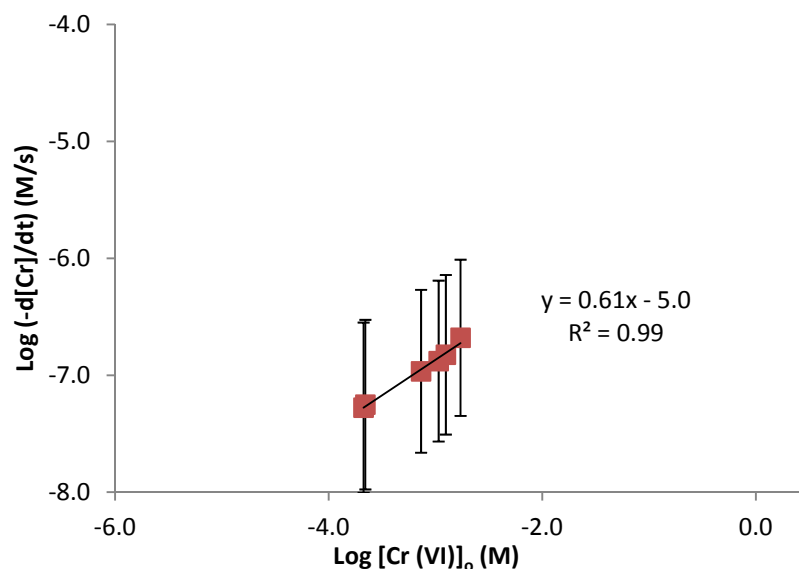


Figure 3.13. Determination of reaction order with respect to initial Cr (VI) concentration. Reaction conditions: Aliquat-336: 0.04392 M, Decanol: 1.0325 M, pH = 5.14, $\Delta t = 4$ min.

Figure 3.14 shows the determination of the reaction order with respect to initial Aliquat-336 concentration. The concentrations of Cr (VI), decanol, and H^+ are held constant while the organic phase Aliquat-336 concentration is varied. The plot illustrates the log of the apparent rate constant ($\log k_{obs}$) as a function of initial Aliquat-336 concentration. The slope of the regression equation ($m = 0.57$) is the reaction order with respect to the initial Aliquat-336 concentration.

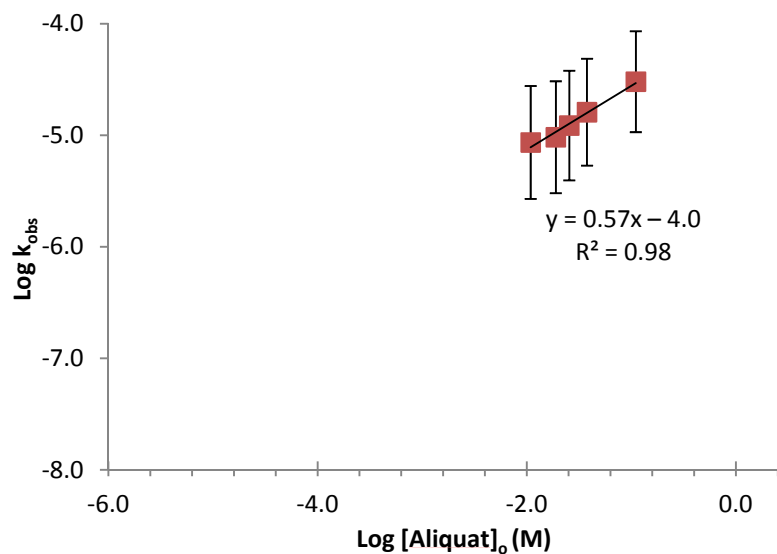


Figure 3.14. Determination of reaction order with respect to initial Aliquat-336 concentration. Reaction conditions: Cr (VI): 0.0009616 M, Decanol: 1.0325 M, pH = 5.14, $\Delta t = 4$ min.

Figure 3.15 shows the determination of the reaction order with respect to initial decanol concentration. The concentrations of Cr (VI), Aliquat-336, and H^+ are held constant while the organic phase decanol concentration is varied. The plot illustrates the log of the apparent rate constant ($\log k_{obs}$) as a function of initial decanol concentration. The slope of the regression equation ($m = -0.17$) is the reaction order with respect to the initial decanol concentration.

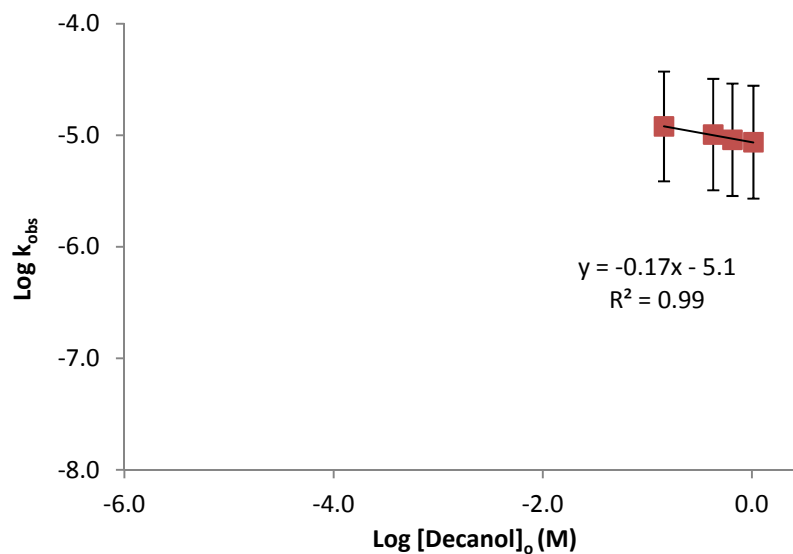


Figure 3.15. Determination of reaction order with respect to initial decanol concentration. Reaction conditions: Cr (VI): 0.0009616 M, Aliquat-336: 0.04392 M, pH = 5.14, $\Delta t = 4$ min.

Figure 3.16 shows the determination of the reaction order with respect to initial H^+ concentration. The concentrations of Cr (VI), Aliquat-336, and decanol are held constant while the organic phase decanol concentration is varied. The plot illustrates the log of the apparent rate constant ($\log k_{obs}$) as a function of initial proton concentration. The slope of the regression equation ($m = -0.27$) is the reaction order with respect to the initial H^+ concentration.

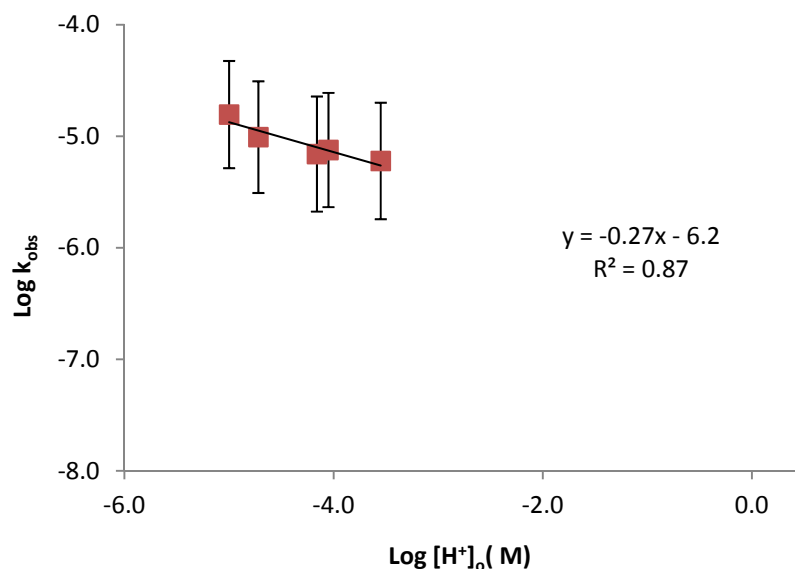


Figure 3.16. Determination of reaction order with respect to initial proton concentration. Reaction conditions: Cr (VI): 0.0009616 M, Aliquat-336: 0.04392 M, Decanol: 1.0325 M, $\Delta t = 4$ min.

The results of the Lewis cell studies are in Table 3.11. The rate law provides information about the charge and composition of the transition state for a reaction.³⁴ This means that the reaction orders indicate how many molecules are present in the transition state. The transition state of the reaction occurs at the interface of the aqueous and organic phase. The results indicate a 1:1 ratio of Cr ion and carrier molecule in the transition state for both Cr (III) and Cr (VI). Furthermore, the results suggest that the proton reaction order is approximately zero for both cases, which indicates that there is little effect of pH on the reaction rate in the pH range studied. To date, there are no reported reaction orders for decanol in the extraction of Cr. We suspect that the reaction orders in decanol for Cr (III) and Cr (VI) are probably not “true” reaction orders. Alternatively, it is likely that the decanol functions in the systems as a phase modifier by simply modifying the polarity of the organic phase (e.g. a modest solvent effect over the range of concentrations studied). The function of decanol as a phase modifier is well documented in the literature.

Table 3.11. Apparent reaction orders of Cr^{+x}, carrier, decanol, and proton for Cr (III) and Cr (VI) as well as apparent rate constants determined by liquid-liquid extraction kinetics.

	Cr (III) (95% confidence)	Cr (VI) (95% confidence)
Cr	1.3 (0.4)	0.61 (0.10)
Carrier	1.3 (0.2)	0.57 (0.17)
Decanol	0.34 (0.09)	-0.17 (0.06)
[H ⁺]	0.06 (0.02)	-0.27 (0.19)
<i>k</i>	9.4e-4 (3.2 e-4) M ⁻³ s ⁻¹	7.4e-7 (4.6 e-7) M ^{-0.25} s ⁻¹

Upon further reflection of the kinetic pH results, the role of pH in the extraction of Cr was questioned. Could variation in pH change the speciation of Cr? Could the non-integer reaction orders for Cr (III) and Cr (VI) result from more than one Cr (III) or Cr (VI) species present at the given pH? The Pourbaix diagram, shown in Figure 1.2, illustrates the dependence of Cr species on pH and potential. Since the potential of natural systems generally is not variable, the Pourbaix diagram provides the dominate Cr species at a given pH. The non-integer reactions orders for Cr (III) and Cr (VI) could result from more than one Cr (III) or Cr (VI) species present at the given pH. Therefore, fundamental principles of acid-base chemistry were employed to examine the species distribution of Cr (III) and Cr (VI) over the pH ranges used in the LLE kinetics experiments. Using the Henderson-Hasselbalch equation, the ratio of dominate Cr species was computed and graphed for Cr (III) and Cr (VI). Figures 3.17 and 3.18 illustrate the species distribution for Cr (III) and Cr (VI), respectively, over the LLE pH ranges studied (denoted by the red vertical lines). Figure 3.17 illustrates that the ratio of Cr(OH)₂⁺ to Cr(OH)²⁺ remains approximately constant over the range of pHs studied (within 10%). Furthermore, the

dominant form of Cr (III) is $\text{Cr}(\text{OH})^{2+}$. The results for the Cr (VI) species are shown in Figure 3.18. The ratio of CrO_4^{2-} to HCrO_4^- is approximately zero over the pH range studied, which means that the dominate form of Cr (VI) is HCrO_4^- .

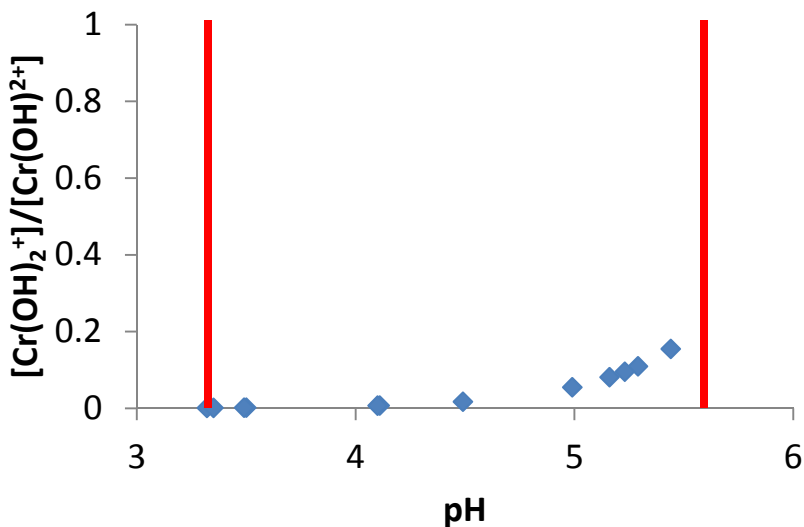


Figure 3.17. Species distribution of Cr (III). The red vertical lines denote the pH range studied in the liquid-liquid extraction kinetics experiments.

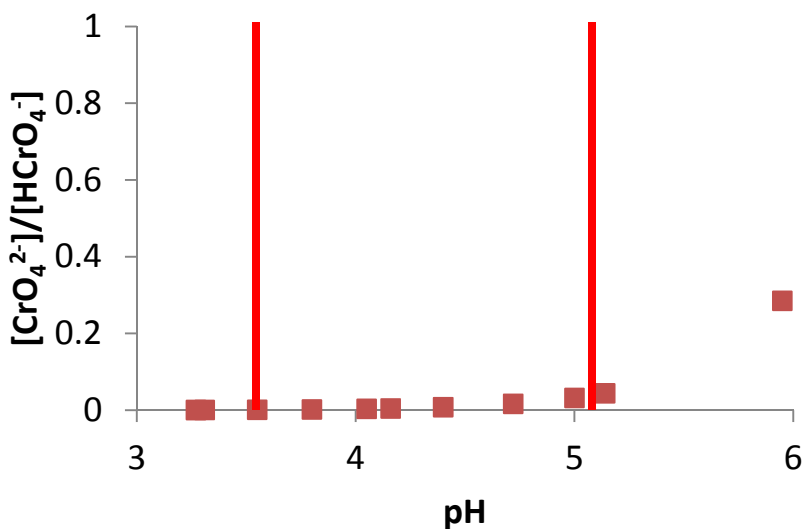


Figure 3.18. Species distribution of Cr (VI). The red vertical lines denote the pH range studied in the liquid-liquid extraction kinetics experiments.

The non-integer reaction orders are unlikely attributable to the presence of more than one Cr species. It is hypothesized that the non-integer reaction orders reflect the fact that the reaction order is an ensemble average of the components of the transition state. This means that it is possible to have more than one Cr and/or carrier molecule present in the transition state. For instance, the reaction order of 1.3 for Cr (III) and D2EHPA means that there could be two molecules of each present in the transition state at times, such that the number of 2 molecule ion-pairs and 4 molecule ion-pairs averages out to be 1.3. The existence of more than one D2EHPA molecule is plausible considering the reports in the literature of the dimerization of D2EHPA.^{35,36}

The overall rate laws for Cr (III) and Cr (VI) are written by substituting the rate constants and reaction orders from Table 3.11 into Equation 3.1. Equations 3.9 and 3.10 are the overall rate laws for Cr (III) and Cr (VI), respectively. The calculated rate constants have been adjusted to reflect the shape and appearance of the experimental data. Figure 3.19 illustrates how well the overall Cr extraction rate laws fit the observed LLE kinetic data.

$$Rate_{Cr(III)} = (8.0 \times 10^{-3} M^{-3} s^{-1}) [Cr]^{1.3} [D2EHPA]^{1.3} [Decanol]^{0.34} [H^+]^{0.06} \quad (3.9)$$

$$Rate_{Cr(VI)} = (1.2 \times 10^{-6} M^{0.25} s^{-1}) [Cr]^{0.61} [Aliquat - 336]^{0.57} [Decanol]^{-0.17} [H^+]^{-0.27} \quad (3.10)$$

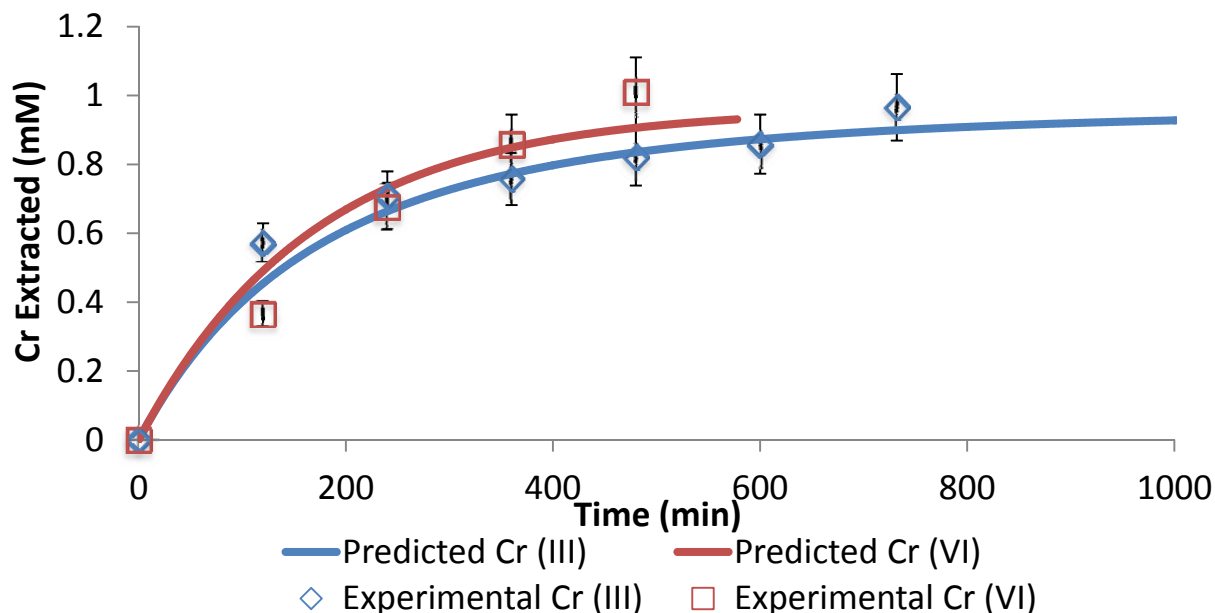


Figure 3.19. Overlay of extraction rate laws (equations 3.9 and 3.10) on experimental Cr liquid-liquid extraction.

Since the extraction rate laws have been adjusted to mirror the 24 hour experimental data, the rate laws can be applied to the long-term sampler extraction studies (see Section 4.3.1 for details). The application of the rate laws to the longer-term sampler extraction data provides information about the mechanism of liquid-liquid extraction in the sampler as well as the apparent rate constants. Information about the charge and composition of the transition state in the sampler extraction mechanism (i.e., how many molecules of each component are present in the transition state) can also be obtained. If the rate laws obtained from the LLE kinetics studies (equations 3.9 and 3.10) model the sampler extraction data, then it is reasonable to suspect that the same mechanism of extraction occurs in both systems. This is assumed to be true. However, the LLE studies only model the first step of the SLM-based extraction mechanism. Recall that the SLM-based mechanism consists of two consecutive LLEs. Hence, agreement in the two

experiments means that the second LLE step in the SLM process (extraction of the Cr ion into the acceptor phase from the organic phase) is a faster than the first LLE step (extraction of the Cr ion into the organic phase from the feed phase).

In Figure 3.20, the three week sampler extraction data is presented as open diamonds and open squares for Cr (III) and Cr (VI), respectively. The solid lines represent the predicted Cr uptake based on the rate laws established from the LLE kinetics data (equations 3.9 and 3.10). The predicted values have approximately the same shape as the experimental data. However, the rate laws predict that the Cr will be extracted before the first data point (day 1). Clearly, equations 3.9 and 3.10 predict a faster Cr extraction than what is observed.

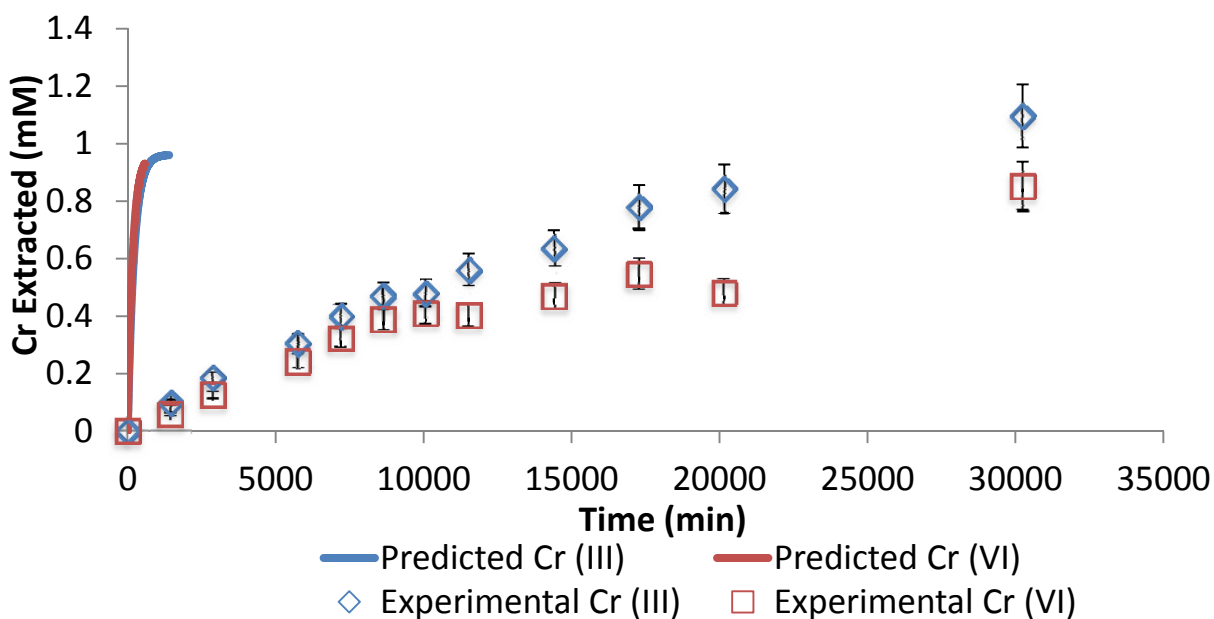


Figure 3.20. Overlay of extraction rate laws (equations 3.9 and 3.10) on experimental sampler extraction data.

Two possible explanations for the discrepancy in the predicted versus experimental SLM-based extraction data are the second LLE step or the presence of the membrane. If the second LLE step is a slower process than the first LLE step, the shape of the predicted and experimental extraction curves would be different. Figure 3.20 shows that the shapes are similar. Thus, the second LLE step is not the contributing factor for the delay between the experimental and theoretical values. Therefore, the membrane is responsible for the significant difference shown in Figure 3.20. The membrane is an essential part of the SLM-based extraction process; the hydrophobic membrane provides the necessary physical boundary that separates the two aqueous phases (feed and acceptor). Channels exist through the polymeric material of the membrane. These paths slow the extraction speed. Instead of the direct extraction of Cr at a liquid-liquid interface, the extraction in the SLM occurs *through* the polymeric membrane. Therefore, the rate of extraction is slowed. If the apparent rate constants from equations 3.5 and 3.6 are manipulated (slowed down), the predicted values and the experimental data become aligned (Figure 3.21).

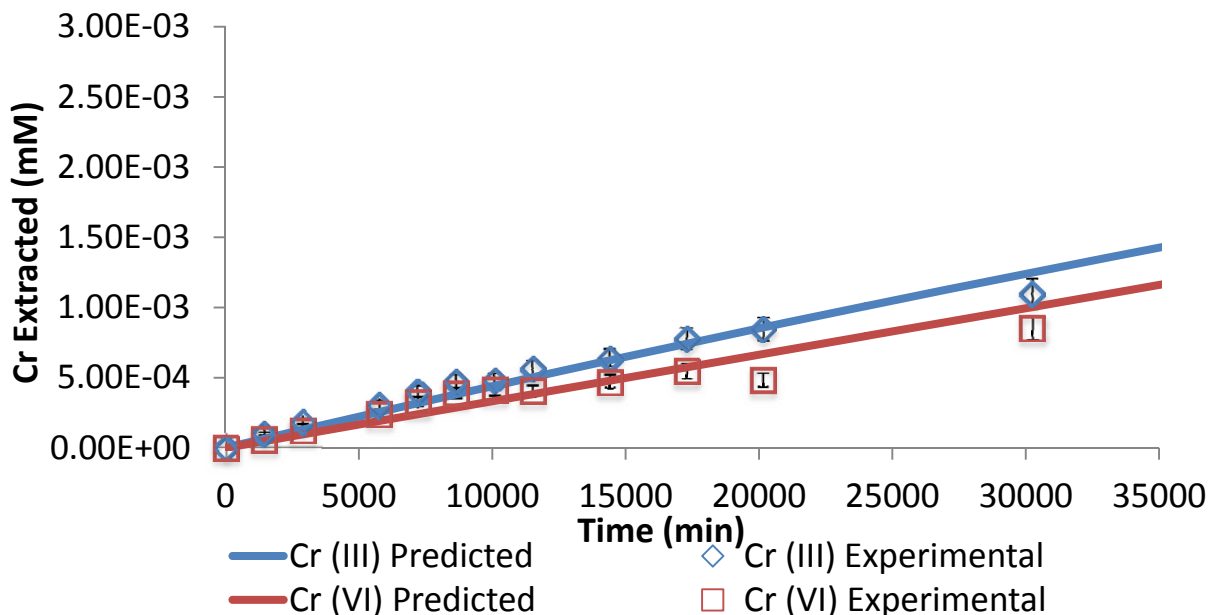


Figure 3.21. Overlay of overall extraction rate laws with adjusted rate constants (equations 3.11 and 3.12) on experimental sampler extraction data.

The new rate laws for the SLM-based sampling systems are given in equations 3.11 and 3.12 for Cr (III) and Cr (VI), respectively. The rate constants are four orders of magnitude lower than the corresponding rate constants in equations 3.9 and 3.10. Figure 3.21 shows that the four order of magnitude modification in the rate constants align the predicted extraction with the experimental data. The adjusted rate laws for the SLM-based extraction can be used to predict Cr extraction as well as to determine initial [Cr] in contaminated sites, given the extraction [Cr], initial pH, initial carrier concentration, initial decanol concentration, and the sampler residence time. The concentrations (extracted Cr, initial decanol, initial carrier, H^+) and sampling time (in seconds) are substituted into equations 3.11 and 3.12. Then, the equations are solved for the initial Cr concentration.

$$Rate_{Cr(III)} = (8.9 \times 10^{-6} M^{-3} s^{-1}) [Cr]^{1.3} [D2EHPA]^{1.3} [Decanol]^{0.34} [H^+]^{0.06} \quad (3.11)$$

$$Rate_{Cr(VI)} = (2.5 \times 10^{-11} M^{0.25} s^{-1}) [Cr]^{0.61} [Aliquat - 336]^{0.57} [Decanol]^{-0.17} [H^+]^{-0.27} \quad (3.12)$$

3.3.3 Occam's Razor

Although the kinetic data presented in Section 3.3.2 indicates that the reactions orders are non-integer values, the ratio of Cr ion to carrier molecule is 1:1 for both Cr (III) and Cr (VI), and the reaction order for decanol and hydrogen ion are negligible. Occam's Razor states that the less complex explanation should be used when there are more than one possible explanations. In the case of the rate laws established from the kinetic data, Occam's Razor favors a simpler model with integer reaction orders, i.e., first order in Cr and carrier, and zero order in decanol and hydrogen ion. The issue to address is whether this simpler model is adequate. The same data analysis was used to fit the data to the experimental LLE and sampler data. The modeling from Section 3.3.2 will be compared to that obtained using the Occam's Razor rate laws.

The calculated rate constants were adjusted to reflect the shape and appearance of the experimental LLE data. Figure 3.22 illustrates how well the Occam's razor extraction rate laws fit the observed kinetics data. The rate constant for Cr (III) is slightly slower in equation 3.13 than that of equation 3.9. The rate constant in equation 3.14 is three orders of magnitude faster than that in equation 3.10. In setting the positive fractional reaction orders to 1 for decanol and hydrogen ion for Cr (III), the rate is subsequently increased. Therefore, the rate constant has to be reduced in the Occam's Razor case to maintain a consistent fit with the experimental data. For the Cr (VI) system, setting the reaction orders to 1 for decanol and hydrogen ion increases the denominator to 1 since the reactions orders of each component (decanol and H^+) was negative.

This has an over decrease on the reaction rate. Therefore, the rate constant must be increased to maintain a consistent fit with the experimental data.

$$Rate_{Cr(III)} = (2.4 \times 10^{-4} M^{-2} s^{-1}) [Cr] [D2EHPA] \quad (3.13)$$

$$Rate_{Cr(VI)} = (2.3 \times 10^{-3} M^{-2} s^{-1}) [Cr] [Aliquat - 336] \quad (3.14)$$

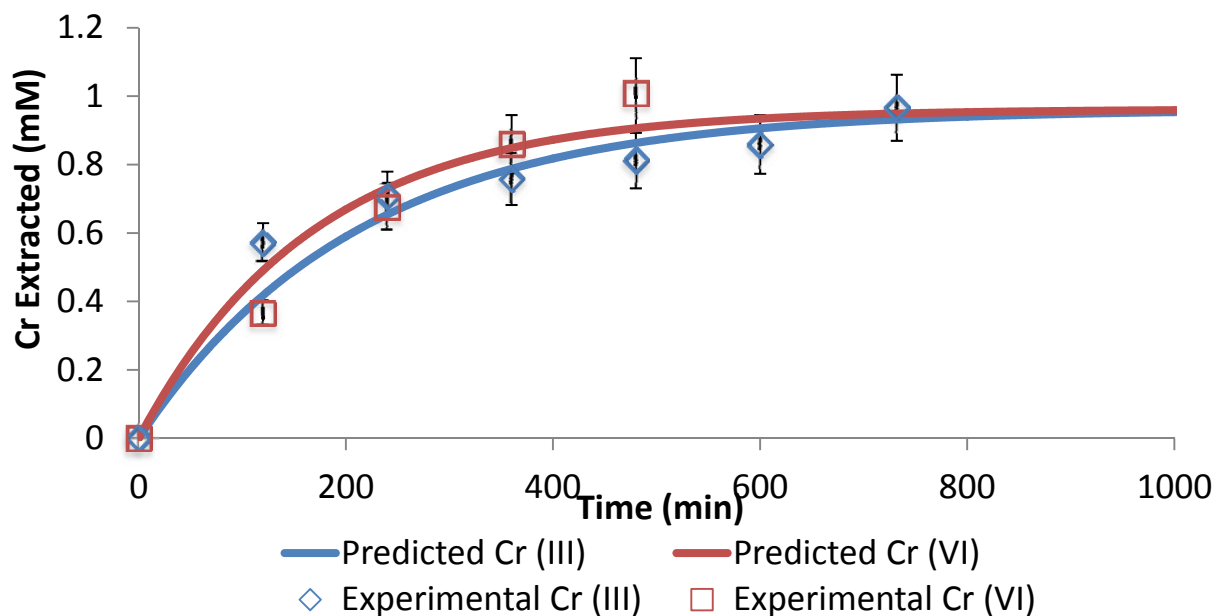


Figure 3.22. Overlay of Occam's Razor extraction rate laws (equations 3.13 and 3.14) on experimental Cr liquid-liquid extraction kinetics data.

The model obtained from the 24 hour Cr extraction experiments was applied to the long-term sampler extraction studies (see Section 5.2.1 for details). In Figure 3.22, the three week sampler extraction data is presented as open diamonds and open squares for Cr (III) and Cr (VI), respectively. The solid lines represent the predicted Cr uptake based on the rate laws established from the LLE kinetics data (equations 3.13 and 3.14). As seen in Figure 3.20, the Occam's Razor

predicted values have approximately the same shape as the experimental data. However, the rate laws predict that the Cr will be extracted before the first data point (day 1). The Occam's Razor rate laws for LLE (equations 3.13 and 3.14) predict a faster Cr extraction than what is observed. This result is consistent with the results in Section 3.3.2.

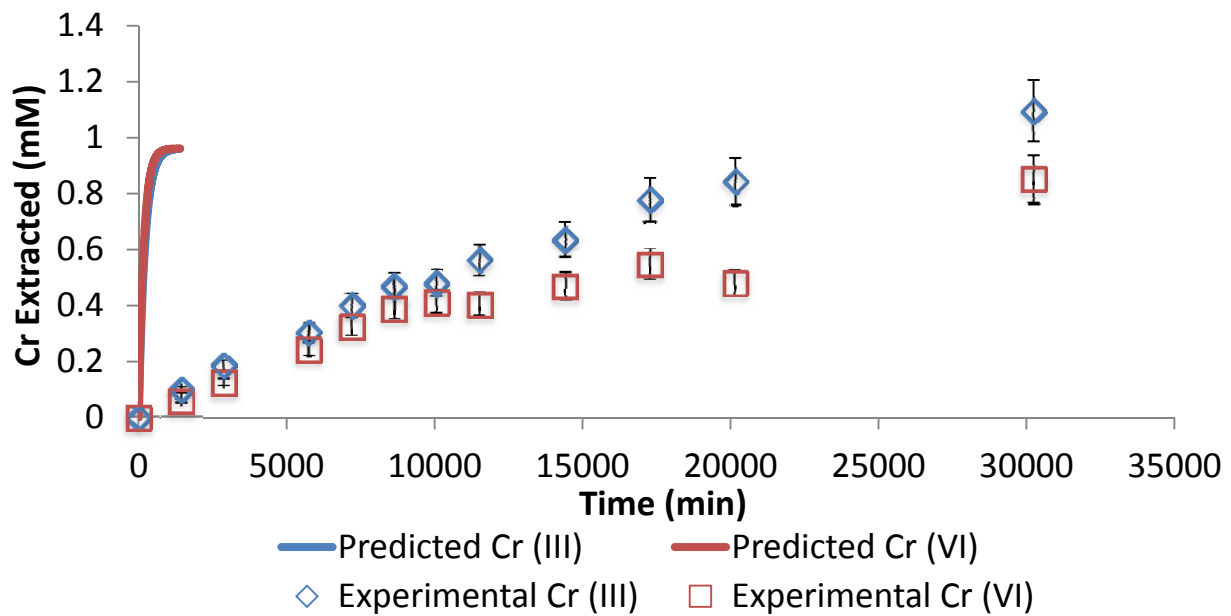


Figure 3.23. Overlay of Occam's Razor extraction rate laws (equations 3.13 and 3.14) on experimental sampler extraction data.

The rate constants of the Occam's Razor rate laws were adjusted to model the experimental sampler extraction data. The new model is shown with the experimental data in Figure 3.24. The Occam's Razor rate laws are given in Equations 3.15 and 3.16. The alignment of Occam's Razor rate laws when the rate constants are reduced (compared to the rate constants

in equations 3.13 and 3.14) to the experimental data supports the hypothesis that the first LLE step is slower than the second step.

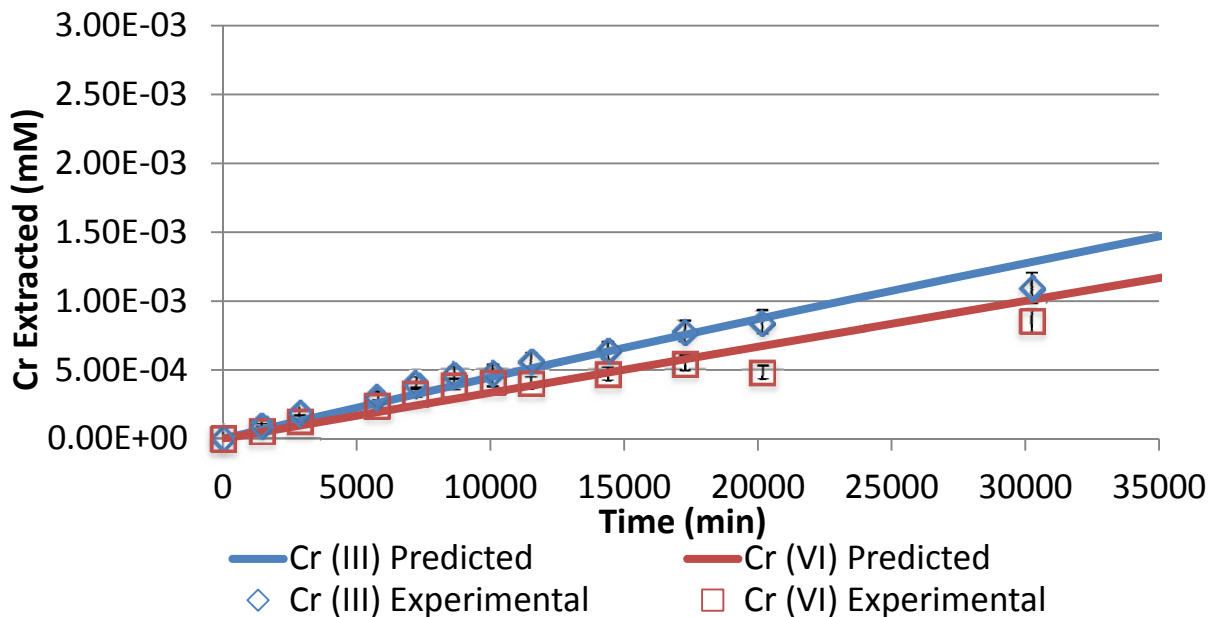


Figure 3.24. Overlay of Occam’s Razor extraction rate laws (equations 3.15 and 3.16) on experimental sampler extraction data.

The rate constants are three and four orders of magnitude slower than those of the LLE rate laws. This result is consistent with the magnitude of decrease seen in Section 3.3.2. Also, the Cr (III) Occam’s Razor rate constant is only slightly slower than the rate constant of equation 3.7. As seen in adjustment of the rate constants in LLE kinetics data, the rate constant must decrease when the positive fractional reaction orders are set to one (1). Conversely, the rate constant of the Cr (VI) Occam’s Razor rate law must increase when the negative fractional reactions orders are set to one (1). Therefore, the rate constant increases three orders of magnitude. It should be noted that the increase of rate constants from equation 3.10 to 3.14 is also three orders of magnitude.

$$Rate_{Cr(III)} = (2.4 \times 10^{-7} M^{-2} s^{-1}) [Cr] [D2EHPA] \quad (3.15)$$

$$Rate_{Cr(VI)} = (6.6 \times 10^{-8} M^{-2} s^{-1}) [Cr] [Aliquat - 336] \quad (3.16)$$

3.4 Summary

Equilibrium liquid-liquid extraction studies were performed in order to optimize the parameters for supported liquid membrane extraction. The optimal conditions for Cr (III) extraction are 10% D2EHPA, 15% decanol, and 0.1 M HCl as the acceptor phase, and the optimal conditions for Cr (VI) extraction are 2% Aliquat-336, 20% decanol, and 5 M HCl as the acceptor phase. Furthermore, LLE studies were performed in order to determine the kinetics of the extraction procedure. The kinetics studies are essential in the SLM parameter optimization procedure. The kinetic studies were also used to predict extraction in the SLM-based sampling systems. These results are the first kinetic measurements involving the sampling system designed in this work.

The kinetics data produced fractional reaction orders for the SLM components (Cr ion, carrier molecule, decanol, and proton). However, the Cr ion and carrier molecule reaction orders were 1:1 for both Cr systems, and the decanol and proton reaction orders were negligible (~0). The method of initial rates results define the experimental rate law and experimental rate constant. Occam's Razor shows that a simple 1:1 model seems to account for the experimental results. Therefore, the kinetics data was reanalyzed to predict Cr extraction in the SLM-based sampling systems under the simplified conditions.

The kinetics data provides a useful theoretical basis when the sampling system will be employed during *in-situ* Cr speciation. The Occam's Razor approach to the kinetics data

indicates that the simplified second-order rate law is as adequate a model of the experimental Cr SLM-based extraction as experimental model with fractional reaction orders. Therefore, the second-order rate laws can be used as a theoretical model to predict extraction behavior in future sampling applications. The initial Cr ion concentration as well as the carrier ion concentration are the two parameters that affect the extraction rate. In future sampling applications, the initial Cr ion concentration is an unknown variable. Therefore, the only parameter that can be controlled and optimized to achieve more efficient Cr extraction is the carrier molecule concentration. Also, the theoretical model developed in this chapter will assist in the selection of the appropriate sampling duration for future sampling applications.

3.5 References

- (1) Yang, X. J.; Fane, A. G.; Soldenhoff, K. *Ind. Eng. Chem. Res.* **2003**, *42*, 392.
- (2) Audunsson, G. *Anal. Chem.* **1986**, *58*, 2714.
- (3) Jonsson, J. A.; Lovkvist, P.; Audunsson, G. *Anal. Chim. Acta* **1993**, *277*, 9.
- (4) Choi, Y.-W.; Moon, S.-H. *Sep. Sci. Technol.* **2004**, *39*, 1663.
- (5) Soko, L.; Cukrowska, E.; Chimuka, L. *Anal. Chim. Acta* **2002**, *474*, 59.
- (6) Buonomenna, M. G.; Oranges, T.; Molinari, R.; Drioli, E. *Water Environ. Res.* **2006**, *78*, 69.
- (7) Alguacil, F. J.; Caravaca, C.; Martin, M. I. *J. Chem. Technol. Biotechnol.* **2003**, *78*, 1048.
- (8) Alonso, A. I.; Pantelides, C. C. *J. Membr. Sci.* **1996**, *110*, 151.
- (9) Castillo, E.; Granados, M.; Cortina, J. L. *Anal. Chim. Acta* **2002**, *464*, 197.
- (10) Jonsson, J. A.; Mathiasson, L. *Trends Anal. Chem.* **1999**, *18*, 318.
- (11) Franken, T. *Membr. Technol.* **1997**, *1997*, 6.
- (12) Alguacil, F. J.; Coedo, A. G.; Dorado, M. T. *Hydrometallurgy* **2000**, *57*, 51.

- (13) De, A. K.; Khopkar, S. M.; Chalmers, R. A. *Solvent Extraction of Metals*; Van Nostrand Reinhold: London, 1970.
- (14) Morrison, G. H.; Freiser, H. *Solvent Extraction in Analytical Chemistry*; J. Wiley & Sons, Inc. : New York, 1957.
- (15) Marcus, Y.; Kertes, A. S. *Ion exchange and solvent extraction of metal complexes*; Wiley-Interscience, 1969.
- (16) Sekine, T.; Hasegawa, Y. *Solvent Extraction Chemistry* Marcel Dekker: New York, 1977.
- (17) Khopkar, S. M. *Solvent Extraction Separation of Elements with Liquid Ion Exchangers*; New Age Science Limited Tunbridge Wells, UK, 2009.
- (18) Watarai, H.; Tsukahara, S.; Nagatani, H.; Ohashi, A. *B. Chem. Soc. Jpn* **2003**, *76*, 1471.
- (19) Niemczewska, J.; Cierpiszewski, R.; Szymanowski, J. *Physicochem. Probl. Mi.* **2003**, *37*, 87.
- (20) Sekine, T.; Komatsu, Y. *Journal of Inorganic and Nuclear Chemistry* **1975**, *37*, 185.
- (21) Komatsu, Y.; Honda, H.; Sekine, T. *J. Inorg. Nucl. Chem.* **1976**, *38*, 1861.
- (22) Islam, F.; Biswas, R. K. *J. Inorg. Nucl. Chem.* **1980**, *42*, 421.
- (23) Islam, F.; Biswas, R. K. *J. Inorg. Nucl. Chem.* **1978**, *40*, 559.
- (24) Islam, M. F.; Biswas, R. K. *J. Inorg. Nucl. Chem.* **1981**, *43*, 1929.
- (25) Biswas, R. K.; Mondal, M. G. K. *Hydrometallurgy* **2003**, *69*, 145.
- (26) Biswas, R. K.; Mondal, M. G. K. *Hydrometallurgy* **2003**, *69*, 117.
- (27) Freiser, H. *Anal. Chem.* **1968**, *40*, 522R.
- (28) McClellan, B. E.; Freiser, H. *Anal. Chem.* **1964**, *36*, 2262.
- (29) Dreisinger, D. B.; Charles Cooper, W. *Solvent Extr. Ion Exc.* **1986**, *4*, 135.
- (30) Dreisinger, D. B.; Charles Cooper, W. *Solvent Extr. Ion Exc.* **1989**, *7*, 335.
- (31) Sato, T.; Kawamura, M.; Nakamura, T.; Ueda, M. *J. Chem. Technol. Biotechnol.* **1978**, *28*, 85.
- (32) Biswas, R. K.; Habib, M. A.; Ali, M. R.; Haque, M. Z. *Pak. J. Sci. Ind. Res.* **1998**, *41*, 121.
- (33) Mathew, D. S.; Juang, R.-S. *Sep. Purif. Technol.* **2007**, *53*, 199.

- (34) Espenson, J. H. *Chemical Kinetics and Reaction Mechanisms*; 2nd ed.; McGraw-Hill Custom Publishing, 2002.
- (35) Huang, T. C.; Juang, R. S. *Ind. Eng. Chem. Fundam.* **1986**, 25, 752.
- (36) Komasaawa, I.; Otake, T.; Higaki, Y. *J. Inorg. Nucl. Chem.* **1981**, 43, 3351.

Chapter 4

Validation of the Supported Liquid Membrane (SLM) Based Samplers in Laboratory-Controlled and Simulated Natural Groundwater Conditions

4.1 Introduction

As the fundamental purpose of this work is to create a sampling system that is capable of the speciation of Cr (III) and Cr (VI) in natural waters, a critical portion of the work lies in the validation of the system. Previous chapters have focused on the design and fabrication (Chapter 2), the selection of optimal operating parameters (Chapter 3), as well as the kinetics involved in the sampling process (Chapter 3). Therefore, sampler validation requires the evaluation of the sampler in laboratory-controlled and simulated natural conditions.

Once the operating parameters of the SLM systems were optimized, studies were conducted to determine the performance of the SLM samplers. These performance studies were executed in the HDPE tanks as described by the experimental details given in Table 3 in Section 2.6. As part of the sampler evaluation process, a series of uptake and depletion studies were conducted for each Cr ion separately. The samplers were placed in the HDPE tanks and were removed at the pre-determined residence times of 1, 2, 4, 5, 6, 7, 8, 10, 12, 14, and 21 days. In some cases, the sampling period is less than 21 days. Inductively Coupled Plasma – Optical Emission Spectroscopy (ICP-OES) was performed on the contents of the sampler bottles to determine the extent of Cr uptake or depletion.

4.2 Experimental

The testing phase of the SLM samplers included a variety of tank studies using the sampling systems. An 8”x 8”x 8” high-density polyethylene (HDPE) tank, purchased from

Fisher Scientific, was used as the feed phase container in these studies and up to 4 samplers were placed in the tank. The arrangement of the samplers is shown in Figure 4.1.



Figure 4.1. Photograph of SLM samplers positioned in HDPE tank.

The tank studies investigated the uptake and depletion of Cr. The studies initially focused on Cr (III) and Cr (VI) separately, but later studies were designed to simulate natural sampling conditions where Cr (III) and Cr (VI) would be present together. The experimental conditions of each tank study are given in Table 4.1.

Table 4.1. Experimental conditions for SLM tank studies.

ION	STUDY	FEED PHASE	ORGANIC PHASE	ACCEPTOR PHASE
Cr (III)	Uptake	10 ppm Cr (III)	10% D2EHPA; 15% Decanol	0.1 M HCl
	Depletion	0.1 M HCl	10% D2EHPA; 15% Decanol	10 ppm Cr (III)
	Depletion with EDTA	0.1 M HCl ~1 mM EDTA	10% D2EHPA; 15% Decanol	10 ppm Cr (III)
	Uptake – no carrier	10 ppm Cr (III)	15% Decanol	0.1 M HCl
	Depletion – no carrier	0.1 M HCl	15% Decanol	10 ppm Cr (III)
	Uptake – selectivity	10 ppm Cr (III)	2% Aliquat-336; 20% Decanol	0.1 M HCl
	Depletion – selectivity	0.1 M HCl	2% Aliquat-336; 20% Decanol	10 ppm Cr (III)
	Simulated natural uptake (1&2)	Simulated groundwater with ~0.2 ppm Cr (III)	10% D2EHPA; 15% Decanol	0.1 M HCl
	Simulated natural uptake (3)	Simulated groundwater with 10 ppm Cr (III)	10% D2EHPA; 15% Decanol	0.1 M HCl
Cr (VI)	Uptake	10 ppm Cr (VI)	2% Aliquat-336; 20% Decanol	5 M HCl
	Depletion	5 M HCl	2% Aliquat-336; 20% Decanol	10 ppm Cr (VI)
	Uptake – no carrier	10 ppm Cr (VI)	20% Decanol	5 M HCl
	Uptake – selectivity	10 ppm Cr (VI)	10% D2EHPA; 15% Decanol	5 M HCl
	Simulated natural uptake (1&2)	Simulated groundwater with ~0.2 ppm Cr (VI)	2% Aliquat-336; 20% Decanol	5 M HCl
	Simulated natural uptake (3)	Simulated groundwater with 10 ppm Cr (VI)	2% Aliquat-336; 20% Decanol	5 M HCl

4.2.1 Cr (III) Uptake

The tank was filled with ~2.5 L 10 ppm Cr (III). The membrane was prepared according to the wet preparation procedure described by Yang and Fane.¹ Accordingly, a Teflon[®] membrane was soaked in a 10 mL organic phase solution containing 10% D2EHPA and 15% decanol in kerosene. The membrane was removed from the solution and placed on the

opposite side of the Teflon[®] plate bonded to the bottle cap. A second Teflon[®] plate (minus the bottle cap) was placed on top of the first plate to sandwich the membrane. Screws were placed through the holes in the corners of the plates to secure the membrane between the plates of the sampler. The acceptor phase (50.0 mL of 0.1 M HCl) was pipetted into the Teflon[®] bottle. Then, the bottle was attached to the bottled cap (screwed on). The completed samplers were placed in the tank on their sides. A Teflon[®] plate was placed under the bottle of the sampler to ensure that the entire membrane was covered by the acceptor phase solution. The tank was covered with its lid and the samplers were allowed to sit in the tank undisturbed until the predetermined removal date. The removal dates were based on residence time in the tank and were selected to be 1, 2, 4, 5, 6, 7, 8, 10, 12, 14, and 21 days.

4.2.2 Cr (VI) Uptake

The tank was filled with ~2.5 L 10 ppm Cr (VI). As with the Cr (III) uptake studies, the membrane was prepared using the wet preparation method (Section 4.2.1). The organic phase (10 mL) for the Cr (VI) uptake studies consisted of 2% Aliquat-336 and 20% decanol in a kerosene matrix. The membrane was soaked for 10 minutes then removed from the solution and assembled in the Teflon[®] samplers as described in Section 2.2.7. The acceptor phase (50.0 mL of 5 M HCl) was pipetted into the Teflon[®] bottle, which was attached to the bottle cap to complete the sampling system. The completed samplers were placed in the tank according to the procedure described in Section 2.2.7 and removed according to the schedule also described in the previous section.

4.2.3 Cr (III) Depletion

The Cr (III) Depletion experiments following the same procedure detailed in Section 4.2.1, except the contents of the feed and acceptor phases are switched. The tank

contains ~2.5 L 0.1 M HCl in the depletion experiments and the acceptor phase is 50.0 mL of the 10 ppm Cr (III) solution.

4.2.4 Cr (III) Depletion with EDTA

The experimental details for the Cr (III) Depletion studies with EDTA are the same as those described in Section 4.2.3, except for the contents of the tank. In these experiments, the tank contains ~1 mM EDTA dissolved in 0.1 M HCl.

4.2.5 Cr (VI) Depletion

The Cr (VI) Depletion experiments following the same procedure detailed in Section 4.2.2, except the contents of the feed and acceptor phases are switched. The tank contains ~2.5 L 5 M HCl in the depletion experiments and the acceptor phase is 50.0 mL of the 10 ppm Cr (VI) solution.

4.2.6 Cr (III) Uptake with no carrier

The Cr (III) uptake experiments conducted without the organic carrier present follow the same preparation procedure detailed in Section 4.2.1, except the organic carrier (D2EHPA) is omitted from the organic phase solution. Therefore, the soaked membrane does not contain the carrier agent. The tank contains ~2.5 L 10 ppm Cr (III) and the acceptor phase is 50.0 mL of the 0.1 M HCl solution.

4.2.7 Cr (VI) Uptake with no carrier

The Cr (VI) uptake experiments conducted without the organic carrier present follow the same preparation procedure detailed in Section 4.2.2, except the organic carrier (Aliquat-336) is omitted from the organic phase solution. Therefore, the soaked membrane does not contain the carrier agent. The tank contains ~2.5 L 10 ppm Cr (VI) and the acceptor phase is 50.0 mL of the 5 M HCl solution.

4.2.8 Cr (III) Depletion with no carrier

The Cr (III) depletion experiments conducted without the organic carrier present follow the same preparation procedure detailed in Section 4.2.3, except the organic carrier (D2EHPA) is omitted from the organic phase solution. Therefore, the soaked membrane does not contain the carrier agent. The tank contains ~2.5 L of a 0.1 M HCl solution and the acceptor phase is 50.0 mL of the 10 ppm Cr (III) solution.

4.2.9 Cr (III) Uptake – Selectivity

The purpose of this experiment is to determine the selectivity of the organic carrier. The organic phase used in the studies contains the organic carrier that has the same charge of the Cr ion in the feed phase. Therefore, the system is not expected to transport any Cr into the acceptor phase. If this condition holds, the system displays selectivity. The feed phase for these studies is ~2.5 L of a 10 ppm Cr (III) solution. The membrane is soaked in a solution (10 mL) of 2% Aliquat-336 and 20% decanol in kerosene. The acceptor phase (bottle contents) is 50.0 mL of 0.1 M HCl.

4.2.10 Cr (VI) Uptake – Selectivity

The purpose of this experiment and expected outcome is the same as described in Section 4.2.9. The feed phase for these studies is ~2.5 L of the 10 ppm Cr (VI). The membrane is soaked in a solution (10 mL) of 10% D2EHPA and 15% decanol in kerosene. The acceptor phase (bottle contents) is 50.0 mL of 5 M HCl.

4.2.11 Cr (III) Depletion – Selectivity

The purpose of this experiment and expected outcome is the same as described in Section 4.2.9. One exception to the expected outcome is that there is no transported expected **from** the acceptor phase. The feed phase for these studies is ~2.5 L 0.1 M HCl. The membrane

conditions are the same as those described in Section 4.2.9. The acceptor phase (bottle contents) is 50.0 mL of 10 ppm Cr (III).

4.2.12 Simulated Natural Sampling

An important part of the testing phase of this work is the analysis of the sampler's performance in tank studies designed to simulate natural sampling conditions. A study of 30 groundwater sources (wells) in the Kanawha River Basin area of the Appalachian Plateau (West Virginia) conducted by the United States Geological Survey (USGS) was selected as the reference for the preparation of simulated natural water.² The study investigated major ion (cation and anion) composition of the 30 water samples as well as the pH of the samples. The data median values were presented in a table and percentiles (10th, 25th, 75th, and 90th) were estimated from the graphical representations. Table 4.2 summarizes the data from the Appalachian Plateau groundwater studies.

Table 4.2. Components and ppm concentrations of 30 groundwater sources found in the Appalachian Plateau region of West Virginia.²

Component	10th Percentile	25th Percentile	Median	75th Percentile	90th Percentile
Calcium	8	17	24	38	60
Magnesium	2.1	4	5.8	11	19
Sodium	3.5	9	19	60	90
Potassium	0.4	0.5	1.4	2.1	2.7
Chloride	1.24	2	3.3	8.5	28
Sulfate	1	3.5	8.6	18	65
Bicarbonate	82	100	168	250	310

The chemical composition of groundwater is governed by the weathering of minerals and dissolution of salts contained within the adjoining aquifer system. Hence, the components of the soil matrix and rock systems above a particular area of groundwater influence the water's composition. Precipitation from the Earth's atmosphere does not contain all of the chemical components found in groundwater and contributes only a small amount of these components. However, as the precipitation percolates through the soil into a groundwater system and through the system, anions and cations are washed or weathered from the minerals of the soil and rock. Also, the percolation of water used in crop irrigation has been found to transport "substantial quantities of salt" into groundwater systems.³ Depending on the type of soil and rock present in the area between earth's surface and the groundwater system as well as use of the land above, various ions at different concentrations are transported into the groundwater.

In addition to the weathering of minerals caused by water flow through a system, ions can enter groundwater systems by various decomposition pathways. The decomposition of organic matter contained in the soil is a source of bicarbonate (HCO_3^-). Carbon dioxide is released from the organic decomposition and converted to HCO_3^- , which is the most common anion found in groundwater.³

Based on the data presented from the Appalachian Plateau study, a simulated groundwater was prepared using the following chemicals: calcium carbonate (CaCO_3), sodium bicarbonate (NaHCO_3), magnesium hydroxide ($\text{Mg}(\text{OH})_2$), potassium chloride (KCl), sodium chloride (NaCl), and sulfuric acid (H_2SO_4). The mass of each chemical was calculated based on 2.5 L of simulated natural water and the solution was prepared according to the recipe in Table 4.3. Each component was weighed and dissolved in a small amount of Milli-Q water, then quantitatively transferred into a 2.0 L volumetric flask. The $\text{Mg}(\text{OH})_2$ and CaCO_3 solutions

exhibited some solubility issues, which resolved after 5 minutes in a sonicator. For the Cr (III) simulated natural uptake studies, chromium (III) nitrate ($\text{Cr}(\text{NO}_3)_3 \cdot 9 \text{H}_2\text{O}$) was added to the volumetric flask. Potassium dichromate ($\text{K}_2\text{Cr}_2\text{O}_7$) was added to the flask for the Cr (VI) simulated natural uptake studies. The concentration of Cr in the simulated natural groundwater was ~ 0.2 ppm. This value is an order of magnitude greater than the Cr concentration of NIST SRM 1643d (natural water standard reference material) as indicated on the certificate of analysis.⁴

Table 4.3. Components of Appalachian Plateau simulated natural groundwater.

Compound	Mass (g)
CaCO_3	0.2329
NaHCO_3	0.3827
$\text{Mg}(\text{OH})_2$	0.0348
KCl	0.0067
NaCl	0.0084
H_2SO_4	0.0220
$\text{Cr}(\text{NO}_3)_3 \cdot 9 \text{H}_2\text{O}$	0.0039
$\text{K}_2\text{Cr}_2\text{O}_7$	0.0015

Once all components were added to the volumetric flask, the solution was diluted to volume with Milli-Q H_2O . The flask contents were added to the HDPE tank and the pH was tested using an Orion pH electrode. The remaining 500 mL of solution volume (Milli-Q H_2O) was added in small increments and the pH was monitored during addition. The initial solution pH is around 8.5. The pH was adjusted to ~ 6.5 with concentrated HNO_3 and KOH pellets (if

necessary). The final ionic composition of the simulated natural groundwater is given in Table 4.4.

Table 4.4. Ionic composition and concentration of the simulated natural groundwater prepared for the simulated natural uptake studies. [†]The concentration of each component was compared to the data in Table 4.4. [‡]The carbonate concentration was assumed to be approximately equal to the bicarbonate concentration presented in Table 4.4.

Component	Concentration (ppm)	Range[†]
Calcium	37.304	Median-75th
Magnesium	6.3452	Median-75th
Sodium	43.198	Median-75th
Potassium	1.4055	~Median
Chloride	3.3127	~Median
Sulfate	8.6976	~Median
Carbonate [‡]	165.21	~Median
Cr (III)	0.2027	N/A
Cr (VI)	0.2121	N/A

The prepared groundwater solution was the feed phase for the simulated natural uptake experiments. The organic phase for the Cr (III) studies consisted of 10% D2EHPA and 15% decanol dissolved in kerosene on a Teflon[®] membrane. For the Cr (VI) studies, the organic phase was composed of 2% Aliquat-336 and 20% decanol dissolved in kerosene on a Teflon[®] membrane. The acceptor phase was 50 mL of HCl: 0.1 M HCl for the Cr (III) systems and 5 M HCl for the Cr (VI) systems.

Results of the simulated natural uptake studies with the simulated groundwater that is chemically-similar to the water of the New River Valley indicate that there is a lack of Cr uptake into the sampling systems. ICP-OES was conducted on the other cations present in the Appalachian Plateau water (Table 4.4) and the results validate the proper ion-pairing transport mechanism; the cations are present in the D2EHPA (negatively-charged carrier) systems and absent in the Aliquat-336 (positively-charged carrier) systems. The hydrolysis constant of Cr (III) is ~ 4 , the pH of the solution influences the availability of Cr (III). At $\text{pH} \geq \text{p}(\text{Hydrolysis})$, the Cr (III) species will precipitate out of solution as $\text{Cr}(\text{OH})_3$. Therefore, it was determined that the groundwater composition should be simplified and the pH should be altered for future natural sampling studies.

Accordingly, groundwater representing that found in Elizabeth City, NC was used in a second series of simulated natural sampling experiments. The composition of this groundwater is 7 mM NaCl and 0.86 mM CaSO_4 and 0.2 ppm Cr.⁵ For each experiment, 2.5 L was prepared. Table 4.5 gives the recipe for the Elizabeth City simulated natural groundwater.

Table 4.5. Components of Elizabeth City, NC simulated natural groundwater.⁵

Compound	Mass (g)
NaCl	1.0227
CaSO_4	0.2927
$\text{Cr}(\text{NO}_3)_3 \cdot 9 \text{H}_2\text{O}$	0.0039
$\text{K}_2\text{Cr}_2\text{O}_7$	0.0015

Since the hydrolysis constant for Cr (III) indicates that the Cr (III) ion will precipitate out of solution as a hydroxide ($\text{Cr}(\text{OH})_3$) as the pH of the solution increases above 4, two

experiments were conducted for each Cr system in the Elizabeth City studies: feed phase pH ~ 6.5 and feed phase pH < 4. The pH of each system was adjusted by drop-wise addition of either 1M NaOH or concentrated HNO₃. The samplers were equipped with the appropriate membrane system and removed from the tank at the pre-determined residence times of 2, 4, and 6 days. ICP-OES was performed on the contents of the sampler bottles to determine the Cr concentration and uptake profile of each experiment.

A third series of natural sampling studies were conducted using the Elizabeth City simulated natural groundwater conditions and increased Cr concentration over the previous studies. The goal of these experiments was to determine if the low concentration of Cr (0.2 ppm) found in the previous simulated natural sampling studies was a limiting factor. In these studies, 2.5 L of the simulated Elizabeth City groundwater (7 mM NaCl and 0.86 mM CaSO₄) was prepared along with 10 ppm Cr. The recipe for the modified Elizabeth City simulated natural groundwater is found in Table 4.6.

Table 4.6. Composition of modified Elizabeth City simulated natural groundwater.

Compound	Mass (g)	1000 ppm stock (mL)
NaCl	1.0227	----
CaSO ₄	0.2927	----
Cr(NO ₃) ₃ · 9 H ₂ O	----	25.0
K ₂ Cr ₂ O ₇	----	25.0

Each Cr ion was studied using the modified Elizabeth City simulated natural groundwater. The pH of each system was not regarded. Three samplers were prepared and

equipped with the appropriate membrane system. The samplers were removed from the tank at the pre-determined residence times of 2, 4, and 6 days. ICP-OES was performed on the contents of the sampler bottles to determine the Cr concentration and uptake profile of each experiment.

4.3 Results and Discussion

The data from the SLM performance studies is presented in tabular and graphical forms. The tables give the [Cr] determined from the ICP experiments in units of ppm ($\mu\text{g}/\text{mL}$) as well as statistical information associated with the data. The graphs display either the uptake of Cr into the acceptor phase or the depletion of Cr from the acceptor phase. These graphs are presented in the introduction subsection for each experiment. Uptake and depletion graphs presented separately for purposes of clarity.

The x-axis for all graphs represents the sampler's residence time (days) in the tank. The y-axis of the graphs presented in this chapter depends on the experiment. For the uptake studies, the y-axis of the graphs is the concentration of Cr in the acceptor phase (ppm). The data are corrected for the Cr concentration in the corresponding blank samples. The uptake data are corrected by subtracting the Cr concentration in the HCl stock solution from the sample concentration. The y-axis of the depletion graphs shows the normalized concentration of Cr in the acceptor phase. The data are normalized such that the acceptor phase concentration is divided by the initial concentration of the sampler bottle. Error bars (95% confidence interval) for the Cr concentration are present. However, most error bars cannot be seen because they are covered by the data marker. A legend appears with each graph to illustrate the data series. The data markers used in the graphs are shown in Table 4.7. If more than one data series of each type is present on the graph, the fill is removed from one series to emphasize the difference between the data sets.

Table 4.7. Data markers used in Chapter 4 graphs.

Data Series	Marker
Cr (III) uptake	Blue diamond (◆)
Cr (VI) uptake	Red square (■)
Cr (III) depletion	Green circle (●)
Cr (VI) depletion	Purple triangle (▲)

4.3.1 Uptake

Uptake studies for both Cr (III) and Cr (VI), separately, were conducted as part of the SLM sampler evaluation. The goals of these experiments were to determine the efficiency of Cr uptake and to determine enrichment of each of the systems. The results of the uptake experiments are presented in Figure 4.1 and Tables 4.8 and 4.9. Each system will be discussed in more detail in the following sections: Section 4.3.1.1 (Cr (III) Uptake) and Section 4.3.1.2 (Cr (VI) Uptake). A summary section follows.

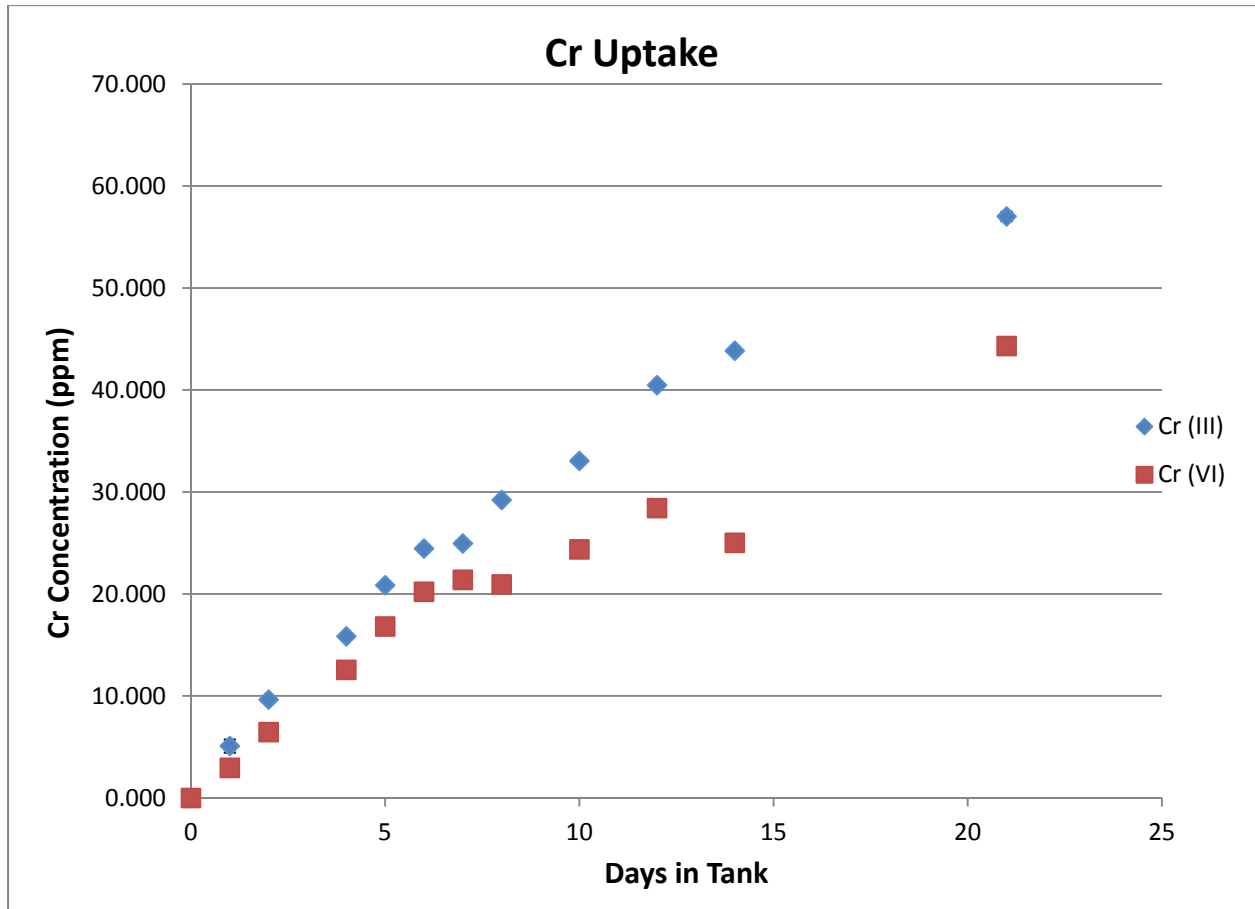


Figure 4.2. Graph of Cr uptake using the SLM-based sampling systems.

4.3.1.1 Cr (III)

The numerical data collected during the Cr (III) uptake experiment is shown in Table 4.8. The Cr (III) uptake profile is linear in shape. The system displays enrichment after 2 days or residence in the tank. The concentration doubles again (20 ppm) at 5 days of residence. After 8 days in the tank, the system reaches approximately 30 ppm. The 40 ppm mark is achieved at 12 days residence. The sampler surpasses 50 ppm at day 21.

Table 4.8. Cr (III) uptake data (in units of ppm) with 95% confidence error (n = 5).

Days in Tank	[Cr] (ppm)	95% Confidence (ppm)
0	0.000	
1	5.094	0.639
2	9.645	0.083
4	15.85	0.13
5	20.86	0.16
6	24.46	0.32
7	24.96	0.19
8	29.22	0.27
10	33.05	0.33
12	40.48	0.30
14	43.85	0.18
21	57.02	0.46

4.3.1.2 Cr (VI)

The Cr (VI) uptake profile is similar to that of Cr (III); the concentration increases linearly throughout the experiment. The numerical data is given in Table 4.9. Enrichment is achieved after 4 days in the tank. The Cr (VI) concentration exceeds 20 ppm at day 6. The

30 ppm mark is approached on days 12, but is not surpassed until day 21. At this point, the concentration of Cr (VI) exceeds 40 ppm.

Table 4.9. Cr (VI) uptake data (in units of ppm) with 95% confidence error (n = 5).

Days in Tank	[Cr] (ppm)	95% Confidence (ppm)
0	0.000	
1	2.956	0.083
2	6.457	0.065
4	12.56	0.10
5	16.81	0.09
6	20.22	0.19
7	21.39	0.11
8	20.94	0.60
10	24.38	0.16
12	28.43	0.36
14	25.02	0.08
21	44.31	0.15

4.3.1.3 Uptake Summary

From the data presented in Figure 4.3, it can be determined that both systems (Cr (III) and Cr (VI)) have similarly-shaped uptake curves, which suggests that both systems function in a

similar fashion. However, the data indicate that Cr (III) uptake is faster than Cr (VI). This result is consistent with the results obtained from the kinetic uptake analysis (Section 3.3). Also, it should be noted that Cr (III) uptake is more complete at the end of the sampling period (21 days). The extent of Cr (III) extraction compared to Cr (VI) extraction is also consistent with the observed faster Cr (III) kinetics (Section 3.3).

Despite the differences in rate, both systems display enrichment, which occurs when the concentration of the acceptor phase exceeds the concentration of the feed phase. Since the acceptor phase has a smaller volume than the feed phase (50 mL vs. 2500 mL), the transport of Cr into the acceptor phase concentrates or enriches the concentration of Cr compared to that of the original solution (feed phase). This is especially important when one considers the fact that Cr in natural systems can occur in trace amounts.

4.3.2 Depletion

Since the SLM technique is based on a concentration gradient between the feed and acceptor phases, it is hypothesized in this work that Cr can be transported from the acceptor phase as well. To test this hypothesis, depletion experiments were conducted. In these experiments, the feed and acceptor phase contents have been switched; the feed phase contains the HCl solution and the acceptor bottle contains the Cr solution.

Depletion studies for both Cr (III) and Cr (VI), separately, were conducted as part of the SLM sampler evaluation. The goals of these experiments were to determine if the reverse function of the SLM process (removal of Cr from sampler bottle back into the tank) and to determine the extent (if any) of this depletion. The results of the depletion experiments are presented in Figure 4.3 and Tables 4.10, 4.11, and 4.12. The data for each day of residence is

normalized against the initial concentration of Cr in the sampler bottle. Each system will be discussed in more detail in the following sections: Section 4.3.2.1 (Cr (III)), Section 4.3.2.2 (Cr (VI)), and Section 4.3.2.3 (Cr (III) with EDTA), with a summary of the data to follow in Section 4.3.2.4.

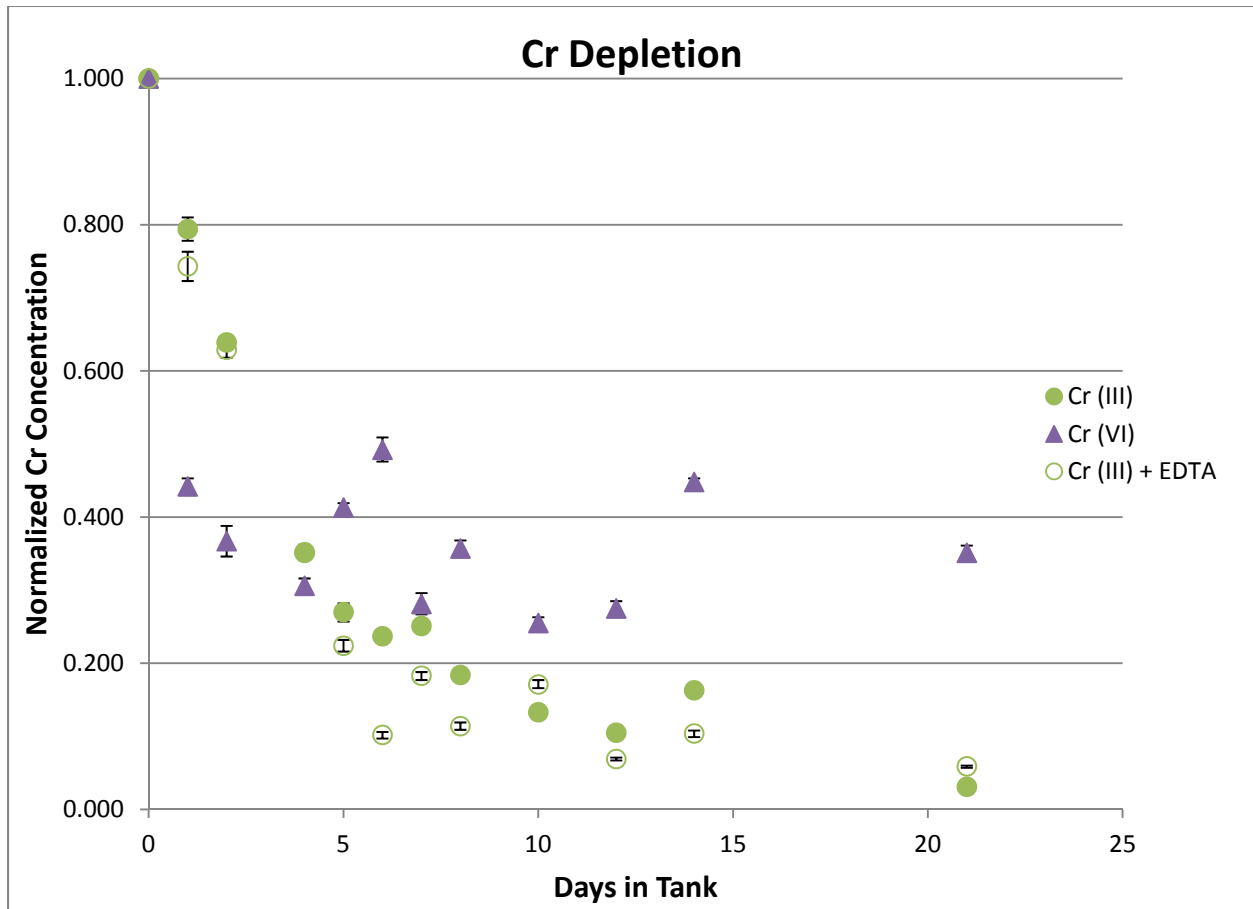


Figure 4.3. Graph of Cr depletion using the SLM-based sampling systems.

4.3.2.1 Cr (III) Depletion

The Cr depletion experiment displays exponential decay. The numerical data is given in Table 4.10. The data are normalized against the initial Cr (III) concentration. The half life (τ) is approximately 3 days. The normalized data approaches a lower limit of ~ 0.100 . Since the

transport mechanism is based on an equilibrium process, it is not reasonable to expect the Cr concentration to reach zero. The observation of a lower limit of ~0.100 (normalized) supports the SLM theory.

Table 4.10. Normalized (against initial Cr (III) concentration) Cr (III) depletion data with 95% confidence error (n = 5).

Days in Tank	Normalized [Cr]	95% Confidence (ppm)
0	1.000	
1	0.794	0.016
2	0.639	0.009
4	0.351	0.006
5	0.270	0.013
6	0.237	0.006
7	0.251	0.005
8	0.184	0.004
10	0.133	0.006
12	0.105	0.003
14	0.163	0.004
21	0.031	0.004

4.3.2.2 Cr (VI) Depletion

The numerical data is given in Table 4.11. The data are normalized against the initial Cr (VI) concentration. The Cr (VI) depletion data exhibits exponential decay through day 4. The data collected beyond 4 days residence in the tank are very scattered and do not follow a discernible trend. The samples are subjected to very harsh sampling conditions during the Cr (VI) depletion experiments. The samplers were submerged in 5 M HCl, which is far more acidic than any potential groundwater sampling environment. The plastic screws and nuts used to hold the sampler plates together are not designed nor expected to withstand extremely acidic solution for extended periods of time (i.e. several days). Accordingly, the screws and nuts disintegrate in the 5 M HCl tank contents. Thus, the plates that sandwich the membrane separate. This plate separation compromises the integrity of the sampling system for the Cr (VI) depletion study. The membrane can potentially slip out of place, which would uncover the hole. In this situation, a direct channel would be established for the unassisted flow of Cr to and from the acceptor bottle. It should be noted that there was no obvious visual evidence of membrane slippage upon removal from the tank.

Furthermore, the epoxy used to bond the bottle cap to the plate does not withstand the harsh sampling conditions. Unlike the screw/nut problem, the plate/cap assembly remained intact in the 5 M HCl solution. However, the epoxy-bonded assembly was weakened such that the bottle cap and plate came apart upon subsequent assembly for additional experiments. The damaged samplers were repaired according to the procedure detailed in chapter 2. It was determined that the sampling conditions for the Cr (VI) depletion studies are too harsh for the samplers to withstand. The damage to the samplers is too detrimental to warrant further Cr (VI) depletion experiments. Therefore, only Cr (III) depletion data will be presented from this point.

Table 4.11. Normalized (against initial Cr (VI) concentration) Cr (VI) depletion data with 95% confidence error (n = 5).

Days in Tank	Normalized [Cr]	95% Confidence (ppm)
0	1.000	
1	0.442	0.011
2	0.367	0.021
4	0.306	0.010
5	0.413	0.007
6	0.492	0.017
7	0.281	0.015
8	0.357	0.012
10	0.255	0.008
12	0.275	0.010
14	0.448	0.005
21	0.351	0.010

The rationale for using a high acid concentration in these studies was to determine if the rate of depletion of Cr (VI) from the sampler bottles was slower than that of Cr (III). The slower uptake values obtained for Cr (VI) in the Cr uptake studies warranted a second look at the extraction rate (this time from the sampler bottle into the tank). However, this information was unattainable due to the damage sustained as a result of the harsh sampling environment. It should

be noted that the sampling systems were designed to function in natural systems. The sampling environment in natural systems is very mild compared to the 5 M HCl used in the Cr (VI) depletion experiments. The samplers will never experience conditions as harsh when sampling groundwater sources.

4.3.2.3 Cr (III) Depletion with EDTA

EDTA was added to the tank solution to determine if the rate of depletion would be enhanced. EDTA is a chelating ligand that is capable of forming a coordinate covalent bond with metal cations. The ratio of EDTA to metal cation is 1:1. If EDTA is placed in the tank, the Cr (III) depletion should be affected according to Le Chatlier's principle. Therefore, the removal of Cr (III) from the sampler bottle should occur at a faster rate.

However, the EDTA-Cr (III) data presented in Figure 4.3 and Table 4.12 indicates that the presence of EDTA does not affect the rate of Cr (III) depletion. The data are normalized against the initial Cr (III) concentration. The shape and rate of the Cr (III) and EDTA-Cr (III) depletion curves are the same. It is plausible that the concentration of EDTA (~1 mM) was not sufficient to cause any discernible removal of Cr (III) from the extracted solution. Also, the pH of the tank solution does not provide a favorable environment for the active form of EDTA (Y^{-4}). The activity of EDTA increases as the pH decreases.⁶ As a result, the amount of active form of EDTA (Y^{-4}) present decreases, thereby decreasing the effectiveness of Cr (III) removal.

Table 4.12. Normalized (against initial Cr (III) concentration) Cr (III)-EDTA depletion data with 95% confidence error (n = 5).

Days in Tank	Normalized [Cr]	95% Confidence (ppm)
0	1.000	
1	0.743	0.020
2	0.629	0.012
4	0.352	0.010
5	0.224	0.008
6	0.102	0.005
7	0.183	0.006
8	0.114	0.005
10	0.171	0.006
12	0.069	0.003
14	0.104	0.005
21	0.059	0.002

4.3.2.4 Depletion Summary

The depletion of Cr (III) from the sampler bottle fits an exponential decay model. The approximate half-life (τ) was calculated to be 3 days ($\tau \approx 3$ days). Only data points for 1, 2, and 4 days of residence are reported for the Cr (VI) depletion studies. The acceptor phase present in the tank is far too acidic for the samplers. Hence, no long-term studies were performed for this system.

4.3.3 No Carrier

Uptake studies for both Cr (III) and Cr (VI), separately, were conducted as part of the SLM sampler evaluation. The goal of these experiments was to validate the carrier molecule's function in the SLM speciation of Cr ions. Based on the SLM theory, there should be no transport of Cr through the organic phase if there is no carrier present. If there is no uptake of Cr into the acceptor phase in the uptake studies or no depletion of Cr from the acceptor phase in the depletion studies, then the role of the carrier molecule in the SLM process is validated.

The results of the SLM experiments without the carrier molecule present in the organic phase are presented in Figure 4.4 (uptake) and Figure 4.5 (depletion). Each system is discussed in more detail in the following sections: Section 4.3.3.1 (Cr (III) Uptake) and Section 4.3.3.2 (Cr (VI) Uptake) and Section 4.3.3.3 (Cr (III) Depletion). The data obtained in these experiments are summarized in Section 4.3.3.4.

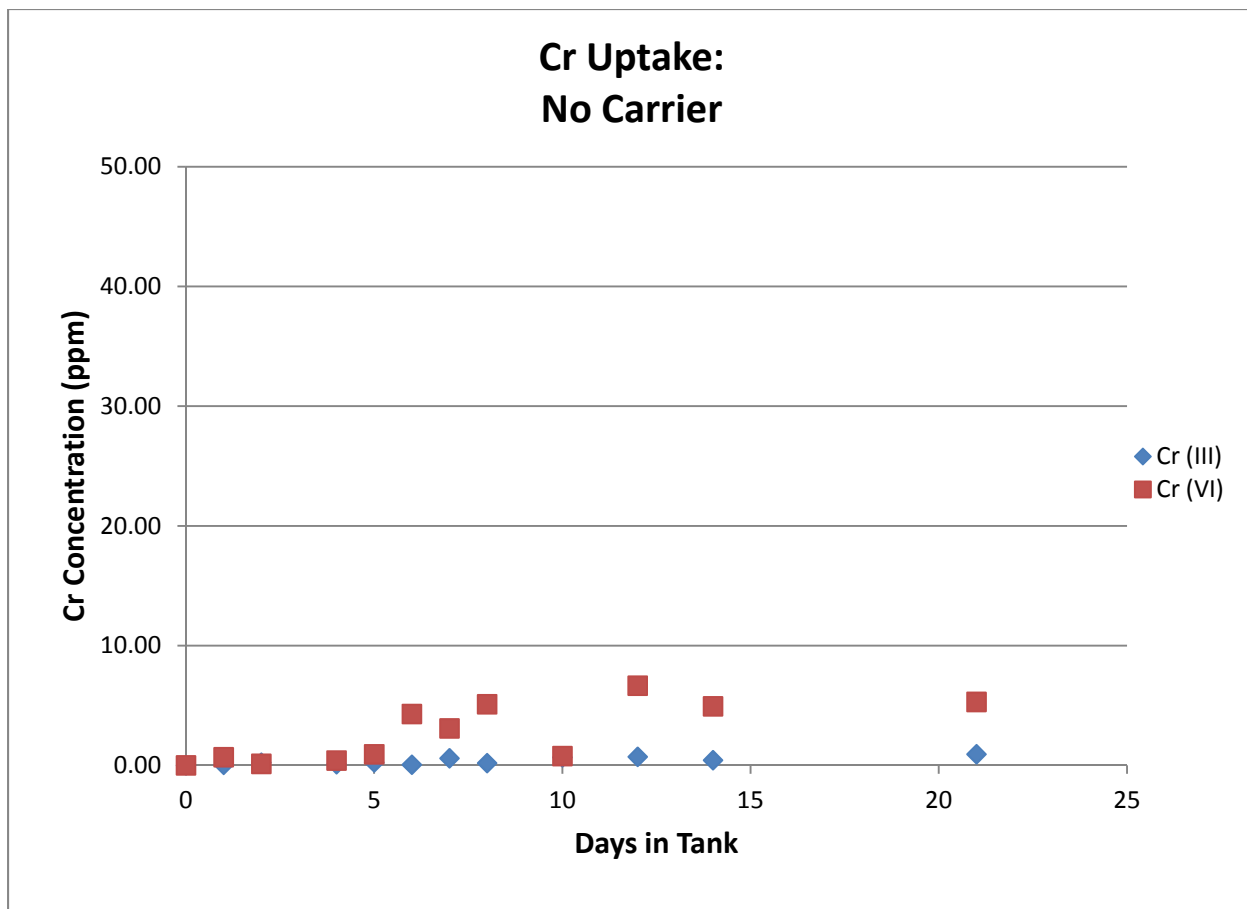


Figure 4.4. Cr uptake with no carrier present in the organic phase.

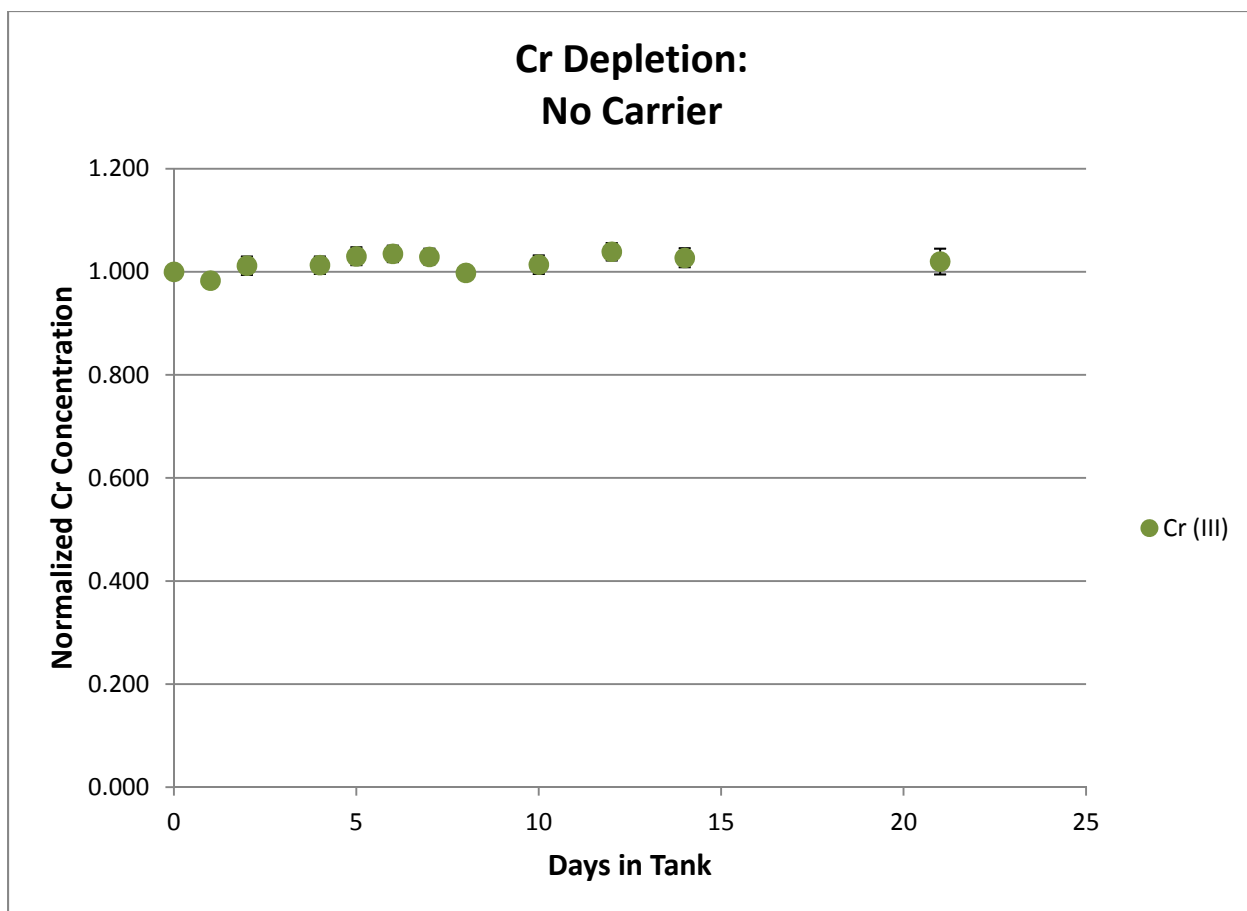


Figure 4.5. Cr depletion with no carrier present in the organic phase.

4.3.3.1 Cr (III) Uptake

The numerical data is given in Table 4.13. The Cr (III) uptake data obtained from the no carrier studies is what is expected given the experimental conditions (i.e. no carrier molecule present means no Cr transport). The maximum uptake concentration is 0.929 ppm at day 21. When this value is compared to the corresponding data point in the normal sampling conditions (57.0 ppm), the uptake is negligible (1.63%). This data validates the role of D2EHPA in the Cr (III) SLM transport mechanism.

Table 4.13. Cr (III)-no carrier uptake data with 95% confidence error (n = 5).

Days in Tank	[Cr] (ppm)	95% Confidence (ppm)
0	0.000	
1	0.046	0.027
2	0.230	0.011
4	0.100	0.010
5	0.238	0.079
6	0.051	0.008
7	0.593	0.086
8	0.188	0.010
10	0.667	0.025
12	0.714	0.070
14	0.431	0.029
21	0.929	0.015

4.3.3.2 Cr (VI) Uptake

The shape of the Cr (VI) uptake curve is similar to that of Cr (III) and adheres to what is expected from these sampling conditions. In the absence of Aliquat-336 (carrier molecule), no Cr (VI) will be transported according to the SLM extraction mechanism. However, it should be noted that the Cr (VI) uptake is greater than what is observed in the Cr (III) experiments. The numerical data is given in Table 4.14. The Cr (VI) no carrier system reaches a maximum value

of 6.656 ppm at day 12. This value is 23.4% of the value obtained on day 21 of the normal Cr (VI) uptake studies. The data are also scattered and a discernible pattern of Cr (VI) uptake cannot be established. These results indicate that Cr (VI) is transported into the sampler bottle, which is contradictory to the SLM theory, and is most likely a failure of the physical sampler.

Table 4.14. Cr (VI)-no carrier uptake data with 95% confidence error (n = 5).

Days in Tank	[Cr] (ppm)	95% Confidence (ppm)
0	0.000	
1	0.682	0.046
2	0.126	0.027
4	0.404	0.039
5	0.926	0.051
6	4.292	0.164
7	3.090	0.193
8	5.104	0.190
10	0.777	0.078
12	6.656	0.218
14	4.932	0.312
21	5.299	0.192

The sampling systems were inspected after removal from the tank. The samplers in contact with the 5 M HCl solution inside the tank of the Cr (VI) depletion studies displayed

structural failure when removed from the tank. The sampler plates appeared to be slightly misaligned upon removal. This misalignment is thought to have resulted in a compromised sampler seal. The seal of the sampler plate is crucial to sampler integrity. If the sampler is not sealed properly, the membrane may not cover the hole in the sampler plate, then Cr enters the acceptor bottle without being transported there via the SLM mechanism. Once the sampler plates were disassembled, the membrane was inspected. If there is a hole in the membrane, then a direct channel is created whereby Cr enters the acceptor bottle and bypasses the SLM extraction mechanism. It was found that the structural integrity of the membranes was maintained (i.e. no holes). Therefore, direct channel establishment was ruled out as a possible cause of unexpected Cr (VI) transport. The sampler bottles were the next area investigated. The bottles had not loosened from the cap of the sampler assembly and the cap/plate bond did not exhibit weakness upon twisting. Therefore, the gaps found between the sampler plates was selected as the cause of Cr (VI) transport.

Investigation into the plate seal malfunction revealed that the screws can be easily over-tightened, thereby stripping the threads and compromising the integrity of both the sampler and the data obtained from the sampler. Since the screws were not tightened properly, the plates of the sampler were not completely sealed and did not remain flush during the experiment. In this situation, solution from the feed phase of the tank can enter the sampler through the space between the plates then enter the sampler bottle through the membrane/plate gap.

4.3.3.3 Cr (III) Depletion

The numerical data is given in Table 4.15. The data are normalized against the initial Cr (III) concentration. The results are shown in Figure 4.5. The normalized concentration

remains at a constant value of one throughout the 21 day sampling period. This indicates that the Cr (III) ion does not leave the sampler bottle. These results indicate proper SLM function given that the carrier molecule is not present in the organic phase of the sampling systems (i.e. no carrier means no transport). Therefore, the mechanism of the SLM extraction is validated in the depletion experiments.

Table 4.15. Cr (III)-no carrier depletion data with 95% confidence error (n = 5).

Days in Tank	Normalized [Cr]	95% Confidence (ppm)
0	1.000	
1	0.983	0.007
2	1.012	0.018
4	1.013	0.017
5	1.030	0.018
6	1.035	0.016
7	1.029	0.016
8	0.998	0.011
10	1.014	0.018
12	1.039	0.017
14	1.027	0.019
21	1.020	0.025

4.3.3.4 No Carrier Summary

The results of the experiments without a carrier molecule present indicated that the SLM sampling systems exhibit proper function. In the absence of carrier molecule, there is no transport of Cr ion. These results also validate the mechanism of the SLM extraction as well as the integrity of the samplers themselves. Evidence of transport of Cr ions into/out of the sampler bottle would indicate a failure of the sampler. The Cr (VI) no carrier uptake studies revealed a vulnerability of the samplers; the screws are susceptible to stripping through over-tightening. This process creates an improper seal in the sampling systems and leads to a gap between the sampler plates, which can cause a gap in the membrane/plate seal. Thereby, Cr entered the sampler bottle despite the absence of carrier molecule due to a malfunction in the sampling system.

4.3.4 Selectivity

Uptake studies for both Cr (III) and Cr (VI), separately, were conducted as part of the SLM sampler evaluation. The experimental details of these experiments are found in Table 4.1 in Section 4.2. The goals of these experiments were to determine the efficiency of Cr uptake and to determine enrichment of each of the systems. The results of the uptake experiments are presented in Figure 4.6 and the results of the depletion studies are presented in Figure 4.7. Each system is discussed in more detail in the following sections: Section 4.3.4.1 (Cr (III) Uptake), Section 4.3.4.2 (Cr (VI) Uptake), and Section 4.3.4.3 (Cr (III) Depletion). A summary section follows.

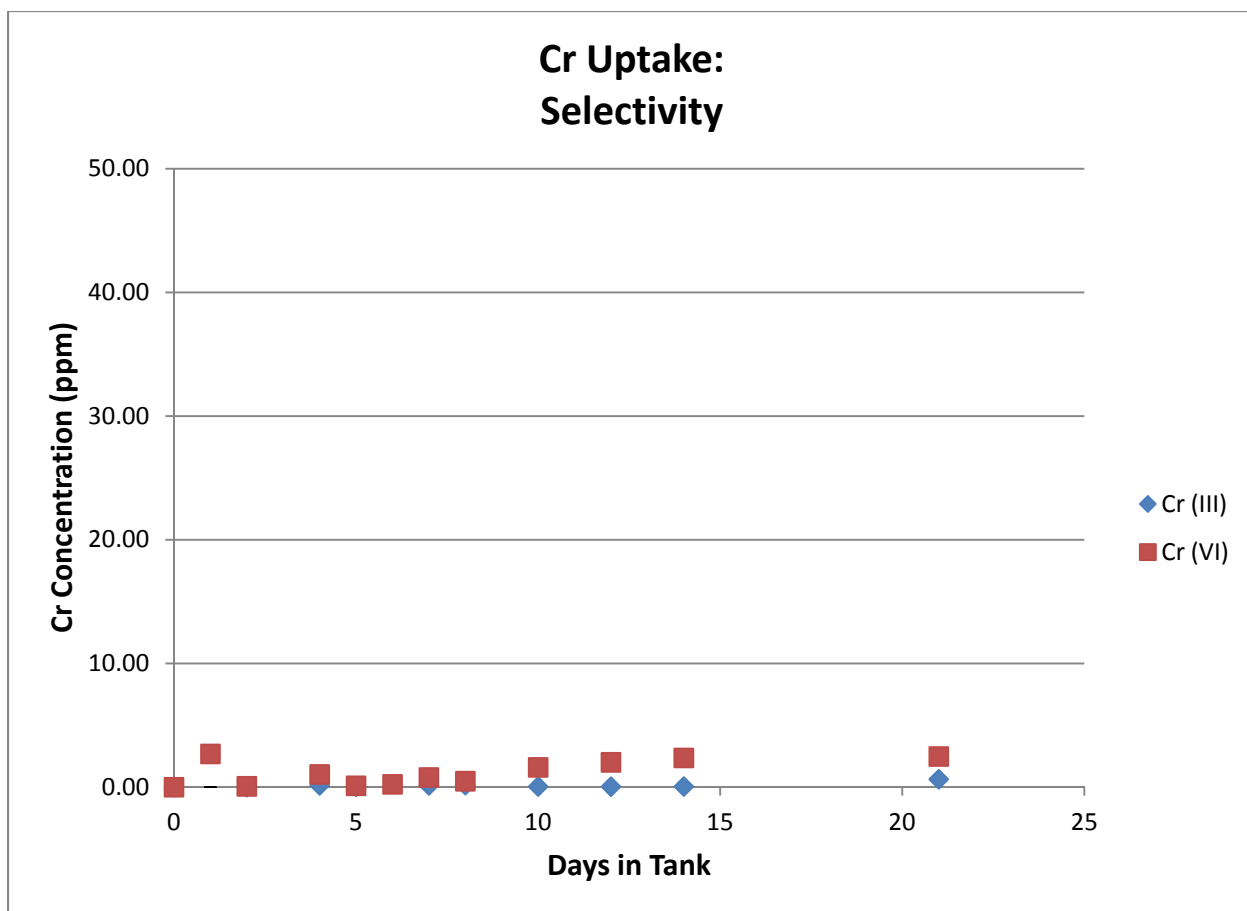


Figure 4.6. Selectivity of organic carrier molecule as a function of Cr uptake.

4.3.4.1 Cr (III) Uptake

The numerical data is given in Table 4.16. The Cr (III) ions are not transported into the acceptor phase during the selectivity experiments. These results illustrate the proper function of the SLM extraction. The ion-pairing mechanism cannot occur in these experiments. The positively-charged Aliquat-336 molecule is present in the organic phase of the Cr (III) systems. Since the Cr (III) ions are positively-charged, ion-pairing between the carrier molecules and the Cr (III) ions will not occur. Thus, there will be *no* transport of Cr (III) into the acceptor phase. The results validate the SLM-based extraction mechanism as well as the selectivity of the carrier

molecule. Furthermore, the sampler data is consistent with the LLE selectivity data presented in Section 3.2.4.

Table 4.16. Cr (III)-selectivity uptake data with 95% confidence error (n = 5).

Days in Tank	[Cr] (ppm)	95% Confidence (ppm)
0	0.000	
1	-0.014	0.016
2	0.002	0.022
4	0.141	0.015
5	0.028	0.016
6	-0.003	0.013
7	0.138	0.014
8	0.163	0.013
10	0.054	0.062
12	0.042	0.062
14	0.053	0.062
21	0.641	0.244

4.3.4.2 Cr (VI) Uptake

The numerical data is given in Table 4.17. The Cr (VI) ions are not transported into the acceptor phase during the selectivity experiments. These results illustrate the proper function of the SLM extraction. The ion-pairing mechanism cannot occur in these experiments. The

negatively-charged D2EHPA molecule is present in the organic phase of the Cr (VI) systems. Since the Cr (VI) ions exist as oxyanions and are negatively-charged, ion-pairing between the carrier molecules and the Cr (VI) ions will not occur. Thus, there will be **no** transport of Cr (VI) into the acceptor phase. The results validate the SLM-based extraction mechanism as well as the selectivity of the carrier molecule. Furthermore, the sampler data is consistent with the LLE selectivity data presented in Section 3.2.4.

Table 4.17. Cr (VI)-selectivity uptake data with 95% confidence error (n = 5).

Days in Tank	[Cr] (ppm)	95% Confidence (ppm)
0	0.000	
1	2.691	0.120
2	0.068	0.021
4	1.033	0.034
5	0.113	0.029
6	0.226	0.024
7	0.787	0.021
8	0.482	0.034
10	1.597	0.345
12	2.009	0.217
14	2.366	0.210
21	2.482	0.204

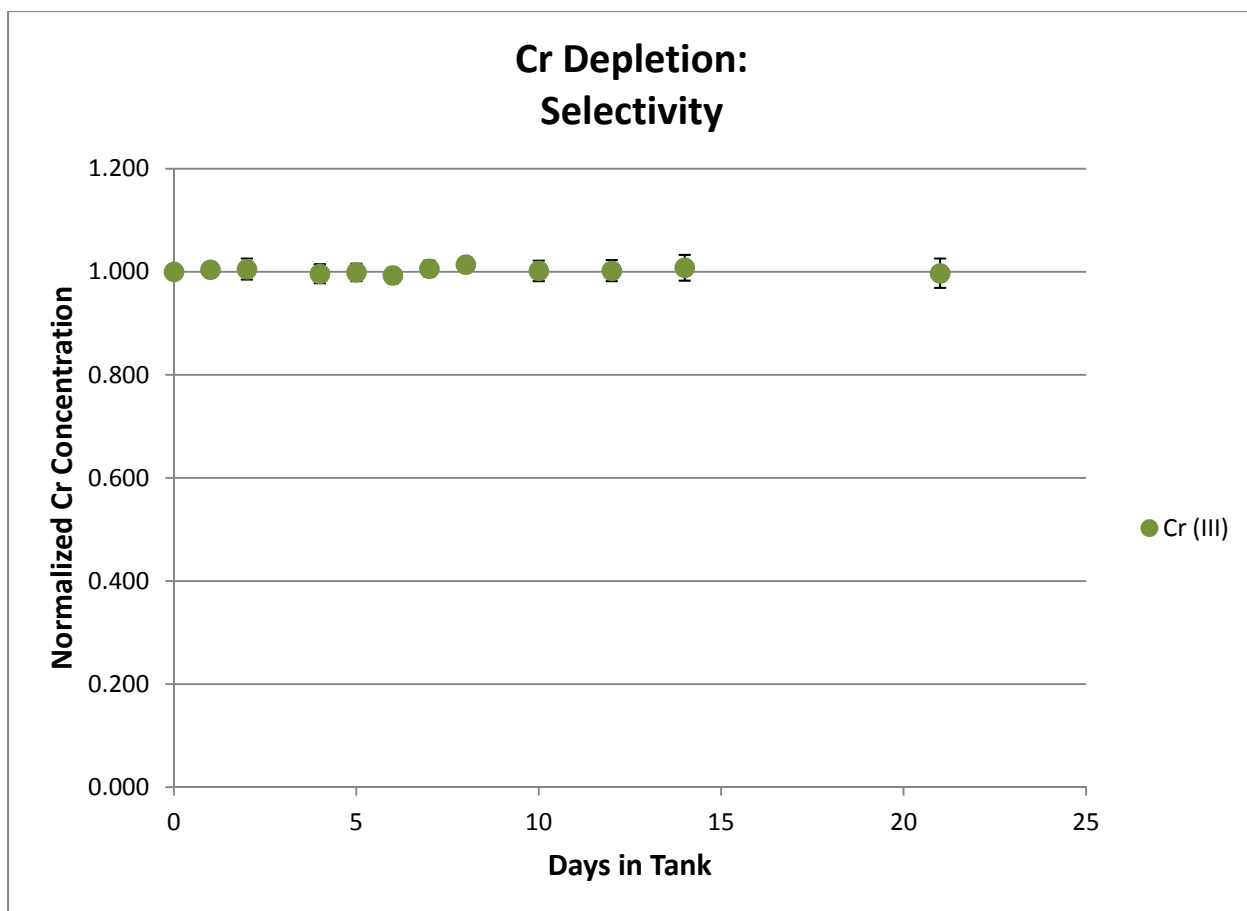


Figure 4.7. Selectivity of Cr depletion.

4.3.4.3 Cr (III) Depletion

The numerical data is given in Table 4.18. The data are normalized against the initial Cr (III) concentration. The Cr (III) ions are not removed from the acceptor phase during the selectivity experiments. These results illustrate the proper function of the SLM extraction. The ion-pairing mechanism cannot occur in these experiments. The positively-charged Aliquat-336 molecule is present in the organic phase of the Cr (III) systems. Since the Cr (III) ions are positively-charged, ion-pairing between the carrier molecules and the Cr (III) ions will not occur. Thus, there will be **no** transport of Cr (III) from the acceptor phase. The results validate the

SLM-based extraction mechanism as well as the selectivity of the carrier molecule. Furthermore, the sampler data is consistent with the LLE selectivity data presented in Section 3.2.4.

Table 4.18. Cr (III)-selectivity depletion data with 95% confidence error (n = 5).

Days in Tank	Normalized [Cr]	95% Confidence (ppm)
0	1.000	
1	1.004	0.012
2	1.005	0.021
4	0.996	0.019
5	0.999	0.017
6	0.993	0.015
7	1.006	0.016
8	1.014	0.007
10	1.002	0.020
12	1.002	0.021
14	1.008	0.025
21	0.997	0.029

4.3.4.4 Selectivity Summary

The results of the selectivity studies validate the role of the carrier molecule in the SLM extraction process. In these studies, the carrier molecules are switched within the Cr systems:

Aliquat-336 with Cr (III) (instead of with Cr (VI)) and D2EHPA with Cr (VI) (instead of with Cr (III)). This creates a situation where the carrier molecule and the Cr ion have the same charge. Ion-pairing cannot occur, which means there will be no transport of Cr within the system according to the SLM mechanism. As seen in the no carrier studies, the integrity of the samplers is validated during the selectivity studies also. The experimental design dictates no Cr transport, which means that any transport of Cr observed in the sampling systems is due to a failure within the sampler (i.e. improper sealing, stripped screws, plate/plate or membrane/plate gaps, etc.). Since there is no observed Cr transport in the selectivity studies, the structural integrity of the sampling systems is validated as well as the role of the carrier molecule in proper SLM function.

4.3.5 Double Membrane

Double membrane studies were performed for Cr (III) depletion. The experimental details of these experiments are found in Table 4.1 in Section 4.2. The goals of these experiments were to determine the efficiency of Cr uptake and to determine enrichment of each of the systems. The results of the depletion experiments are presented in Figure 4.8.

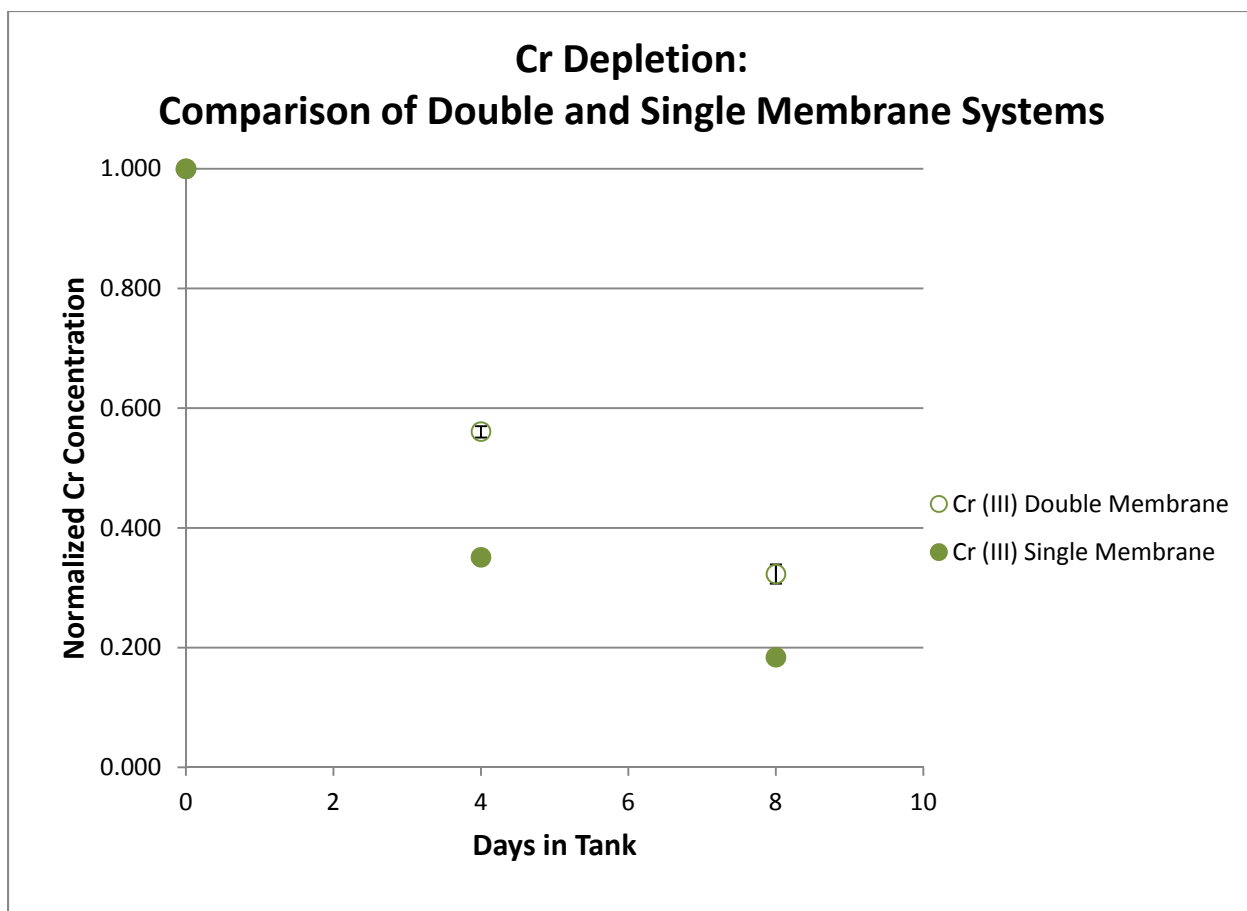


Figure 4.8. Comparison of double and single membrane depletion for Cr (III).

According to Fick’s Law, the flux of Cr through the SLM system is directly proportional to the diffusion coefficient (D_m) and inversely proportional to the thickness of the membrane. Accordingly, an experiment was conducted to determine the influence of membrane thickness on SLM sampler performance. In this experiment, two membranes were soaked in the organic phase solution and placed in the sampler. Two samplers were placed in the tank and allowed to remain there for four (4) and eight (8) days.

The results obtained from the double membrane experiments are shown in Table 4.19. The data from Table 4.19 were compared to the data from the corresponding single membrane experiments. Figure 4.8 illustrates a graphical comparison of the two sets of data. It can be seen

that the presence of a second membrane negatively impacts the rate of Cr uptake/depletion as expected.

Table 4.19. Cr (III) double membrane depletion data with 95% confidence error (n = 5).

Days in Tank	Normalized [Cr]	95% Confidence (ppm)
0	1.000	
4	0.561	0.010
8	0.323	0.016

4.3.5.3 Cr (III) Depletion

The numerical data is given in Table 4.19. Figure 4.8 shows that the depletion of Cr (III) occurs more slowly in the double membrane experiments compared to the same data points from the single membrane experiments. These results are consistent with the inverse proportionality of Cr flux and membrane thickness.

4.3.5.4 Double Membrane Summary

The results seen in the double membrane studies are expected according to the flux theory. Although the membrane plays a crucial role in the SLM mechanism (physical barrier that separates two aqueous phases), it also plays an inhibitory role to the rate of the extraction. A second membrane provides an additional barrier and distance for the Cr-carrier ion pair to diffuse through. Therefore, the extraction process is further slowed. As seen in Section 3.3.2, specifically Figures 3.20 and 3.23, the membrane has a tremendous effect on the rate of the

extraction in the SLM process. The rate constants must be reduced at least three orders of magnitude for the LLE kinetics data to model the experimental extraction observed with the sampling systems.

4.3.6 Mixed Systems

Uptake studies for both Cr (III) and Cr (VI), separately, were conducted as part of the SLM sampler evaluation. The experimental details of these experiments are found in Table 4.1 in Section 4.2. The goals of these experiments were to determine the efficiency of Cr uptake and to determine enrichment of each of the systems. The results of the uptake experiments are presented in Figure 4.9.

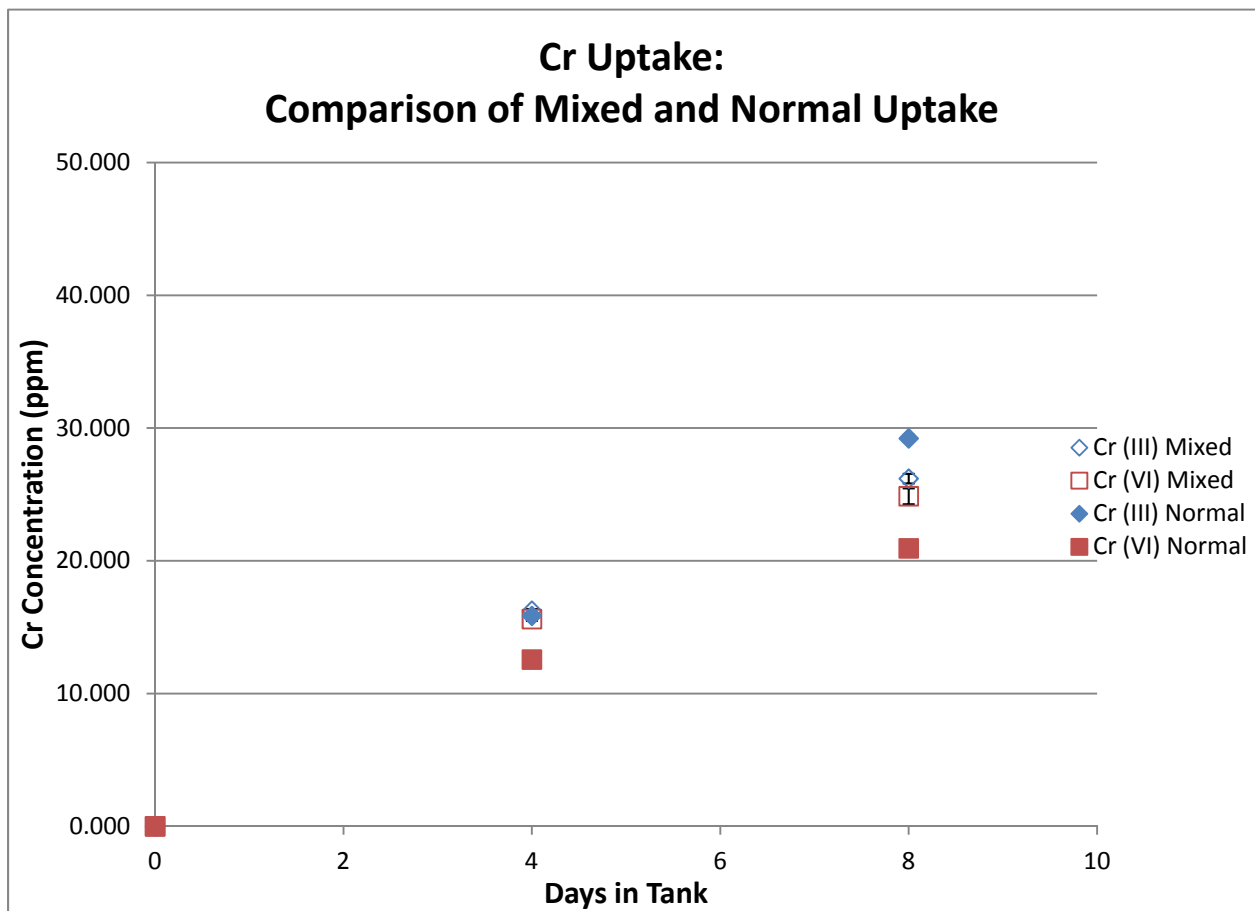


Figure 4.9. Comparison of mixed and normal uptake for Cr (III) and Cr (VI).

The numerical data is given in Table 4.20. The results show similar uptake of the mixed tank studies when compared to the single systems. These results indicated that the presence of both Cr ions does not affect the performance of the single ion samplers. The lack of interference from the Cr ions on the single ion sampler performance supports the viability of the SLM-based sampling systems in the speciation of Cr ions. If a Cr (III) sampler's performance was affected by the presence of a Cr (VI) ion (and vice-versa), then the samplers could not be used reliably in the speciation of Cr ions.

Table 4.20. Mixed system uptake data with 95% confidence error (n = 5).

Days in Tank	[Cr (III)] (ppm)	95% Confidence (ppm)	[Cr (VI)] (ppm)	95% Confidence (ppm)
0	0.000		0.000	
4	16.24	0.13	15.61	0.14
8	26.19	0.36	24.86	0.59

4.3.6.1 Mixed Systems Summary

The presence of both Cr ions in a single tank does not significantly interfere with the proper function of the SLM-based samplers. The uptake of Cr from the Cr (III)/Cr (VI) system is comparable to what is found in the single ion studies (Sections 4.3.1.1 and 4.3.1.2). Therefore, the presence of the opposite Cr ion does not present a significant interference.

4.3.7 Simulated Natural Sampling

Since the overall goal of this work was to design and fabricate a sampler based on the SLM extraction/speciation technique that is capable of *in-situ* speciation of Cr contamination in groundwater sources, the performance of the SLM samplers was evaluated in conditions that

simulated those found in natural groundwater in the area. The uptake behavior of the Cr (III) and Cr (VI) systems in simulated natural groundwater conditions were studied separately. The results of the simulated natural studies were compared to the normal (single species) uptake behavior of each system. The uptake behavior of the Cr (III) and Cr (VI) systems were also studied in simulated natural groundwater conditions that contained Cr (III) and Cr (VI); this is referred to as mixed simulated natural uptake (SNU).

In the individual Cr uptake experiments, only one sampler was placed in the tank and removed after two weeks residence. For the mixed simulated natural uptake study, two samplers (one for Cr (III) and one for Cr (VI)) were added to the tank containing a simulated groundwater with ~0.2 ppm of each Cr ion. The samplers remained in the tank for a period of two weeks. The data was compared to both the normal uptake data as well as the uptake studies performed with the individual samplers. After the two week sampling period, the bottle contents were analyzed using ICP-OES to determine the Cr concentration.

4.3.7.1 Simulated Natural Cr Uptake

As discussed in Section 4.2.12, the presence of the carbonate and bicarbonate components in the Appalachian Plateau simulated natural groundwater creates a situation where the pH is buffered to a value greater than the hydrolysis constant of Cr (III) ($\text{pH} > 4$). Therefore, Cr (III) is rendered insoluble and the uptake is negligible. Therefore, the simulated natural water was changed to reflect the composition found in the sandy aquifer system of Elizabeth City, NC (Table 4.6).

4.3.7.2 Elizabeth City Simulated Natural Sampling

The complexity of the simulated natural groundwater (Section 4.3.7.1) created a situation where Cr (III) became insoluble and thus the experiment did not fully demonstrate the sampler's

ability to speciated Cr. Therefore, a second simulated natural uptake study was conducted for both Cr systems individually as well as a mixed simulated natural uptake study. This simulated groundwater is based on that found in Elizabeth City, NC (Table 4.6).

The results of the mixed SNU studies are shown in Figure 4.10. The results of the laboratory-controlled Cr (III) and Cr (VI) are also provided on the graph. These results of the Cr SNU are consistent with the laboratory-controlled Cr uptake. The presence of the additional ions (Na^+ , Cl^- , Ca^{+2} , SO_4^{-2}) does not inhibit the transport of Cr from the simulated natural groundwater to the acceptor phase.

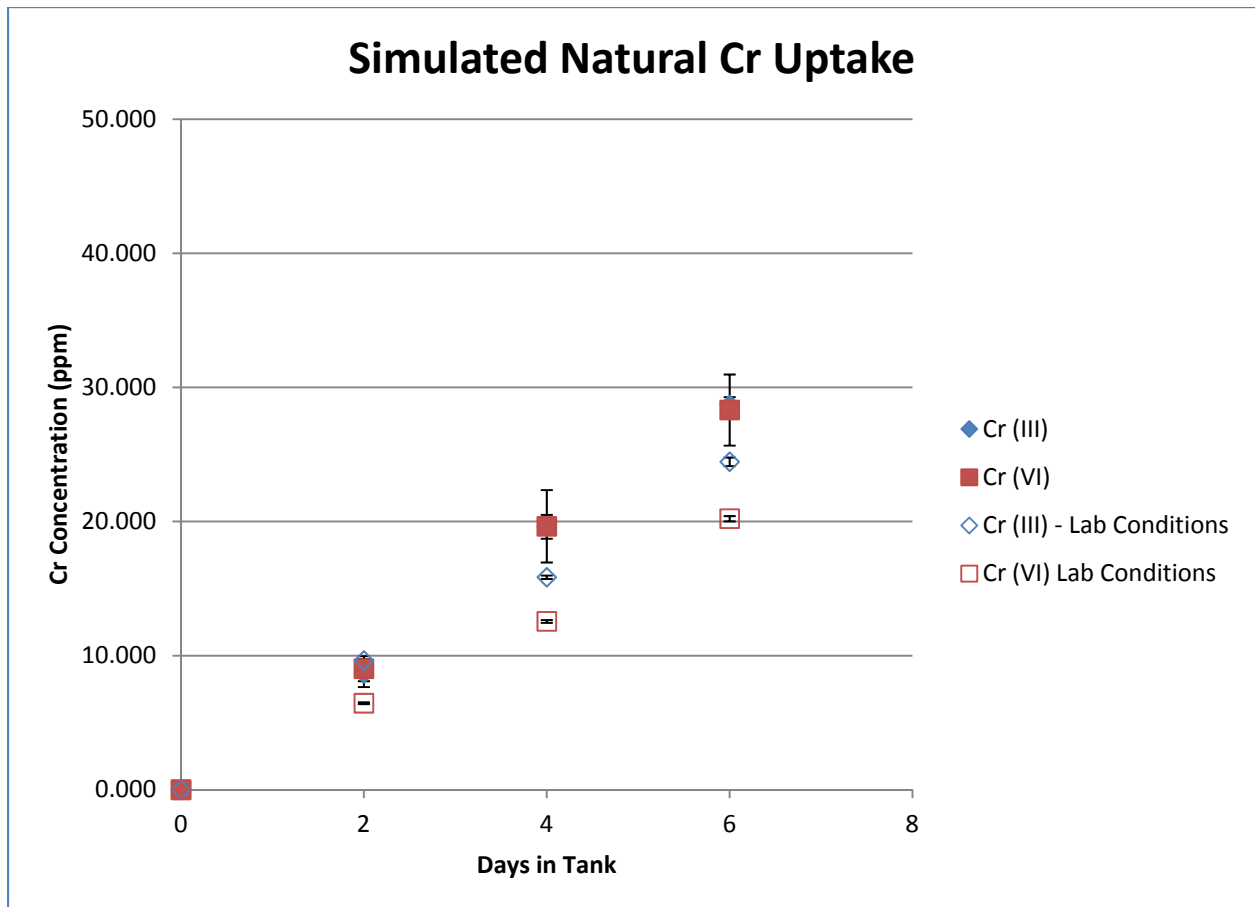


Figure 4.10. Uptake of Cr (III) and Cr (VI) in Elizabeth City simulated groundwater sampling conditions.

4.3.7.3 Simulated Natural Systems Summary

Uptake studies that simulated the conditions of groundwater were conducted for both Cr (III) and Cr (VI), separately, as part of the SLM sampler evaluation. The presence of carbonate and bicarbonate anions in the Appalachian Plateau simulated natural groundwater rendered the Cr (III) ions insoluble. The simulated natural groundwater was changed to reflect that of a sandy aquifer (Elizabeth City, NC simulated natural groundwater), which doesn't contain carbonate/bicarbonate. The modification to the simulated natural groundwater eliminated the pH issue that caused Cr (III) to precipitate from the Appalachian Plateau solution.

The results of the Elizabeth City simulated natural groundwater indicate that the sampling systems perform (uptake and speciation) as well in simulated natural sampling conditions as in laboratory-controlled conditions. The presence of additional ions does not decrease the uptake efficiency and does not impact the speciation of the sampling systems.

4.4 Summary

The overall goal of this work was to design and fabricate a sampling system that is capable of the speciation of Cr (III) and Cr (VI) in natural waters. However, the SLM-based sampler has to be validated in laboratory-controlled conditions as well as simulated natural conditions before it could be incorporated into existing sampler technology (multi-layer sampler, MLS) and used in environmental sampling applications. This chapter examined the performance of the sampling systems in laboratory-controlled uptake and depletion experiments designed to test the sampler's proper function as well as structural integrity. Additionally, the sampling systems were tested in the laboratory under simulated natural sampling conditions. These experiments were designed to mimic Cr contamination in groundwater systems. The sampling systems performed equally well in the simulated natural sampling conditions as in the

laboratory-controlled experiments. These results suggest that the SLM-based sampling system designed and fabricated in this work is a viable method for speciation of Cr (III) and Cr (VI) in groundwater sources.

4.4 References

- (1) Yang, X. J.; Fane, T. J. *Membr. Sci.* **1997**, *133*, 269.
- (2) Sheets, C. J., Kozar, M.D. *Ground-water quality in the Appalachian Plateaus, Kanawha River Basin, West Virginia*, U.S. Geological Survey 2000.
- (3) Todd, D. K.; Mays, L. W. *Groundwater Hydrology*; Wiley: Hoboken, NJ, 2005.
- (4) NIST; Vol. 2009.
- (5) Su, C.; Puls, R. W. *Environ. Sci. Technol.* **2003**, *37*, 2582.
- (6) Harris, D. C. *Exploring Chemical Analysis*; W.H. Freeman: New York, 2009.

Chapter 5

Summary and Potential Applications

5.1 Summary

Cr contamination, resulting from improper disposal of Cr-containing industrial waste, has become an important environmental problem within recent decades. Due to the differences in toxicity, bioavailability, and mobility of Cr ions in natural systems, the need to speciated Cr is crucial: Cr (III) is an essential micronutrient with low bioavailability and mobility in natural systems, whereas Cr (VI) is toxic, and highly mobile and bioavailable in natural systems. Current techniques in environmental speciation remove a sample from the natural system and analyze the sample for Cr content and species distribution at a laboratory facility off-site. This method is problematic due to the possibility of interconversion of sample species between the time of collection and analysis. Redox-active elements are capable of interconversion between species between the time of collection and analysis. Techniques that remove a redox-active element, such as Cr, from where it naturally occurs present problems in terms of representative sampling. Therefore, a sampling system that is capable of *in-situ* speciation is desired. Additionally, an ideal sampler would have the ability to store speciated Cr ions until laboratory analysis so that representative sampling is preserved.

Given the current methods of chemical speciation in natural systems, the need for a sampling system capable of *in-situ* speciation of Cr is apparent. Therefore, a sampler has been fabricated to facilitate the *in-situ* speciation of Cr. The design of the sampler is based on the Supported Liquid Membrane (SLM) extraction technique, which is heavily used in industrial wastewater treatment and recovery operations. The SLM technique utilizes charged organic carrier molecules loaded onto a polymeric (Teflon[®]) support membrane, which provides a

physical barrier between two aqueous phases. Electrostatic transport selectively transfers Cr ions from one aqueous phase to the other through the polymeric membrane. Cr ions in the feed solution, which have a charge opposite of that of the carrier molecule, form an ion-pair with the carrier and are transported through the membrane and deposited into a second aqueous phase, which is referred to as the acceptor phase. A counter-ion from the acceptor phase is exchanged for the Cr ion to complete the extraction process. The acceptor phase is contained in a Teflon[®] bottle. Teflon[®] was selected as the material for the samplers because of its inert chemical nature.

The SLM-based sampling systems described in the literature and discussed in this work are utilized to remove metals from process and wastewater streams. The accounts in the literature detail the tweaking of parameters in order to optimize metal recovery. A formal discussion that provides fundamental understating of the mechanism of the SLM-based extraction process is absent in the literature. Therefore, investigations were conducted to provide more information about the mechanism of Cr extraction in an SLM-based sampling system. Specifically, kinetic studies of LLE were performed in order to develop a model capable of predicting SLM-based Cr extraction.

The SLM-based sampling system discussed in this dissertation is capable of speciation and storage of Cr ions. The speciated Cr ions are transferred to the acceptor phase, which is contained in a Teflon[®] bottle. Interconversion that occurs after speciation does not affect the species distribution. Any Cr found in the sampler bottle was present in the groundwater source as a single Cr species. The ability of the SLM sampler to speciate and store Cr ions provides a major advantage over current speciation techniques.

The SLM extraction technique involves two concerted liquid-liquid extractions (LLEs). Equilibrium LLE studies were conducted on both systems (Cr (III) and Cr (VI)) to determine the optimal operating parameters (carrier concentration, decanol concentration, and acceptor phase concentration) of the SLM system. The optimal operating conditions were 10% D2EHPA and 15% decanol with 0.1 M HCl acceptor phase for Cr (III) and 2% Aliquat-336 and 20% decanol with 5 M HCl acceptor phase for Cr (VI).

Validation of the sampling systems occurred in both the equilibrium LLE studies and the SLM-based sampling studies. The LLE systems display appropriate Cr transport according to SLM theory. LLE studies, including extractions with no carrier molecule present as well as selectivity studies, were conducted in order to validate proper LLE function. The LLE extractions showed proper function (no Cr transport in the absence of carrier molecule and selectivity).

A total of nine Teflon[®] SLM-based samplers were prepared and validated to ensure structurally soundness. The performance of the samplers was evaluated in a series of tank studies that focused on the uptake of Cr into the acceptor phase as well as the depletion of Cr ion from this phase. The goal of the performance studies was to determine the mechanical and chemical stability of the SLM samplers. The samplers were found to be stable over a three week period when in conditions similar to those found in natural systems. As part of the validation process, selectivity studies and studies without the carrier molecule were conducted to ensure that the systems were functioning according to SLM theory. The opposite carrier molecule (with the same charge as the Cr ion) was used in the selectivity studies. No transport of Cr into the acceptor phase from the feed phase should occur according to the electrostatic pairing model of the SLM extraction technique. Consequently, the selectivity studies support the SLM theory (no

Cr transport to the acceptor phase) and validate proper sampler function. Tank studies that simulated natural sampling condition were also conducted. These studies demonstrate the viability of the SLM-based sampling system in the speciation of Cr ions in groundwater sources.

Kinetic studies of Cr transport in LLE were conducted in order to model the Cr transport in the SLM-based sampling systems. These studies provide the first kinetic analysis of Cr speciation in an SLM-based sampler. The results of the LLE kinetic studies provide a greater understanding of the Cr extraction mechanism. After the application of an Occam's Razor analysis of the kinetic data, the presence of decanol and H^+ were found to have a negligible effect on the overall Cr extraction. The composition of the transition state was found to be one Cr ion for each carrier molecule. Therefore, the rate laws that model LLE Cr extraction are second order overall and first order in both Cr and carrier molecule.

The rate laws obtained from the LLE studies were applied to the SLM-based extraction data. The predicted Cr extraction was significantly faster than the observed SLM-based experimental data. However, the shape of the predicted extraction matches the laboratory-controlled data. The membrane of the SLM-based extraction systems was determined to be the factor that impedes Cr extraction. The rate constants for Cr (III) and Cr (VI) were adjusted (decreased) and the predicted data models the experimental data.

Overall, the results of the tests conducted in the laboratory indicate that the SLM samplers are a stable, reliable, and viable method for Cr speciation. Thus, a new method of Cr speciation in groundwater sources has been designed, fabricated, and validated. This advance in environmental sampling will improve current methods for analyzing Cr in groundwater sources as well as the monitoring of remediation efforts in contaminated sites. The future directions of

this project will be discussed in Section 5.2 and include the incorporation of the SLM sampler into the existing Multi-layer Sampler (MLS) technology as well as the analysis of the stability and performance of the incorporated systems in the *in-situ* speciation application.

5.2 Potential Applications

The potential applications of this project include utilizing the kinetic data to create a calibration curve, which can be used to predict Cr uptake in the SLM sampling system, as well as the incorporation of the SLM sampler with existing multilayer sampler (MLS) technology. The SLM-MLS apparatus will be studied in laboratory-controlled studies (mimicking natural systems) as well as in the field in areas of known contamination.

The results of the LLE kinetics studies have been adapted to predict the uptake of Cr in the sampling system. The rate constant was manipulated to account for the presence of the membrane, which provides a substantial barrier to Cr transport. Thus, the rate constant of the SLM rate law is significantly (three orders of magnitude) less than that of the LLE rate law. Furthermore, the SLM rate law can be used to predict the uptake of Cr into the SLM sampling systems. The Cr concentration of the sampler bottle can be analyzed using ICP-OES at 283.569 nm. Using equation 3.15, the initial Cr (III) concentration can be determined, substituting the optimal carrier (10%). An analogous method can be used to determine the initial Cr (VI) concentration from equation 3.16.

The final application of the project will consist of the incorporation of the SLM sampling system into the existing MLS technology. The MLS is a spine-like apparatus that is placed in contaminate plumes. The SLM samplers can be attached at perpendicular to one another at different levels on the MLS. Not only does this arrangement provide speciation information, it is also capable of providing spatial information regarding depth of Cr contamination. The first

challenge will be the actual incorporation of the SLM sampler to the MLS system. Although ease of MLS incorporation was envisioned when designing the SLM sampling systems, undoubtedly, issues concerning mechanical stability will be encountered during the incorporation process. Work will be done to ensure preservation of sampler integrity and stability during this stage. Sampler modifications will be fabricated from Teflon[®] materials to maintain a metal-free sampler design.

Once the SLM-MLS sampling apparatuses have been produced, they will be tested in laboratory-controlled experiments designed to mimic Cr contamination in groundwater sources. After the SLM-MLS apparatus is validated in laboratory-controlled experiments, the apparatus will be tested *in-situ* in areas of known Cr contamination. Furthermore, the SLM-MLS apparatus can be utilized to monitor groundwater remediation processes.